AN ABSTRACT OF THE THESIS OF

Kenton Alldritt for the degree of Master of Science in Wood Science and Civil Engineering presented on June 18, 2013
Title: Designing a Strand Orientation Pattern for Improved Shear Properties of Oriented Strand Board

Abstract approved:

Arijit Sinha Thomas H. Miller

As oriented strand board (OSB) increases in use as an engineered wood product, improving the in-plane shear properties will allow more efficient use of the material as well as open up other opportunities for OSB to be used in engineered wood products with high shear stresses. Based on classical laminated plate theory, composite laminates with ±45° laminate alignment patterns produce higher in-plane shear modulus and strength when compared to typical 0°/90°/0° laminate alignment. This research consisted of manufacturing 13.3 mm thick OSB with 0°/+45°/-45°/-45°/+45°/0° and 0°/90°/0° alignment patterns and comparing the in-plane shear, bending, nail connection, and small-scale shear wall properties with typical commercial OSB. The results showed an increase of 24% in measured average shear modulus for 0°/+45°/-45°/-45°/+45°/0° alignment when compared to 0°/90°/0° alignment using a method similar to the ASTM D2719-Method C in-plane shear test. The results show a 10% reduction in measured bending modulus of elasticity in the parallel direction. The small-scale shear wall tests were insensitive to changes in in-

plane shear properties. The nail connection tests showed no reduction in yield load of the connection, implying that ±45° panels can be used in similar applications as 0°/90°/0° OSB without adversely affecting the connection properties.

Designing a Strand Orientation Pattern for Improved Shear Properties of Oriented Strand Board

by
Kenton Alldritt

A THESIS

submitted to

Oregon State University

in partial fulfillment of
the requirements for the
degree of

Master of Science

Presented June 18, 2013
Commencement June 2014

Master of Science thesis of Kenton Alldritt presented on June 18, 2013.

APPROVED:

Co-Major Professor, representing Wood Science and Engineering

---

Co-Major Professor, representing Civil Engineering

Head of the Department of Wood Science and Engineering

Head of the School of Civil and Construction Engineering

Dean of the Graduate School

I understand that my thesis will become part of the permanent collection of Oregon State University libraries. My signature below authorizes release of my thesis to any reader upon request.

Kenton Alldritt, Author

ACKNOWLEDGMENTS

I would like to deeply thank my wonderful Lord, Jesus Christ. He created me in His image because He loves me and wants me to have abundant life through Him. But because of my sin, I was separated from Him and there was nothing I could do to bridge the gap between me and a Holy God. God sent the ultimate and final cure to my sin in the form of a Man who was blameless but took the punishment that I deserved because of my willing disobedience through sin. Now my payment is paid in full and I will stand before God blameless and without a single blemish. With such an amazing gift that was so freely given to me but at a great cost to Him, I have no other desire but to praise His great name with every word from my mouth, every thought in my mind, and every action of my hand. He is the reason I live and He has empowered me to complete this research project with steadfast excellence. To Him be the glory and Him alone.

CONTRIBUTION OF AUTHORS

Dr. Arijit Sinha and Dr. Thomas H. Miller have provided significant guidance in this research project.

TABLE OF CONTENTS

TABLE OF CONTENTS (Continued)

Page

LIST OF FIGURES

LIST OF TABLES

LIST OF APPENDICES

LIST OF APPENDIX FIGURES

LIST OF APPENDIX FIGURES (Continued)

LIST OF APPENDIX FIGURES (Continued)

Figure Page

LIST OF APPENDIX FIGURES (Continued)

<u>Figure</u> <u>Page</u>

LIST OF APPENDIX TABLES

LIST OF APPENDIX TABLES (Continued)

INTRODUCTION

Oriented strand board (OSB) is used in many applications including structural sheathing, flooring, I-joist web material, structural insulated panels, upholstered furniture, and various material handling products. OSB is typically made from low-density trees such as aspen (*Populus tremuloides*) (Barbuta *et al*., 2011). By using low-density wood species, high value products can be made from a relatively low value wood species. As OSB is used in an increasing number of products, refinement and adjustment of its mechanical properties are of importance. By applying composite laminate mechanical theories to OSB manufacturing, specific desired properties can be refined to meet the needs of the end product.

The mechanical properties investigated in this study were in-plane shear modulus and shear strength. In-plane shear refers to shear stress and distortion relative to the x-y plane as seen in Fig. i. Another term used in ASTM D2719 (ASTM 2007) for in-plane shear is "shear through-the-thickness." In-plane shear is an important mechanical property of OSB in products such as I-joist web stock and structural sheathing for buildings (McCutcheon, 1985, Shrestha, 1999, and Grandmont *et al*., 2010). According to Grandmont *et al*. (2010), I-joist web stock performance is highly sensitive to in-plane shear properties. In-plane shear modulus also has a significant role in the deflection of OSB sheathed shear walls (McCutcheon, 1985).

Typically, researchers have modeled the mechanical behavior of OSB using Classical Laminate Plate Theory (CLPT) (Moses *et al*., 2003 and Weight and Yadama, 2008). CLPT involves mathematical modeling of each individual layer of a composite laminate with individual mechanical properties in the x, y, and z directions. Thus, CLPT can predict the change in mechanical properties of the entire laminate with any alignment orientation of each individual laminate layer.

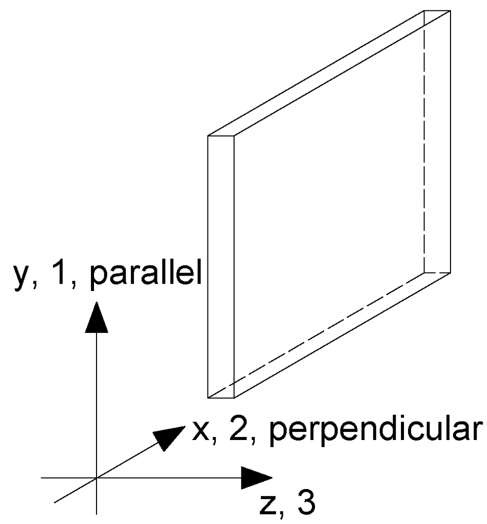

Figure i. Reference coordinate system

Due to wood being an orthotropic material, the orientation of the strands within OSB has a significant impact on the mechanical properties in the x and y directions (McNatt *et al*. 1992). McNatt *et al*. (1992) studied the contribution of strand alignment to performance of OSB in bending, internal bond, and linear expansion properties of OSB. McNatt *et al*. (1992) manufactured 72 panels using six strand orientation patterns while keeping the same furnish, resin type, and resin content. The orientations of face strands and core strands were varied. The strand patterns included the following: strands randomly distributed, face strands aligned parallel to panel length with core strands random, face strands aligned parallel to panel length with core strands cross aligned, face strands aligned parallel to the panel width with core strands cross aligned, and unidirectional alignment. McNatt *et al*. (1992) concluded that the alignment of face strands improved bending strength and stiffness in the direction of alignment but caused a reduction in bending strength and stiffness in the direction perpendicular to the alignment. McNatt *et al*. (1992) improved the bending properties of OSB by investigating strand alignment, which is a very important property when OSB is used as flooring.

Moses *et al*. (2003) studied ±45° alignment of laminated strand lumber (LSL) panels. LSL is a strand composite similar to OSB, but with longer strands (25 cm as opposed to 10 cm of OSB) and unidirectional strands. LSL is typically unidirectional, however, Moses *et al*. (2003) manufactured LSL panels with strand alignment patterns that included: fully oriented; randomly oriented; surfaces oriented, core randomly oriented; surfaces randomly oriented, core fully oriented; and eight fully oriented layers aligned at angles of 0° and ±45°. Smaller test specimens were cut from the manufactured panels and tested for their tension and compression properties, and compared to a mathematical model but no large panel in-plane shear testing was performed. The model showed that the ±45° alignment could produce an increase in shear modulus compared to a 0°/90°/0°alignment for LSL panels. Moses *et al*. (2003) concluded that the influence of strand alignment on the in-plane properties of the panels could be predicted using the composite laminate model used in Moses *et al*. (2003).

A similar study presented by Chen *et al*. (2008) involved a mathematical model for bending stiffness of OSB based on strand alignment. Very little research has been conducted on the effect of strand orientation not in the parallel and perpendicular directions due to the difficulty in achieving the target strand orientation (Chen *et al*., 2008).

Sturzenbecher *et al*. (2010) introduced the need for more applied design of laminate alignment, wood quality, and compaction of OSB for specific applications. The authors perform an excellent study quantifying the effects of material properties and strand geometry on stiffness and strength of OSB. The authors performed out-of-plane shear tests on the panels but did not perform an in-plane shear tests. No off-axis strand orientation was investigated; only parallel, perpendicular, and random alignment was investigated.

A preliminary study using OSU Laminates (Nairn, 2008) to investigate the optimum alignment angle for in-plane shear modulus of Douglas-fir OSB in a 6 layer laminate with equal weight ratios showed that ±45° core layers was most beneficial while 90° core layers were least beneficial. Equal weight ratios refer to each layer of the laminate having the same weight of wood strands. Fig. ii shows the results from the OSU Laminates calculations.

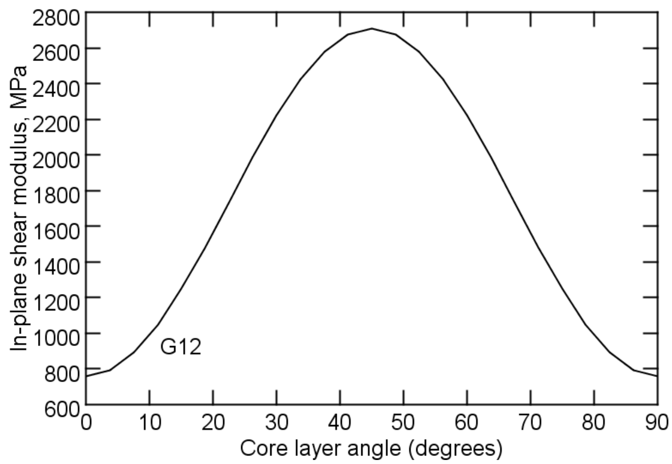

Figure ii. OSU Laminates core layer angle versus in-plane shear modulus

Objectives

The objective of this study was to observe the effect that the 0°/+45°/-45°/-45°/+45°/0° strand alignment has on the in-plane shear properties of OSB. In addition, an objective was to observe behavior of the small-scale shear wall test, nail connection, and bending properties when in-plane shear properties of the OSB have been modified using the 0°/+45°/-45°/-45°/+45°/0° layup pattern. To assist in data interpretation, a control layup pattern of 0°/90°/0° was also manufactured and tested. Commercial OSB was also tested in shear, bending, small-scale shear wall, and nail connection tests. All other factors in manufacturing were held constant between the 0°/90°/0° and the [0°/+45°/-45°/-45°/+45°/0°] laboratory manufactured panels.

ORGANIZATION

The thesis herein is organized in a manuscript format which includes one manuscript in the following section. Following the manuscript is a series of appendices that supplement and support the research presented in the manuscript.

MANUSCRIPT

DESIGNING A STRAND ORIENTATION PATTERN FOR IMPROVED SHEAR PROPERTIES OF ORIENTED STRAND BOARD

Kenton Alldritt, Arijit Sinha, Thomas H. Miller

American Society of Civil Engineers
Journal of Materials in Civil Engineering

ASCE Journal Services
1801 Alexander Bell Drive
Reston, VA 20191

Submitted 2013

Abstract

As oriented strand board (OSB) increases in use as an engineered wood product, improving the various mechanical properties of OSB is of importance. Improving the in-plane shear properties of OSB will allow more efficient use of the material as well as open up other opportunities for OSB to be utilized in engineered wood products with high shear stresses. Based on classical laminated plate theory, composite laminates with ±45° laminate alignment patterns produce higher in-plane shear modulus and strength when compared to typical 0°/90°/0° laminate alignment. This research consisted of manufacturing 13.3 mm thick OSB with 0°/+45°/-45°/-45°/+45°/0° and 0°/90°/0° alignment patterns, and comparing the in-plane shear, bending, nail connection, and small-scale shear wall properties with typical commercial OSB. The results showed an increase of 24% in measured average shear modulus for the 0°/+45°/-45°/-45°/+45°/0° alignment when compared to the 0°/90°/0° alignment using a method similar to the ASTM D2719 Method C in-plane shear test. The results show a 10% reduction in measured bending modulus of elasticity in the parallel direction. The small-scale shear wall tests were insensitive to changes of in-plane shear properties. Nail connection tests showed no reduction in yield load of the connection, implying that these panels can be used in similar applications as for OSB without affecting the connection properties.

Introduction

Oriented strand board (OSB) is used in many applications including structural sheathing, flooring, I-joist web material, structural insulated panels, upholstered furniture, and various material handling products. OSB is typically made from low-density trees such as aspen (*Populus tremuloides*) (Barbuta *et al*., 2011). By using low-density wood species, high value products can be manufactured from a relatively low value wood species. As OSB is used in an increasing number of products, refinement and adjustment of OSB mechanical properties is important. By adjusting manufacturing specifications of OSB to alter mechanical properties, specific desired properties can be refined to meet the needs of the end product.

Mechanical properties investigated in this study include in-plane shear modulus and shear strength. In-plane shear is the shear stress and deformation in the x-y plane as seen in Fig. 1. Another term used in ASTM D2719 (ASTM 2007) for in-plane shear is "shear through-the-thickness." In-plane shear is an important mechanical property of OSB in products such as I-joist web stock and structural sheathing for buildings (McCutcheon, 1985, Shrestha, 1999, and Grandmont *et al*., 2010). According to Grandmont *et al*. (2010), I-joist web stock performance is highly sensitive to in-plane shear properties. In-plane shear modulus also has a significant role in the deflection of OSB sheathed shear walls (McCutcheon, 1985).

Typically, researchers have modeled the mechanical behavior of OSB using Classical Laminate Plate Theory (CLPT) (Moses *et al*., 2003 and Weight and Yadama, 2008). CLPT involves mathematical modeling of each individual layer of a composite laminate with individual mechanical properties in the x, y, and z directions. Thus, CLPT can predict the mechanical properties of the entire laminate using any alignment orientation of each individual laminate layer.

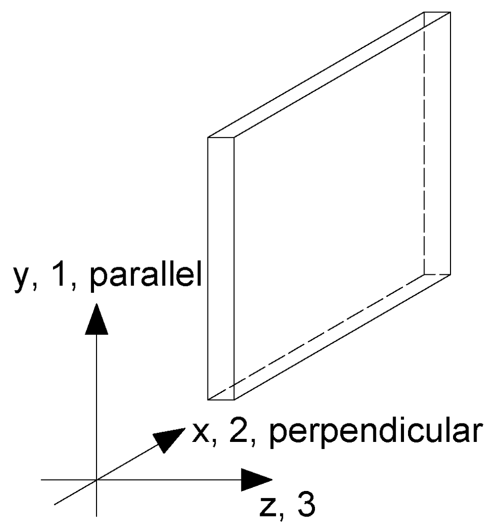

Figure 1. Reference coordinate system

Due to wood being an orthotropic material, the orientation of the strands within OSB has a significant impact on the mechanical properties in the x and y directions (McNatt *et al*. 1992). They studied the contribution of strand alignment to performance of OSB in bending, internal bond, and linear expansion properties of OSB. McNatt *et al*. (1992) concluded that the alignment of face strands improved bending strength and stiffness in the direction of alignment but caused a reduction in bending strength and stiffness in the direction perpendicular to the alignment. They improved the bending properties of OSB by investigating strand alignment, which is a very important property when OSB is used as flooring.

Moses *et al*. (2003) manufactured ±45° alignment of laminated strand lumber (LSL) panels and produced a mathematical model for mechanical properties based on tension tests. The model showed that ±45° alignment could produce an increase in shear modulus compared to 0°/90°/0° alignments for LSL panels. They concluded that the influence of strand alignment on the in-plane properties of the panels could be predicted using the composite laminate model. A mathematical model was presented by Chen *et al*. (2008) for bending stiffness of OSB based on strand alignment. Chen *et al*. (2008) stated that very little research has been conducted on the effect of strand orientation not in the parallel and perpendicular directions due to the difficulty in achieving the target strand orientation. Stürzenbecher *et al*. (2010) examined more applied design of laminate alignment, wood quality, and compaction of OSB for specific applications.

A preliminary study using OSU Laminates (Nairn, 2008) to investigate the optimum alignment angle for in-plane shear modulus of Douglas-fir OSB in a 6 layer laminate with equal weight ratios showed that ±45° core layers were most beneficial while 90° core layers were least beneficial. Fig. 2 shows the results from the OSU Laminates calculations.

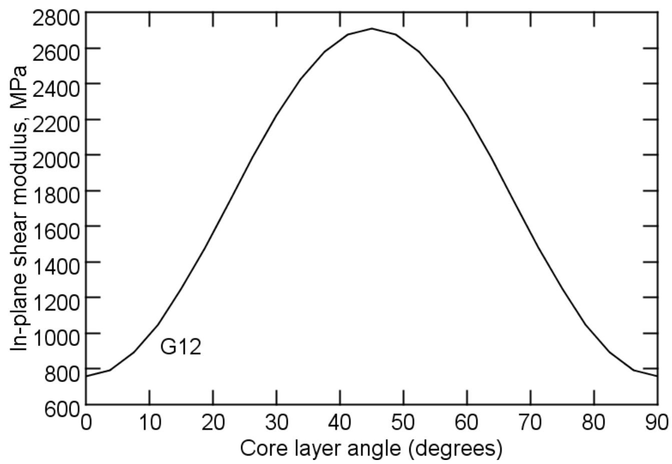

Figure 2. OSU Laminates core layer angle versus in-plane shear modulus

Objectives

The objective of this study was to observe the effect that the 0°/+45°/-45°/-45°/+45°/0° strand alignment has on the in-plane shear properties of OSB. In addition, an objective was to observe behavior of the small-scale shear wall test, nail connection, and bending properties when in-plane shear properties of the OSB have been modified using the 0°/+45°/-45°/-45°/+45°/0° layup pattern. To assist in data interpretation, a control layup pattern of 0°/90°/0° was manufactured and tested. Commercial OSB was also tested in shear, bending, small-scale shear wall, and nail connection tests. All other factors in manufacturing were held constant between the 0°/90°/0° and the 0°/+45°/-45°/-45°/+45°/0° laboratory manufactured panels.

Materials and Methods

A six-layer alignment pattern of 0°/+45°/-45°/-45°/+45°/0° and a typical 3-layer pattern of 0°/90°/0° were manufactured in the current study as seen in Fig. 3. Both panel types were manufactured with the same target density and same furnish weight. Therefore, the 0°/+45°/-45°/-45°/+45°/0° panel had 1/6 of the total panel weight per each layer while the 0°/90°/0° panel had 1/3 of the total panel weight per layer. The weight ratio for the 0/90/0 panels was 1/3:1/3:1/3 and for the [0/+45/-45]s panels it was 1/6:1/6:1/6:1/6:1/6:1/6. For this research, the 0°/+45°/-45°/-45°/+45°/0° alignment pattern will be referred to as [0/+45/-45]s, where "s" represents "symmetric." The pattern is symmetric about the central axis. The 0°/90°/0° layup pattern will be referred to as 0/90/0. To preserve the bending properties of OSB, both alignment designs had the face layers with 0° alignment. OSB also tends to warp after cooling from hot-pressing if the alignment pattern is not symmetric about the central axis, thus the symmetrical [0/+45/-45]s alignment prevents warping during cooling.

Wood Strand Preparation

Wood strands for OSB panels were sourced from Weyerhaeuser Natural Resources Company (Federal Way, Washington). The stands were of aAspen from the Great Lakes area. The wood strands were dried by Weyerhaeuser Natural Resources Company to a moisture content of 6% to 8%. The wood strands were approximately 10 cm in length. The length to width aspect ratio of the wood strands was 4:1.

Resin Application

The strands were placed in a rotating drum blender which was set to spin at 5 rpm. The diameter and depth of the drum blender were 1.83 m and 0.89 m, respectively. A spinning disk atomizer (Coil Model EL4, Surrey, British Columbia) sprayed the adhesive onto the wood strands inside the blender. The rate of the spinning disk atomizer was 10000 rpm. The target density of each panel was 0.64g/cm^3 with a target thickness of 12.7 mm. The calculated amount of resin added to the blender was 524 ml. Typical weight of resin coated wood strands per layer was 2675 grams for the 0/90/0 panels and 1340 grams for the [0/+45/-45]s panels. The resin was liquid phenol formaldehyde with a solids content of 55.5%. The target furnish moisture content was 9%. The resin solids content based on total dry weight of furnish was 4%. The resin was procured from Momentive Specialty Chemicals Inc. (Springfield, Oregon).

Strand Alignment

Strand alignment was achieved by passing the strands by hand in a forming box though a vibratory screen consisting of aluminum vanes spaced at 50 mm as shown in Fig. 4. The vanes were 127 mm deep. The forming box was 914 mm by 914 mm with the alignment screen having an adjustable height above the surface of the strand mat. The free-fall distance of the wood strands from the bottom of the alignment vanes to the surface of the mat was not greater than the typical length of a wood strand (approximately 100 mm). The vibration was achieved from a variable speed electric motor attached to the side of the forming box. The motor was connected to an off-center counter weight. The speed of the motor was adjusted to achieve the greatest amount of vibration of the forming screen. Two forming screens were used consisting of vanes set at 0° and 45°. The forming screens were removed, rotated 90°, and reinstalled to create the different alignment patterns. Photos of the alignment patterns of the OSB strands before pressing are shown in Fig. 5. A thin thermocouple wire was placed in the center of the panel to monitor core temperature during pressing. The weight of strands used in each panel was held constant.

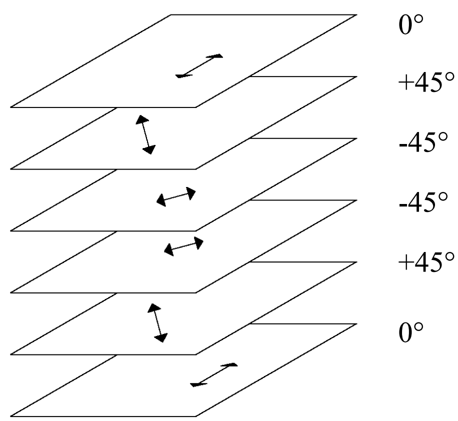

Figure 3. Strand alignment pattern of 0°/+45°/-45°/-45°/+45°/0°

Figure 4. Strand alignment screen and vibratory forming box

Figure 5. Strand alignment of 0° (a), 90° (b), +45° (c), and -45° (d) before pressing

Hot Pressing

After forming the mat of OSB strands, the mat was placed into a hydraulic hot press. The mat was pressed on a screen on the lower platen. The platen temperature was set to 180°C. The panel was pressed using displacement control until the press reached the desired thickness of 12.7 mm. The panel was held in the press until the core temperature was above 100°C for at least two minutes. The panels were pressed for an average of 9 minutes. The same pressing schedule was used for all panels. The pressed panel was then removed and allowed to cool. The measured average thickness of the 0/90/0 panels was 13.3 mm. The measured average thickness of the [0/+45/-45]s panels was 13.2 mm.

Panel Cut Schedule

A total of 32 panels were manufactured. Specimens for in-plane shear and bending test were cut as per ASTM D2719 Method C (ASTM 2007) and ASTM D3043 (ASTM 2011) respectively. The cutting pattern is shown in Fig. 6. Cut numbers 1-7 were parallel bending specimens, cut numbers 8-13 were perpendicular bending specimens and the large center section was reserved for in-plane shear tests. The exterior 67 mm was removed to reduce edge effects. In-plane shear and bending test specimens were cut from 20 panels and the remaining 12 panels were used for ASTM E564 (ASTM 2012) small-scale shear wall tests. Half of all the panels manufactured was 0/90/0 alignment pattern and the other half was [0/+45/-45]s pattern. Sixteen commercial panels (10 for shear/bending and 6 for small shear walls) were cut to the similar specifications as the laboratory manufactured panels. The average density of the commercial panels was 0.59 g/cm^3. The average thickness of the commercial panels was 11.5 mm. The commercial panels were manufactured by LP Building Products at mill #510 in Fort St. John, British Columbia on November 27th 2012. The commercial panels meet the PS-2 sheathing grade which is rated for exposure 1.

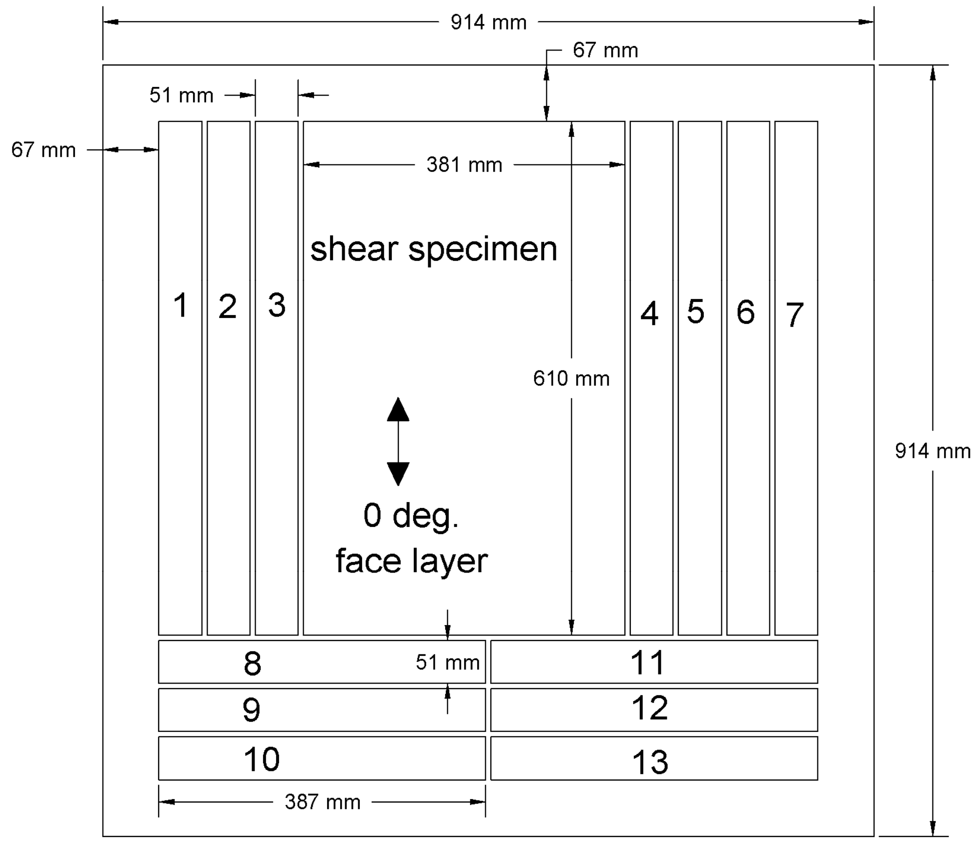

Figure 6. Panel cut pattern

In-Plane Shear Test

One specimen per panel was tested for in-plane shear based on the ASTM D2719 Method C (ASTM 2007). The size of the specimen was 610 mm in height by 390 mm in width. The ASTM D2719 Method C procedure requires bonding heavy lumber rails to the long edges of the shear specimen with adhesive. Steel brackets were bolted to the specimen and were used in place of the adhesive attached lumber rails as shown in Fig. 7 (similar to the testing bracket used in Shrestha (1999)). The brackets were made from 19 mm thick steel plate with 7 holes in each for 12.7 mm diameter bolts to clamp the brackets to the specimen. The holes were drilled through the specimen for the bolts to clamp the steel brackets together. The space between the brackets was 203 mm. The brackets were then pulled in tension to create a shearing force on the specimen. The specimen was loaded at a rate of 1.3 mm per minute. The testing machine consisted of an MTS 407 Hydraulic Controller attached to a MTS 160 kN Hydraulic Actuator (model # 244.23) on a MTS Load Unit test bed.

(a) (b)

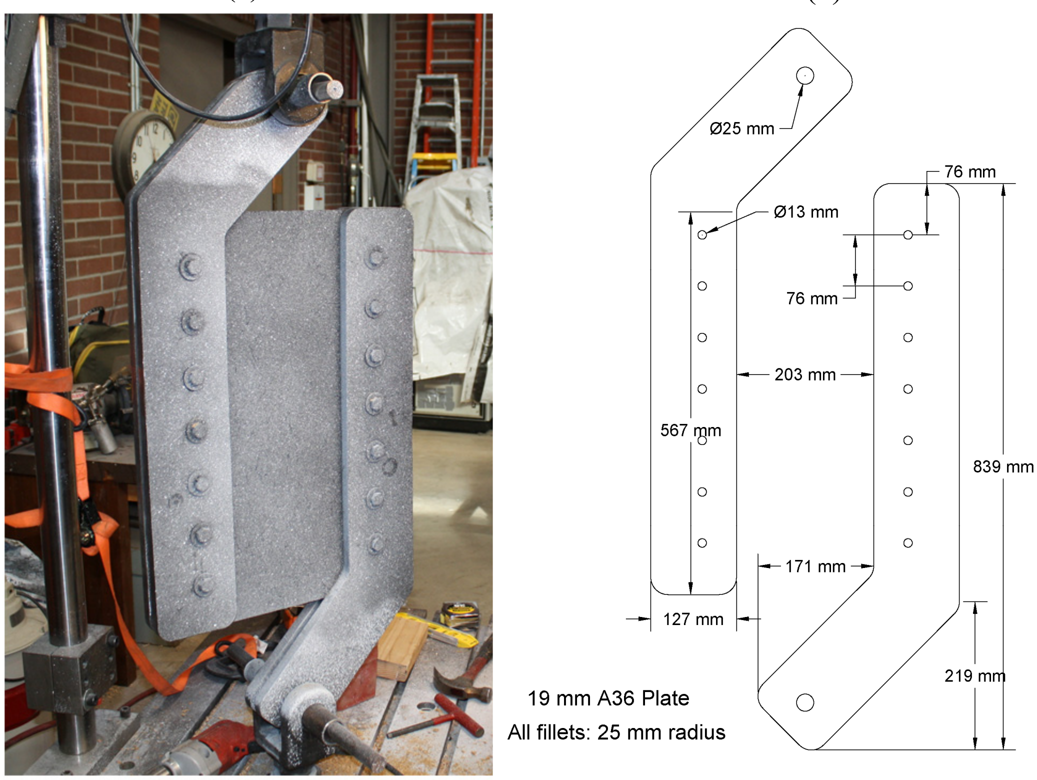

Figure 7. Specimen in modified ASTM D2719 shear test apparatus and painted with DIC speckle pattern (a). Corresponding dimensioned schematic (b).

Digital Image Correlation

An optical non-contract, strain measurement system based on the digital image correlation (DIC) technique was used to measure shear strain (ε_{xy}) on the surface of the shear and wall test specimens. DIC has been successfully used in the wood product industry by Sinha and Gupta (2009). DIC uses a pair of high definition digital cameras that image a surface coated with a contrasting black and white speckle pattern. A series of images are then captured during testing. The software measures the movement of a specified block of pixels in the image during the test in subsequent images. The size of the block of pixels used was 21 and the step between pixel blocks was 5 pixels. The cameras are calibrated using a surface with a known speckle pattern on a special calibration plate. The cameras were set to capture an image every second during the loading of the specimen. Each image was tagged to specific load data received from the MTS 407 hydraulic controller. The DIC software then maps the surface by correlating the movement of the contrasted pixels to calculate strain. Shear strain can be extracted from the DIC output data. Thus, full-field shear strain contour plots were developed for the in-plane shear and small-scale shear wall tests. The resolution of the shear strain measured was ±0.0002 strain. An assumption made by using optical surface strain measurement was that the strain on the surface of the OSB material represented the strain through the thickness of the material due to strain compatibility. Factors that would cause local variations in the surface strains include the presence of voids in the material, as well as resin and density distribution.

In-plane Shear Data Analysis

Shear strain (ε_{xy}) from the in-plane shear test was measured using the DIC measurement technique. Shear modulus, G_{xy}, was calculated using the following equation:

$$G_{xy} = \left(\frac{P}{\varepsilon_{xy}}\right) * \left(\frac{1}{L * t * 2}\right)$$

Here, (P/ε_{xy}) was the slope of the plotted load vs shear strain curve in the linear region, which was at a load between 18 kN and 27 kN. L was the length of the specimen; and t was the thickness of the specimen.

Shear strength was found using the following equation:

$$\tau_{xy} = \left(\frac{P_{max}}{L * t}\right)$$

where P_{max} was the peak load measured on the specimen during the shear test. The sample size for the in-plane shear tests was ten for each panel type (n = 10).

Bending Tests

The parallel and perpendicular bending tests followed the ASTM D3043 – Method B (ASTM 2011) two-point flexure test procedure. The terms parallel and perpendicular refer to parallel and perpendicular to the 0° strand orientation of the panel face as shown in Fig. 1. The tests were conducted on an INSTRON Series 5582 Universal Testing Machine. The span length for the parallel bending test was 558 mm and for the perpendicular bending test was 330 mm. The length between the load points for the parallel bending test was 186 mm and for the perpendicular bending test was 110 mm. The span-to-depth ratios for the parallel and perpendicular test were 44 and 26, respectively. All bending test specimens were cut to approximately 51 mm in width. The load rate of the parallel bending test was 6.8 mm/min and for the perpendicular span was 0.094 mm/min. The load rate was calculated to keep the extreme fiber strain rate limited to 0.0015 mm/mm/min in accordance with ASTM D3043 (ASTM 2011). Seven parallel and six perpendicular bending samples were cut from each panel. Thus, there was a total of 70 parallel and 60 perpendicular specimens for each of the alignment patterns as well as for the commercial panels.

Bending Test Data Analysis

Bending modulus of elasticity (MOE) and modulus of rupture (MOR) were calculated using a method similar to ASTM D3043 – Method B, however, ASTM D3043 – Method B requires measuring the vertical deflection of the neutral axis at the center of the span relative to the supports. The procedure used herein used the deflection of the load head at the load points recorded by the INSTRON Series 5582 UTM. A load-deflection diagram was acquired. The equations for MOE and MOR were:

$$\mathrm{MOE} = \frac{7 * L^3}{324 * I} * \frac{P}{\Delta}$$

$$\mathrm{MOR} = \frac{P_{max} * L * t}{12 * I}$$

Here, L was span length, t was the thickness of the specimen, I was the moment of inertia of the specimen, P_{max} was maximum load on the specimen, and P/Δ was the slope of the load deflection curve. The span between the load points was L/3.

The linear portion of the curve was used for MOE calculations. The linear portion of the curve was found to be at loads between 89 N and 178 N for the parallel direction and between 89 N and 133N for the perpendicular direction. The peak load was used for MOR calculations. The thickness of each specimen was used for MOE and MOR using equations provided in ASTM D3043. The sample size for the bending tests was 70 for each panel type in the parallel direction (n = 70) and 60 for each panel type in the perpendicular direction (n = 60).

Nail Connection Test

The lateral nail connection tests were conducted in accordance to ASTM D1761 (ASTM 2006). Lateral nail resistance was determined for 0/90/0, [0/+45/-45]s, and commercial panels. Two types of tests were conducted, using 38 mm x 89 mm lumber loaded perpendicular and parallel to grain. The nail used was manufactured by Senco Inc. (Cincinnati, Ohio) and was 75 mm in length and 3.8 mm in diameter. The nail had a full round head and was labeled as 10d. The nail was driven by hand with a hammer. The edge distance for both tests was 19 mm. The loading rate was 5 mm/min. The specimen width was 50 mm and one nail connection test was performed for each panel.

Nail Connection Test Data Analysis

The resultant load and deflection data were analyzed to find the yield point using the linear offset method (AFPA 2012). The linear portion of the load and deflection curve is offset by 5% of the diameter of the nail shank. The line is then extended to find the yield load where it intersects the original load vs. deflection curve. The sample size for the nail connection tests was ten for each panel type and each direction (n = 10).

Small-Scale Shear Wall Test

The wall test was based on ASTM E564 (ASTM 2012) which was modified to accommodate the 610 mm by 610 mm walls tested. The wall panels for 0/90/0, [0/+45/-45]s, and commercial specimens were nailed to 2x4 nominal (38 mm x 90 mm) select structural lumber studs with a single sill plate, and single top plate. The nails used were manufactured by Senco Brands, Inc. (Cincinnati, Ohio) and were 75 mm in length and 3.8 mm in diameter. The nail had a full round head and was labeled as 10d. The edge distance was approximately 19 mm. The nail spacing was 102 mm around the entire wall. The nails were pneumatically driven. The sill and top plates were bolted to the test machine. The sill plate was rigidly fixed to the test frame base (Fig. 8b), and the top plate was deflected laterally causing a racking force on the specimen. The displacements were measured from the MTS hydraulic cylinder which was attached to the top plate. The specimen was also sprayed with a black and white speckle pattern (Fig. 8a) for the full-field, non-contact, optical strain measurement based on DIC principles. No stud hold-downs were used in the test. The test was halted when the load-deflection curve reached a maximum and a plateau was observed in the curve. A total of six panels of each panel type (0/90/0, [0/+45/-45]s, and commercial) were tested.

(a)

(b)

Figure 8. Small-scale shear wall test viewed from front (a) and back (b)

Small-Scale Shear Wall Data Analysis

The load versus deflection curve was recorded from the hydraulic cylinder deflection. The load versus deflection curves were compared for each wall type. DIC image analysis was also performed on the small scale shear wall tests. The sample size for the small-scale shear wall tests was 6 for each panel type (n = 6).

Results and Discussion

Shear Test

The shear strain (ε_{xy}) was measured using the DIC software. The DIC software can average the shear strain over a specified area, called the “area of interest”. The area of interest for the average shear strain measurement for the shear test was measured between the two bolts on the extreme ends of the testing brackets and between the steel rails. The average shear strain was plotted against the corresponding force to produce a load vs. shear strain (ε_{xy}) curve. The slope of the curve in the linear region was used to calculate the shear modulus (G_{xy}). The average shear moduli for the 0/90/0, [0/+45/-45]s, and commercial panels are presented in Table 1. A two-sample t-test assuming equal variances was performed on the shear results comparing the 0/90/0 alignment with the [0/+45/-45]s alignment. The [0/+45/-45]s showed a 24% increase (p-value = 0.001) in measured average shear modulus when compared to the 0/90/0 alignment pattern. This result matches the predictions from the CLPT calculations which show an increase in shear modulus when alignment is changed from 0/90/0 to [0/+45/-45]s. The average measured shear modulus for the 0/90/0 layup pattern was 23% greater than for the commercial panels. This result was due to the 0/90/0 and [0/+45/-45]s panels having a higher density due to laboratory manufacturing and thus inconsistent with typical commercial OSB manufacturing. The average density of the 0/90/0, [0/+45/-45]s, and commercial in-plane shear test specimens was 0.749 g/cm^3, 0.741 g/cm^3, and 0.578 g/cm^3 respectively. The published average shear modulus from Shrestha (1999) was 1.28 GPa and a shear strength of 7.0 MPa and was similar to the results found herein being 0.99 GPa for shear modulus and 6.83 MPa for shear strength of the commercial panels. Shrestha (1999) used a similar in-plane shear test apparatus as the research presented herein. The results for shear strength, τ_{xy}, from the research herein showed a high coefficient of variation (COV) when compared to commercial OSB. Due to the high COV of the shear strength, a statistical analysis was inconclusive on alignment pattern affecting shear strength. A typical in-plane shear test failure is shown in Fig. 9. The typical failures modes were shear failure directly at the steel rails or a diagonal shear failure across the panel. The failure lines were not straight through the thickness of the panel, but reflected the nonhomogeneous nature of the material, made of discrete strands..

Shear strain contour plots for all three types of panels – commercial, 0/90/0 and [0/+45/-45]s, are presented in Fig. 10. These contour plots represent progressive development of strain as the load increases during a shear test of the panels. The load cases shown are 20 kN (Fig. 10a), 47.7 kN (Fig. 10b), 70 kN (Fig. 10c), and 84.4 kN (Fig. 10d). The panels shown in Fig. 10 represent the typical panel within the alignment categories: commercial, 0/90/0, and [0/+45/-45]s panels. The average shear moduli for the panels shown in Fig. 10 are 1.01 GPa, 1.28 GPa, and 1.63 GPa for the commercial, 0/90/0, and [0/+45/-45]s, respectively. The color contour plot scale to represent shear strain between 0 and 0.008 is also presented in Fig. 10.

The commercial panel develops significant shear strain the earliest out of the three panels. At 20 kN of load, the commercial panel has significant areas of yellow color contour representing shear strain between 0.0015 to 0.002 (Fig. 10a). Commercial panels were of lower density than lab manufactured panels and, as a result, their shear stiffness was lower. The lower density explains the early onset of strain in commercial panels. The color contour difference between the 0/90/0 and [0/+45/-45]s can be seen in the 20 kN load case of Fig. 10 (a). In Fig. 10 (a), the 0/90/0 panel shows a significant amount of yellow (0.0015 to 0.002 shear strain) contour color, while the [0/+45/-45]s panel shows very little yellow color. These results show that at low loads the ±45° alignment results in less shear strain when compared to 0/90/0 alignment. The commercial panel failed at 47.7 kN. Fig. 10(b) represents a snapshot of the commercial panel's strain contour plot just before failure. High strain concentrations are represented by dark blue spots (0.006 to 0.007 shear strain) in the field of the panel which depicts the failure initiation points. There is a significantly high strain area occurring in the 0/90/0 panel at 47.7 kN of load shown in green (0.003 to 0.004 shear strain), while the [0/+45/-45]s panel has a limited amount of green color contour at the same load shown in Fig. 10(b). At 70 kN, the 0/90/0 panel is showing significantly high shear strain represented in purple (>0.007 shear strain) in Fig 10 (c). Interestingly, the shear strain concentration (shown in purple) is a natural progression of the high shear strain line observed for the 47.7 kN loading. The commercial panel failed before 70kN. At 70 kN the [0/+45/-45]s does not show any evidence of high shear strain which is seen in the 0/90/0 panel with the colors blue and purple (0.006 and 0.007 shear strain, respectively). The 0/90/0 panel failed at 77.8 kN. On the other hand, the [0/+45/-45]s continued to carry load past 70 kN and ultimately failed at 84.4 kN. The 0/90/0 and the [0/+45/-45]s panels have the same amount of wood strands and resin with the same manufacturing processes, however, by aligning the strands at ±45° angles, the panels showed a 24% increase in shear modulus compared to the 0/90/0 panel. These results show that ±45° orientation in OSB could allow for higher shear properties without requiring changes to the amounts of resin or wood strands.

Another observation from the shear strain contour plots is that the areas of high shear strain shown in blue and purple (0.006 and 0.007 shear strain) were the exact location where the failure line occurred. Optical measurement with DIC techniques and colored contour plots can display the location of the failure area on the panel before the panel has failed. This can be seen in Fig. 10 where the purple color represents a very high shear strain (>0.007 shear strain), and then the failure occurs on that high shear strain line. The shear stain near the panel edges on the top and bottom approach zero during the entire test. The shear strain in the middle of the panel seems to develop uniformly between the loading brackets but is not uniform near the top and bottom of the panel. Shear strain was only measured between the steel brackets and the top and bottom bolts. By limiting the area-of-interest to this boundary, the non-uniform shear strain near the edges of the panel was not used for calculation of shear modulus.

Table 1. Measured shear modulus G and shear strength τ

Panel Type		G, GPa	τ, MPa
0/90/0	Average	1.22	9.16
	Max.	1.56	11.91
	Min.	0.94	6.08
	SD	0.21	1.84
	COV (%)	(16.8)	(20.1)
[0/+45/-45]s	Average	1.52	9.50
	Max.	1.73	11.27
	Min.	1.33	8.20
	SD	0.16	1.11
	COV (%)	(10.3)	(11.7)
Commercial	Average	0.99	6.83
	Max.	1.10	7.41
	Min.	0.87	6.18
	SD	0.06	0.35
	COV (%)	(6.5)	(5.2)

SD = standard deviation
COV = coefficient of variation

Figure 9. Typical in-plane shear failure

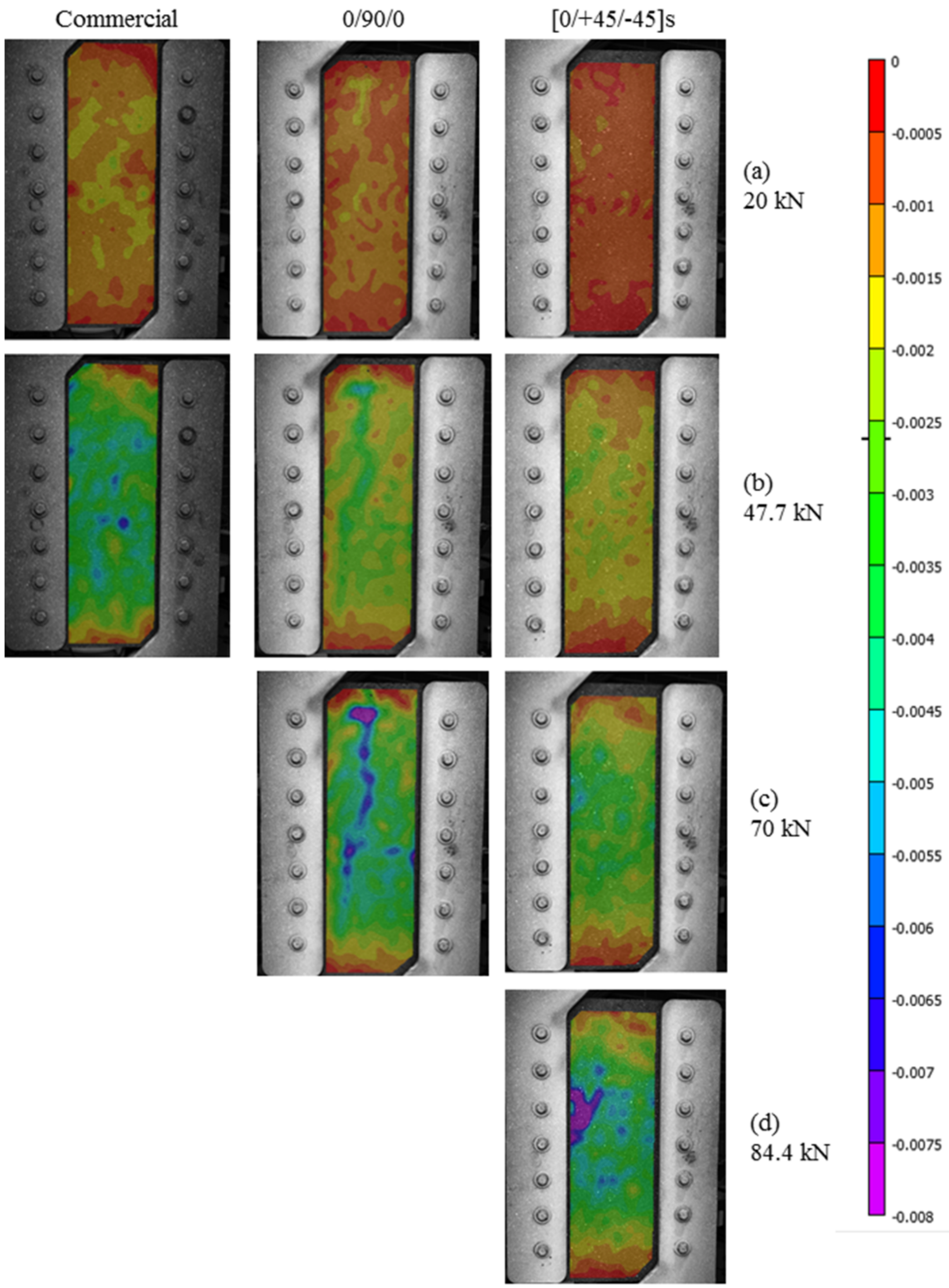

Figure 10. Shear strain at 20kN (a), 47.7 kN (b), 70 kN (c) and 84.4 kN (d)

Bending Test

The [0/+45/-45]s alignment pattern resulted in a lower average bending modulus of elasticity (MOE) in the parallel direction and an increase in average MOE in the perpendicular direction, which is summarized in Table 2. The parallel and perpendicular directions are explained in Fig. 1 with the parallel direction being in line with the surface strands. A two-sample t-test assuming equal variances was performed on the bending results comparing the 0/90/0 alignment with the [0/+45/-45]s alignment. The [0/+45/-45]s parallel MOE reduced by 10% (p value < 0.001) when compared to the 0/90/0 alignment. With a 0/90/0 alignment, 1/3 of the strands are oriented at 0° on the tension surface of a bending specimen while in the [0/+45/-45]s alignment pattern 1/6 of the strands are oriented at 0° on the tension surface. Strands oriented at 0° on the tension surface have a very significant impact on bending properties. This reduction in parallel bending MOE is expected. The [0/+45/-45]s has 1/6 of the total amount of wood strands oriented at 0° on the surface while the 0/90/0 alignment has 1/3. This reduced amount of 0° surface strands corresponds to a reduction in parallel bending MOE as seen in the results. The [0/+45/-45]s alignment pattern could favor a product that needs high shear properties as well as good bending properties. The [0/+45/-45]s perpendicular MOE showed a 8% increase (p value $=$ 0.027) when compared to the 0/90/0 alignment pattern. This result is expected due to the [0/+45/-45]s alignment pattern having more strands oriented toward the perpendicular axis when compared to 0/90/0 alignment. The MOR of the [0/+45/-45]s panels resulted in a 7% reduction in the parallel direction (p value = 0.027) when compared to the 0/90/0 alignment. There was a 5% increase in MOR in the perpendicular direction of the [0/+45/-45]s alignment when compared to the 0/90/0 alignment, however this result was statistically inconclusive due to high variation. Statistically inconclusive results in MOR were due to high horizontal density variability in the specimens. Horizontal density control in the panel manufacturing process was achieved with visual inspection during the strand alignment process. This process seemed to occasionally produce outliers in the data thus causing difficulty in statistical conclusions.

Table 2. Measured MOE and MOR in Parallel and Perpendicular directions with corresponding standard deviations and coefficient of variation

		Parallel to Strong Axis		Perpendicular to Strong Axis	
Panel Type		MOE, GPa	MOR, MPa	MOE, GPa	MOR, MPa
0/90/0	Average	9.53	28.43	2.48	13.23
	Max.	14.13	48.49	3.51	20.88
	Min.	0.40	8.29	0.63	3.90
	SD	1.95	7.28	0.54	3.78
	COV (%)	(20.5)	(25.6)	(21.9)	(27.0)
	n	70	70	60	60
[0/+45/-45]s	Average	8.50	26.35	2.69	13.99
	Max.	10.98	40.10	4.00	20.97
	Min.	5.48	12.04	1.08	6.33
	SD	1.24	6.81	0.66	3.47
	COV (%)	(14.6)	(25.8)	(24.4)	(24.8)
	n	70	70	60	60
Commercial	Average	9.82	27.49	2.09	9.14
	Max.	13.49	48.41	2.90	13.99
	Min.	5.22	14.44	1.47	5.29
	SD	1.39	6.00	0.30	1.79
	COV (%)	(14.1)	(21.8)	(14.5)	(19.6)
	n	70	70	60	60

SD = standard deviation

COV = coefficient of variation

Nail Connection Test

The nail connection tests resulted in no significant difference between the [0/+45/-45]s and 0/90/0 alignment patterns. This result shows that by increasing the shear properties of the panel with ±45° alignment results in no loss in nail connection strength. These results show that an OSB panel with ±45° alignment could continue to be used in products where nail connection mechanical properties are important. There was a noticeable difference between the laboratory manufactured panels ([0/+45/-45]s and 0/90/0) and the commercial panels. This difference was attributed to the difference in density between the laboratory manufactured panels and the commercial panels. The average density of the parallel specimens was $0.753 g/cm^3$, $0.747 g/cm^3$, $0.582 g/cm^3$ for the 0/90/0, [0/+45/-45]s, and commercial panels, respectively. The perpendicular nail connection test specimens for the 0/90/0, [0/+45/-45]s, and commercial panels were, $0.765 g/cm^3$, $0.767 g/cm^3$, and $0.579 g/cm^3$, respectively. The results of the nail connection tests are based mainly on the strength of the nail in bending, the strength of the bottom plate, and nail head sheathing embedment, and less on the in-plane shear properties of the OSB. The results of the nail connection test can be seen in Fig. 11. The error bars represent one standard deviation in each direction. The results also show no difference in average yield point between the parallel and perpendicular loading directions.

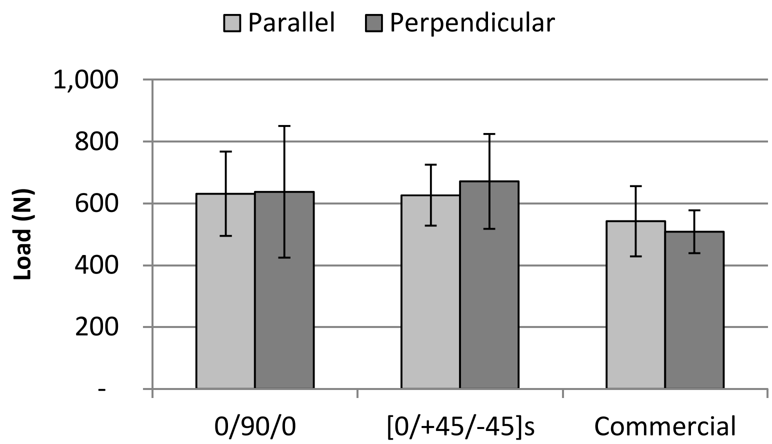

Figure 11. Yield load of nail connection tests in parallel and perpendicular loading direction.

Small-Scale Shear Wall Test

The small-scale shear wall test showed no noticeable difference between the 0/90/0 and [0/+45/+45]s alignment patterns. The variation with one alignment pattern was high and no statistical difference in small-scale shear wall stiffness or strength could be found. This result occurred due to a majority of the wall deflection attributed to the perpendicular nail loading on the bottom plates, which ultimately led to bottom plate failure near the tension corner of the wall as seen in Fig. 12. However, the behavior of the laboratory manufactured panels did behave differently from the commercial panels. There was a slight increase in slope and peak of the load vs. deflection curves between the laboratory panels and the commercial panels as seen in Fig. 13. This result matches the result from the nail connection tests where a difference in density produced different results and the test was insensitive to changes of shear properties.

This result was attributed mostly to the nail bending properties, bottom plate crushing and tension perpendicular to grain and panel density and less on the panel shear modulus. In addition, the shear strain using DIC contour plots were also analyzed but were inconclusive.

(a) 

(b) 

Figure 12. Typical failure of bottom plate in small-scale shear wall test with views (a) end view (b).

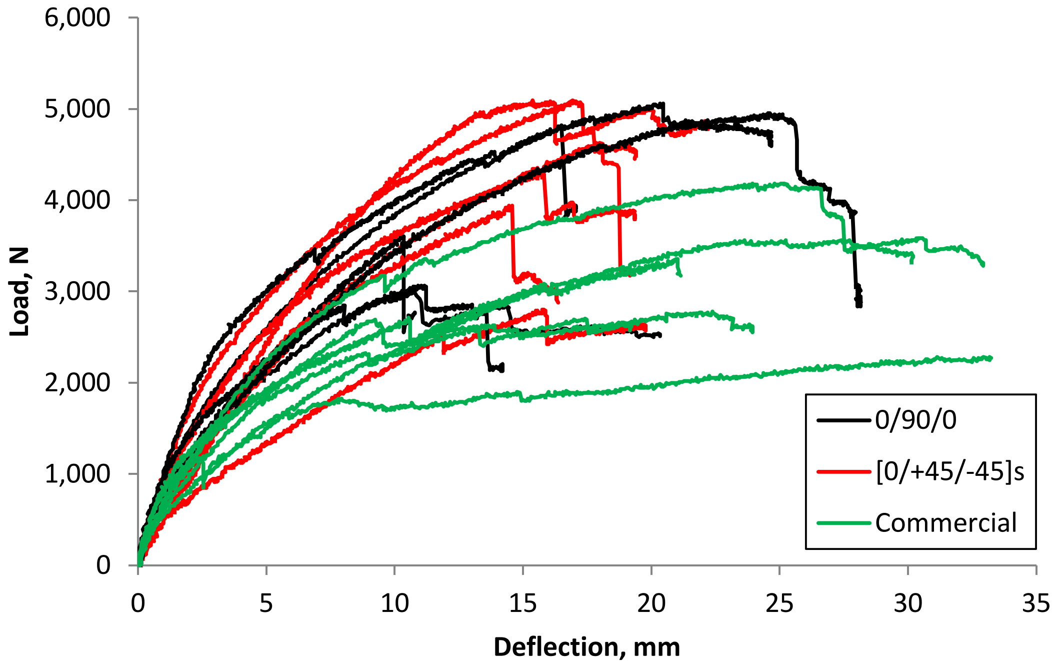

Figure 13. Load vs. deflection curve for small-scale shear wall test

Conclusions

In-plane shear modulus and strength are important mechanical properties of OSB when used as a structural engineered wood product. This research investigated the effect of a 0°/+45°/-45°/-45°/+45°/0° alignment patterns of OSB strands on in-plane shear, bending, nail connection, and small-scale shear wall properties. The [0/+45/-45]s alignment pattern showed an increase of in-plane shear modulus and strength with a reduction in parallel bending MOE and MOR along with an increase in perpendicular bending MOE and MOR. The nail connection and small-scale shear wall tests were insensitive to changes of the strand alignment and showed no difference in strength or stiffness. These results show that strand alignment patterns can be modified to fit the needs of the specific product, or a specific alignment pattern can be designed to improve specific desired mechanical properties while perhaps degrading other less important mechanical properties not needed for the target engineered product. ±45° strand alignment can improve in-plane shear properties of OSB. From the wall test results, the current 0/90/0 alignment performs sufficiently in the small shear wall tests used in this study due to the wall deflection being primarily attributed to the behavior of the connection, however, advanced layup patterns can open more possibilities for OSB to be utilized in non-sheathing products that experience high shear stresses.

Recommendations

With [0/+45/-45]s alignment patterns showing an increase in shear modulus with no change in panel density, further research on applying [0/+45/-45]s alignment to high-shear products is recommended. As concluded in Grandmont *et al*. (2010), the deflection of a shear-controlled I-joist is impacted significantly by the in-plane shear stiffness of the web material. Further research should include using OSB with ±45° alignment patterns as web stock of I-joists and researching changes in its mechanical properties. Furthermore, research on various size holes in the webs of I-joists with ±45° alignment patterns is recommended due to high shear stress concentrations at the holes as explained in Polocoser *et al*. (2013). Another area of interest would be to manufacture ±45° alignment I-joist web stock with less wood strands than typical 0/90/0 web stock and see if one can achieve the same minimum deflection standards for the I-joist. Full size shear walls are also recommended to be researched with various strand alignment patterns to see if changes to in-plane shear properties can be beneficial. Finally, as OSB becomes used for more specific products, designing specific strand alignment patterns for these various products will be of interest.

References

Association American Forest and Paper, AFPA. (2012). “National design specification for wood construction.” Washington, D.C.

ASTM Standard. (2006). “D1761. Standard Test Methods for Mechanical Fasteners in Wood.” West Conshohocken, PA: ASTM International.

ASTM Standard. (2007). “D2719.Standard Test Methods for Structural Panels in Shear Through-the-Thickness*.”* West Conshohocken, PA: ASTM International.

ASTM Standard. (2011). “D3043. Standard Test Methods for Structural Panels in Flexure.” West Conshohocken, PA: ASTM International.

ASTM Standard. (2012). “E564. Standard Practice for Static Load Test for Shear Resistance of Framed Walls for Buildings.” West Conshohocken, PA: ASTM International.

Barbuta, C., Cloutier, A., Blanchet, P., Yadama, V., and Lowell, E. (2011). “Tailor made OSB for special application.” *European Journal of Wood and Wood Products, 69*(4), 511-519.

Chen, S., Fang, L., Liu, X., and Wellwood, R. (2008). “Effect of mat structure on modulus of elasticity of oriented strandboard.” *Wood Science and Technology, 42*(3), 197-210.

Grandmont, J. F., Cloutier, A., Gendron, G., and and Desjardins, R. (2010). “Wood I-Joist Model Sensitivity to Oriented Strandboard Web Mechanical Properties.” *Wood and Fiber Science, 42*(3), 352-361.

McCutcheon, W. J. (1985). “Racking deformations in wood shear walls.” *Journal of Structural Engineering, 111*(2), 257-269.

McNatt, J. D., Bach, L., and Wellwood, R. W. (1992). “Contribution of strand alignment to performance of strandboard.” *Forest Product Journal, 42*(3), 45-50.

Moses, D. M., Prion, H. G., Li, H., and Boehner, W. (2003). “Composite behavior of laminated strand lumber.” *Wood science and Technology, 37*(1), 59-77.

Nairn, J. (2008). OSU Laminates 5.0 Software., Oregon State University, Corvallis, OR

Polocoser, T., Miller, T. H., and Gupta, R. (2013). "Evaluation of remediation techniques for circular holes in the webs of wood I-joists." *Journal of Materials in Civil Engineering*. DOI:10.1061/(ASCE)MT.1943-5533.0000737 (Nov. 20, 2012)

Shrestha, D. (1999). "Shear properties tests of oriented strandboard panels." *Forest Products Journal, 49*(10), 41-46.

Sinha, A., and Gupta, R. (2009). "Strain distribution in OSB and GWB in wood-frame shear walls." *Journal of Structural Engineering, 135*(6), 666-675.

Stürzenbecher, R., Hofstetter, K., Bogensperger, T., Schickhofer, G., and Eberhardsteiner, J. (2010). "Development of high-performance strand boards: engineering design and experimental investigations." *Wood Science and Technology, 44*(1), 13-29.

Weight, S. W., & Yadama, V. (2008). "Manufacture of laminated strand veneer (LSV) composite. Part 1: Optimization and characterization of thin strand veneers." *Holzforschung*, 62(6), 718-724.

CONCLUSIONS

In-plane shear modulus and strength are important mechanical properties of OSB when used as a structural engineered wood product. This research investigated the effect of a 0°/+45°/-45°/-45°/+45°/0° alignment patterns of OSB strands on in-plane shear, bending, nail connection, and small-scale shear wall properties. The [0/+45/-45]s alignment pattern showed an increase of in-plane shear modulus and strength with a reduction in parallel bending MOE and MOR along with an increase in perpendicular bending MOE and MOR. The nail connection and small-scale shear wall tests were insensitive to changes in the strand alignment and showed no difference in strength or stiffness. These results show that strand alignment patterns can be modified to fit the need of the specific product or a specific alignment pattern can be designed to improve specific desired mechanical property while perhaps degrading less important mechanical properties not needed for the target engineered product. ±45° strand alignment can improve in-plane shear properties of OSB. From the wall test results, the current 0/90/0 alignment seems sufficient m in the small shear wall tests used in this study due to wall deflection being primarily attributed to the behavior of the connection, however, advanced layup patterns can open more possibilities for OSB to be utilized in non-sheathing products that experience high shear stresses.

RECOMMENDATIONS

With a [0/+45/-45]s alignment pattern showing an increase in shear modulus with no change in panel density, further research of applying [0/+45/-45]s alignment to high-shear products is recommeded. As concluded in Grandmont *et al*. (2010), the deflection of a shear controlled I-joist is impacted significantly by the in-plane shear stiffness of the web material. Further research should include using OSB with ±45° alignment patterns as web stock of I-joists and researching changes to mechanical properties. Furthermore, research on various size holes in webs of I-joists with ±45° alignment patterns is recommended due to high shear stress concentrations at holes in as explained in Polocoser *et al*. (2013). Another area of interest would be to manufacture ±45° alignment I-joist web stock with less wood strands than the typical 0/90/0 web stock and achieve the same minimum deflection standards of the I-joist. Full size shear walls are also recommended to be researched with various strand alignment patterns to see if changes to in-plane shear properties can be observed on a full size scale. Finally, as OSB becomes used for more specific products, designing strand alignment patterns for these products would be of interest.

BIBLIOGRAPHY

Association American Forest and Paper, AFPA. (2001). “National design specification for wood construction.” Washington, D.C.

ASTM Standard. (2006). “D1761. Standard Test Methods for Mechanical Fasteners in Wood.” West Conshohocken, PA: ASTM International.

ASTM Standard. (2007). “D2719.Standard Test Methods for Structural Panels in Shear Through-the-Thickness.” West Conshohocken, PA: ASTM International.

ASTM Standard. (2011a). “D3043. Standard Test Methods for Structural Panels in Flexure.” West Conshohocken, PA: ASTM International.

ASTM Standard. (2011b). “D3044. Standard Test Methods for Shear Modulus of Wood-based Structural Panels.” West Conshohocken, PA: ASTM International.

ASTM Standard. (2012). “E564. Standard Practice for Static Load Test for Shear Resistance of Framed Walls for Buildings.” West Conshohocken, PA: ASTM International.

Barbuta, C., Cloutier, A., Blanchet, P., Yadama, V., and Lowell, E. (2011). “Tailor made OSB for special application.” *European Journal of Wood and Wood Products, 69*(4), 511-519.

Chen, S., Fang, L., Liu, X., and Wellwood, R. (2008). “Effect of mat structure on modulus of elasticity of oriented strandboard.” *Wood Science and Technology, 42*(3), 197-210.

Durham, J., Lam, F., & Prion, H. G. (2001). “Seismic resistance of wood shear walls with large OSB panels. *Journal of Structural Engineering*, 127(12), 1460-1466.

Geimer, R. L. (1982). “Dimensional stability of strandboards as affected by board specific gravity and strand alignment.” *Forest Prod. J*, 32(8), 44-52.

Grandmont, J. F., Cloutier, A., Gendron, G., and and Desjardins, R. (2010). “Wood I-Joist Model Sensitivity to Oriented Strandboard Web Mechanical Properties.” *Wood and Fiber Science, 42*(3), 352-361.

Khashaba, U. A. (2004). “In-plane shear properties of cross-ply composite laminates with different off-axis angles.” *Composite structures*, *65*(2), 167-177.

Meyers, K. L. (2001). “Impact of strand geometry and orientation on mechanical properties of strand composites.” (Doctoral dissertation, Washington State University, Pullman, WA).

McCutcheon, W. J. (1985). “Racking deformations in wood shear walls.” *Journal of Structural Engineering, 111*(2), 257-269.

McNatt, J. D., Bach, L., and Wellwood, R. W. (1992). “Contribution of strand alignment to performance of strandboard.” *Forest Product Journal, 42*(3), 45-50.

Moses, D. M., Prion, H. G., Li, H., and Boehner, W. (2003). “Composite behavior of laminated strand lumber.” *Wood science and Technology, 37*(1), 59-77.

Nairn, J. (2008). OSU Laminates 5.0 Software, Oregon State University, Corvallis, OR.

Polocoser, T., Miller, T. H., and Gupta, R. (2013). “Evaluation of remediation techniques for circular holes in the webs of wood I-joists.” *Journal of Materials in Civil Engineering*.

Saliklis, E. P., & Falk, R. H. (2000). “Correlating off-axis tension tests to shear modulus of wood-based panels.” *Journal of Structural Engineering*, 126(5), 621-625.

Shrestha, D. (1999). “Shear properties tests of oriented strandboard panels.” *Forest Products Journal, 49*(10), 41-46.

Sinha, A., and Gupta, R. (2009). “Strain distribution in OSB and GWB in wood-frame shear walls.” *Journal of Structural Engineering, 135*(6), 666-675.

Sinha, A., Gupta, R., and Nairn, J. A. (2011). “Thermal degradation of bending properties of structural wood and wood-based composites.” *Holzforschung, 65*(2), 221-229.

Sumardi, I., Ono, K., & Suzuki, S. (2007). “Effect of board density and layer structure on the mechanical properties of bamboo oriented strandboard.” *Journal of wood science*, 53(6), 510-515.

Suzuki, S., & Takeda, K. (2000). “Production and properties of Japanese oriented strand board I: effect of strand length and orientation on strength properties of sugi oriented strand board.” *Journal of wood science*, 46(4), 289-295.

Stürzenbecher, R., Hofstetter, K., Bogensperger, T., Schickhofer, G., and Eberhardsteiner, J. (2010). “Development of high-performance strand boards: engineering design and experimental investigations.” *Wood Science and Technology, 44*(1), 13-29.

Weight, S. W., & Yadama, V. (2008a). “Manufacture of laminated strand veneer (LSV) composite. Part 1: Optimization and characterization of thin strand veneers.” *Holzforschung*, 62(6), 718-724.

Weight, S. W., & Yadama, V. (2008b). “Manufacture of laminated strand veneer (LSV) composite. Part 2: Elastic and strength properties of laminate of thin strand veneers.” *Holzforschung*, 62(6), 725-730.

Zhou, G., Green, E. R., & Morrison, C. (1995). “In-plane and interlaminar shear properties of carbon/epoxy laminates.” *Composites science and technology*, *55*(2), 187-193.

APPENDICES

APPENDIX A

Detailed Literature Review

Oriented strand board (OSB) is used in many applications including structural sheathing, flooring, I-joist web material, structural insulated panels, upholstered furniture, and various material handling products. OSB is typically made from low-density trees such as aspen (*Populus tremuloides*) (Barbuta *et al*., 2011). By using low-density wood species, high value products can be made from a relatively low value wood species. As OSB is used in an increasing number of products, refinement and adjustment of OSB mechanical properties is important. By applying composite laminate mechanical theories to OSB manufacturing, specific desired properties can be refined to meet the needs of the end product.

In-plane shear properties are important characteristics of products such as I-joist web stock and structural building sheathing (McCutcheon, 1985, Shrestha, 1999, and Grandmont *et al*., 2010). Typically, researchers have modeled the mechanical behavior of OSB using Classical Laminate Plate Theory (CLPT) (Moses *et al*., 2003 and Weight and Yadama, 2008). CLPT involves mathematical modeling of each individual layer of a composite laminate with individual mechanical properties in the x, y, and z directions. Thus, CLPT can predict the change in mechanical properties of the entire laminate using any alignment orientation of each individual laminate layer.

Due to wood being an orthotropic material, the orientation of the strands within OSB has a significant impact on the mechanical properties in the x and y directions (McNatt *et al*. 1992). The study by McNatt *et al*. (1992) on the contribution of strand alignment to performance of strand board investigates the effect of alignment of strands on bending strength, internal bond strength, and linear expansion of oriented strand board. 72 panels were manufactured using six unique strand orientation patterns while keeping the same furnish, resin type, and resin content. The orientations of face strands and core strands were varied. The strand patterns included the following: strands randomly distributed, face strands aligned parallel to panel length with core strands random, face strands aligned parallel to panel length with core strands cross aligned, face strands aligned parallel to the panel width with core strands cross aligned, as well as two other alignment patterns. Static bending tests were conducted on the panel specimens and the resulting modulus of elasticity and modulus of rupture were recorded. A mathematical relation was used between modulus of elasticity and percentage of strand alignment developed from research by Geimer (1982), and the prediction of alignment was 35 to 50 percent aligned. The results concluded that alignment of face strands improved bending strength and stiffness in the direction of alignment, but caused a reduction in bending strength and stiffness in the direction perpendicular to the alignment.

Research by McNatt *et al.* (1992) on the contribution of strand alignment on board performance and the research herein on strand alignment in OSB are well correlated. McNatt *et al.* (1992) provided an understanding of the relationship between bending strength and strand alignment layers within OSB. However, a very important property of sheathing is in-plane shear characteristics. McNatt *et al.* (1992) does not investigate the effect of strand alignment on shear properties of OSB. The alignment of the face strands is very important for strand board used in bending applications, but the orientation of the core strands has an important influence on shear strength.

McNatt *et al*. (1992) used the same general scientific approach that was used in the research herein. The manufacturing processes used in the research herein attempted to keep all the manufacturing variables: resin type, resin content, density, and press schedule, similar between panels while changing the alignment of strands in the panel. McNatt *et al*. (1992) also used this same method to investigate the effect of alignment on mechanical properties of OSB. There are many manufacturing factors that affect the mechanical properties of OSB, therefore, limiting the change in variables to solely strand alignment assisted in making conclusions in the project herein.

Barbuta *et al*. (2011) developed an oriented strand board that has high modulus of elasticity in bending by studying the effects of wood species, resin content, density profiles, and weight ratios of the face and core layers for an end use application of engineering wood flooring. Barbuta *et al*. (2011) concluded that a weight ratio 0.45/0.10/0.45 for face/core/face showed a positive impact on bending MOE, as well as, a steep density profile created by a short press closing time.

Barbuta *et al.* (2011) made a significant conclusion that there is a potential to engineer the individual layer properties of OSB to produce a product with characteristics for special end use applications. One goal of the research herein was to adjust alignment properties to produce a panel that has increased in-plane shear modulus for use as a wall sheathing material. Barbuta *et al.* (2011) supports the research of specific end use oriented strand board design.

The manufacturing of the panels in Barbuta *et al*. (2011) showed similar methods to the research herein. Barbuta *et al*. (2011) achieved perpendicular strand orientation by dropping the strands through a mesh with adjustable parallel vanes. This method is similar to the method used in this research.

One property that was studied in Barbuta *et al*. (2011) was the weight ratio of strands in the face and core of the OSB panel. The results show that a weight ratio of 0.45/0.10/0.45 showed the largest positive effect on bending MOE. This supports the researched strand alignment of [0/+45/-45]s which produces a weight ratio of 0.167/0.167/0.167/0.167/0.167/0.167 and would have an effect on bending properties when compared to the 0/90/0 alignment. Barbuta *et al*. (2011) concludes that the weight ratio in the face/core/face of the OSB panel has a significant impact on mechanical properties and should be considered in design of lay-up patterns.

Meyers (2001) investigates the effect of strand geometry on mechanical properties of strand composites as well as investigating the effect of increasing percentage of strand orientation in oriented stand panels. Meyers (2001) manufactured wood strands with different length to width ratios and produced single-layer oriented strand mats. Then, tension and compression properties where evaluated. Meyers (2001) investigated the effect of increasing the percentage of aligned strands on mechanical properties which produced the expected result that increasing the percent of alignment produced an increase in parallel properties and a decrease in perpendicular properties. The average angle of the stands was measured using digital image analysis. Meyers (2001) concluded that the strand geometry did not significantly affect the mechanical properties but the strand geometry did significantly affect the ability to align strands.

Meyers (2001) used the same panel strand alignment process as used in the research herein. Meyers (2001) formed mats by dispersing strands on to an oscillating forming box with vanes spaced at 38 mm. However, this manufacturing process did produce a source of error in that there seemed to be low density regions in the horizontal profile of the panel due to the vanes blocking strands from falling on to the panel. The horizontal density of the panels was not uniform thus creating “columns” of low and high density material throughout the horizontal profile. If the panels do not have the same horizontal density then comparing mechanical property data could not be an accurate method for determining influence of strand orientation.

The use of wood strand composite panels has been increasing significantly over the last decade. Research on wood strand composite panels used as sheathing is abundantly available, however most researchers study wood strand composite panels that are 13 mm thick or greater. There is little research performed on wood strand composite panels that are less than 13 mm thick. Weight and Yadama (2008a) investigated the influence of strand geometry, resin level, and pressing temperature on mechanical and physical properties of thin strand veneers, with thin strand veneers being 3.2 mm thick. In addition to the above objective, the research included ranking these variables according to their effects on thin strand veneers in order to optimize the manufacturing procedure. The research identified the optimum combination of strand geometry, resin level, and pressing temperature and the associated bending and tensile strength values.

The beginning of Weight and Yadama (2008a) lists the previous research performed on oriented strand board with a thickness of 13 mm and greater. This comprehensive list of research allows one to use the results on manufacturing variables and determine their effect on mechanical properties. Weight and Yadama (2008a) focused on optimal configuration of strand geometry, resin level, and pressing temperature. To make the laminated strand veneer panel specimen for this project, the optimum value for resin level and pressure temperature were needed.

One aspect of interest is the process the authors used to calculate percent alignment of the stands in the veneer. The authors took photos of 10 thin strand veneers and analyzed 10 strands on the surface of the veneer to characterize the strand orientation. The manufacturing process used in Weight and Yadama (2008a) resulted in 78% alignment of strands. Weight and Yadama focused on the angle of the aligned strands and whether it has a significant impact on mechanical properties of the veneer. The efforts of Weight and Yadama allow us to see the level of alignment that can be reached with a manufacturing process that is similar to the process used herein.

Part 2 of the laminated strand veneer (LSV) study by Weight and Yadama (2008b), investigates the strength and elastic properties of oriented strand veneers that are laminated to create a 6-ply panel. The orientation of the inner plies was varied and the results compared. Weight and Yadama (2008b) used the optimized thin strand veneers from Weight and Yadama (2008a) to make a 6-ply panel and investigated the strength of the 6-ply strand veneer panels then comparable to commercially sold OSB and plywood panels. The research also includes a comparison between the manufactured LSV panels with a classical lamination theory model. The goal of the comparison was to show that the CLT model could be used to calculate and predict mechanical properties of LSV panels. Weight and Yadama (2008b) researched 6-ply laminated strand veneer panels with the inner panels oriented at a ±45°.

The second half of the Weight and Yadama (2008b) study compares the CLT model to the measured mechanical properties. The authors state that a CLT model produced a very accurate prediction of the panel’s strength properties. This affirms the use of a CLT model to predict strand orientations that produce improved shear characteristics.

Moses *et al*. (2003) studied ±45° alignment of laminated strand lumber (LSL) panels. Smaller test specimens were cut from the manufactured panels and tested for their tension and compression properties and compared to a mathematical model but no large panel in-plane shear testing was performed. The model showed that ±45° alignment could produce an increase in shear modulus compared to 0°/90°/0°

alignment for LSL panels. Moses *et al*. (2003) concluded that the influence of strand alignment on the in-plane properties of the panels could be predicted using the composite laminate model presented. Moses *et al*. (2003) studied the behavior of laminated strand lumber (LSL) to determine the panel properties based on panel lay-up patterns. They developed a predictive model to determine properties of (LSL) panels. They manufactured 760 mm x 760 mm x 38 mm LSL panels with 5 different strand orientation lay-up patterns. The strand patterns include: fully oriented; randomly oriented; surfaces oriented, core randomly oriented; surfaces randomly oriented, core fully oriented; and eight fully oriented layers aligned at angles 0° and ±45°. Smaller test specimens were cut from the manufactured panels and tested for their mechanical properties and compared to a mathematical model. The model can be used by manufacturers of LSL products to provide improved manufactured LSL products.

Moses *et al*. (2003) investigated the tension, compression, and shear behavior of LSL panels. LSL panels differ from oriented strand board (OSB) in that LSL uses longer wood strands at a length of 230 mm. The orientation of the LSL strands was obtained by hand laying strands to form the panels. Typical LSL wood composites are used for beams and columns, however, Moses *et al*. (2003) investigates the properties of specimens cut from a panel. Strand orientation layup pattern research efforts for OSB would be similar to this research which was performed for LSL. The layup pattern with the core strands at ±45° produced an increased shear modulus. While

Moses *et al*. (2003) investigaed ±45° alignment in LSL, they leave a research opportunity in strand alignment patterns with shorter wood strands typically used in OSB. The introduction of Moses *et al*. (2003) states that by changing strand orientation, stiffness and strength properties can be modified for the specific loading application. This same logic was applied to OSB in the research herein. If certain mechanical properties are desired, strand orientation can be altered to reach those desired properties.

A mathematical model was presented by Chen *et al*. (2008) for bending stiffness of OSB based on strand alignment. Very little research has been conducted on the effect of strand orientation not in the parallel and perpendicular directions due to the difficulty in achieving the target strand orientation (Chen *et al*., 2008). Chen *et al*. (2008) produced a mathematical model for the bending stiffness of OSB. Post validation of the model was conducted and then the model was used to produce bending stiffness results for typical OSB panels. The model focused on changing the vertical mat structure by changing strand orientation. OSB panels were manufactured using typical 0/90/0 strand alignment; however, Chen *et al*. (2008) cut out strips of panels at varying angles. This produced panels with varying outer and inner strand orientation layers. The specimens were tested for bending and the data were used to produce a model. The model seemed to predict the panel bending stiffness with reasonable accuracy.

In the introduction of Chen *et al*. (2008), the authors states that very little research has been done on the effect of strand orientation not in the parallel and perpendicular directions due to the difficulty in achieving the target strand orientation. This statement validates the need for research on off-axis OSB strand orientation covered herein.

The goal of the model (Chen *et al*. 2008) was to produce the bending stiffness of OSB panels with respect to different mat alignment structure. The bending stiffness is significantly affected by the face layer and not significantly affected by the core layers due to basic beam theory. The orientation of both core and face layers significantly affect the in-plane shear properties of the panel.

Sturzenbecher *et al*. (2010) introduced the need for more applied design of laminate alignment, wood quality, and compaction of OSB for specific applications. The authors performed out-of-plane shear tests on the panels but did not perform in-plane shear tests. No off-axis strand orientation was investigated; only parallel, perpendicular, and random alignment were investigated.

Shrestha (1999) investigated the in-plane shear (shear through-the-thickness) properties of commercially manufactured oriented strand board using ASTM 2719 – Standard Test Methods for Structural Panels in Shear Through-the-Thickness. Shrestha (1999) identified the difficulties inherent with ASTM 2719 and provided modifications to the test standard that produced reasonable results. The modifications include using L-shaped steel plates in place of wooden rails found in test method C in

ASTM 2719 due to the high shear capacity of oriented strand board. Shrestha (1999) produces shear through-the-thickness moduli with a 10 percent COV.

Shrestha (1999) provided insight on the difficulties involved with shear through-the-thickness tests of OSB. Shrestha (1999) stated that the modified shear test is simple, easy to implement, and relatively inexpensive compared to the lumber rails recommended in ASTM 2719. ASTM 2719 is extremely difficult, expensive, and time consuming according to Shrestha (1999). A similar test fixture has been successfully used at the Alberta Research Council in Canada (Shrestha 1999). Another interesting conclusion made by Shrestha (1999) is that the shear through-the-thickness properties are essentially equivalent for OSB panels in both orientations (G_{xy} and G_{yx}). This conclusion allows future research to only need to test shear through the thickness in one direction, which lowers the amount of specimens needed.

Grandmont *et al*. (2010) investigated the relationship between tension MOE and in-plane shear stiffness of oriented strand board used for webs of I-joists. Tension tests according to ASTM D1037-06a and in-plane shear tests according to ASTM D2719-89-C were performed on OSB web stock material to determine the relationship between density and tension MOE and in-plane shear stiffness. In addition to physically testing in-plane shear stiffness according to ASTM D2719-89-C, a numerical model was used to relate off- axis tension MOE to in-plane shear stiffness. The results show a strong relationship between density and the above mechanical properties. Grandmont *et al*. (2010) confirms the need to improve in-plane shear stiffness of OSB used in engineered products such as webs of I-joists.

Grandmont *et al*. (2010) states that special care was taken to obtain reliable data from large-scale tests to determine G_{xy}, in-plane shear modulus, of the panel. G_{xy} is known to be the most important mechanical property of OSB web material (Grandmont *et al*. 2010).

Grandmont *et al*. (2010) obtained in-plane shear modulus using ASTM 2719-89-C, which is the same test method used in the research herein. The results show that G_{xy} and G_{yx} were very similar due to ASTM 2719-89-C using a large panel producing a near pure shear stress state. The research also obtained in-plane shear modulus using off- axis tension tests and a relationship equation between tension and in-plane shear tests. The coefficient of variation for the G_{xy} obtained from the tension tests was 20 to 40 percent while the coefficient of variation of the ASTM 2719-89-C large specimen test was 4 to 8 percent. This shows that ASTM 2719-89-C produces more consistent results compared to equations relating tension MOE to in-plane shear modulus.

Saliklis and Falk (2000) proposed a new relationship between off-axis tension modulus of elasticity and the in-plane shear modulus of rigidity of wood based orthotropic panels. The proposed relationship is supported by experimental testing of both off-axis tension using ASTM D3500 and in-plane shear testing using the plate twisting test from ASTM D3044. Current empirical models relating off-axis tension modulus of elasticity to the in-plane shear modulus require the knowledge of

Poisson's ratio through experimental testing. The new relationship eliminates the need for Poisson's ratio for the panel by calibrating the E_x/E_y ratio with experimental data. In the case tested, the new relationship provides a better fit to the data than traditional orthotropic elasticity equations.

This research supports the significance of improving in-plane shear modulus of wood composite panels for rigorous design of wood building components such as trusses with gusset plates, box beams, folded plate roofs, roof or floor diaphragms, shear walls, and engineered wood products such as webs of I-joists. The proposed model allows for understanding of in-plane shear modulus without the need from in-plane shear testing which is difficult to perform. The proposed relationship is based on orthotropic composite laminate mechanics, however the research applies the relationship to particle board and oriented strand board. The authors stated that wood composite panel products are traditionally modeled as orthotropic solids. Particle board and oriented strand board are not completely orthotropic solids; however, this new relationship has modified the original orthotropic solid relationship to fit well with particle board and oriented strand board.

Durham *et al*. (2001) presents the results of seismic tests performed on OSB shear walls using static, cyclic, and dynamic loading protocols. Both large (2.4 m x 2.4 m) panels and standard (1.2 m x 2.4 m) panels were used. The results are in line with other standard OSB shear wall research. The results of the large panel testing showed an increase of 26% in shear capacity. All panels reached a drift of approximately 2.5%.

Durham *et al*. (2001) presents results from tests of OSB shear walls, which have been extensively researched in the past, except for the addition of large panel tests in this effort. Therefore, Durham *et al*. (2001) clearly explains the significance of further research in seismic resistance of light- frame wood structures. The authors state that in the 1994 Northridge earthquake, there was extensive financial loss due to damage to wood frame structures. This encouraged the need for further research in preventing damage to wood frame structures from seismic forces by lowering maximum drift, in addition to designing for life safety. Maximum drift of an OSB sheathed shear wall is controlled in part by the in-plane shear stiffness of the OSB panel. Improving the in-plane shear stiffness of the OSB panel could reduce the maximum drift of the shear wall. Lowering the maximum drift will lower the overall damage to the structure, which will reduce the financial loss from earthquake damage.

In McCutcheon (1985), an analytical model to predict wood shear wall racking performance is presented. The model is then compared to experimental results from various other research projects. The model includes linear deformation due to shear distortion of the sheathing material. The model can be used to calculate the nonlinear racking deformations of wood shear walls by using test results from simple small-scale racking tests.

McCutcheon (1985) concludes that at low racking loads nearly 30% of the deformation of the wood wall is due to shear distortion of the sheathing material. For higher loads, the load-slip behavior of the fasteners is the significant factor in wall racking deformations. This supports the significance of improving the in-plane shear stiffness of wood sheathing.

Sumardi *et al*. (2007) studied the effect of board density and strand layup pattern on OSB using bamboo strands. Five different panel densities were manufactured along with three different strand layup patterns. The layup patterns included a randomly oriented homogenous board, a unidirectional oriented homogenous board, and three-layer board with cross-oriented core layer and inline oriented face layers similar to the typical OSB alignment of 0/90/0. The oriented strand panels were manufactured using an aligning screen with thin vanes spaced at 20-mm. The percent of aligned strands was confirmed using digital image analysis. The results of the variation on layup patterns revealed that the three-layer structure provided higher MOR in the parallel direction than the randomly oriented layup pattern with less strength reduction in the perpendicular direction than that of the unidirectional strand layup pattern. The MOR increased with an increase of density.

Sumardi *et al*. (2007) investigates the two OSB variables that have been well understood for typical southern pine and Douglas Fir OSB, board density and aligning the core strand layer perpendicular to the face strands. The research produced expected results for the different panels in that when the MOR in the direction of the orientation of the strands increased while in the perpendicular direction the MOR decreased. The panel with 0/90/0 alignment had less strength loss from the parallel direction to the perpendicular direction when compared to the unidirectional aligned panel. This was due to the unidirectional panel being very strong in only one direction. This shows that if the orientation of the strands is adjusted, the desired mechanical properties can be achieved. This research only investigates MOR from a bending test. No shear tests were done on the panels. Some further steps in this research would be to investigate other strand orientation patterns and in-plane shear properties of test panels.

Suzuki and Takeda (1999) focused on the bending behavior of OSB using sugi (*Cryptomeria japonica*) wood strands manufactured in four different strand orientation layup patterns. The investigated layup patterns include an orientation that is homogeneous unidirectional, a cross-oriented three-layer pattern, an oriented three-layer pattern with random core layer, and completely random orientation. The strands were passed through a strand aligner which consisted of thin plates spaced at 20 mm parallel to each other with a free fall distance of 20 mm. The angle of alignment was measured using digital image analysis. The free fall distance of the strands was varied and the results show that the distribution curve of strand alignment became broader with increasing free fall distance. The bending strength result followed the typical expected result in that the boards expressed decreases in bending strength perpendicular to the strand direction. The cross-oriented three-layer board performed better in bending in the perpendicular direction compared to the three-layered board with a randomly oriented core layer.

Suzuki and Takeda (1999) presented a very standard process of evaluating the bending properties for a new wood species used in OSB. The authors control the variables of resin content and board density while varying other variables, such as free fall distance, strand length, and layup patterns. The results showed that with orientating the core layer of strands perpendicular to the length of the panel, bending strength in the perpendicular direction increased over the unidirectional alignment. However, no shear tests were performed on the specimens.

Zhou (1995) investigated the in-plane shear modulus and strength of carbon/epoxy 32-layer laminates with $[0_4/90_4]_2$s and $[\pm45/90/0]_4$s alignment patterns. The subscripts "2" and "4" refer to the number of layers with that specified angle of alignment. The "s" refers to that pattern being symmetric about the neutral axis. Zhou (1995) used the Iosipescu shear test. The Iosipecu shear test is a well-established in-plane and out-of-plane shear test method for composite laminate materials requiring small samples. The results from Zhou (1995) showed that the alignment with ±45° lamina alignment had an in-plane shear modulus of 17.9 GPa while the [0/90]s alignment had a shear modulus of 4.7 GPa. The ±45° lamina alignment produced a significant increase of in-plane shear modulus.

The conclusion of ±45° alignment improving in-plane shear properties is also made in Khashaba (2004). Khashaba (2004) manufactured glass fiber reinforced epoxy composite laminates with $[0/90]_2$s. These panels were cut into test specimens at different off-axis angles being 0°, 15°, 30°, 60°, 75°, and 90°. Khashaba (2004) performed tension tests on the off-axis specimens to simulate manufacturing of various stacking sequences such as ($[0/90]_2$s, $[15/\text{-}75]_2$s, $[30/\text{-}60]_2$s, $[45/\text{-}45]_2$s, $[60/\text{-}30]_2$s, $[75/\text{-}15]_2$s and $[90/0]_2$s. Khashaba (2004) used a mathematical model to correlate tension test results to in-plane shear properties and concluded that specimens with 45° and 60° alignments resulted in the highest in-plane shear strength while the 0° and 90° alignment patterns resulted in the lowest in-plane shear strength.

APPENDIX B

OSU Laminates

OSU Laminates is a free Java-based program that performs classical composite laminate theory calculations developed by John Nairn at Oregon State University (Nairn, 2008). The program receives user inputs about the type, size, and orientation of the laminates and outputs various types of mechanical data. OSU Laminates was used to decide the alignment pattern to investigate in this study. The only available wood material in OSU Laminates is Douglas Fir. A constant panel thickness of 12.7 mm was entered. The thickness of each ply was divided evenly within the total panel thickness.

The results showed that the largest strong axis bending MOE is from layup A as seen in Table B1, which is the typical configuration of OSB, however, the lowest shear modulus was found from layup A as well. This result supports the significance of research in non-0/90/0 alignment to improve shear modulus. Layup B showed a substantial increase in shear stiffness over layup A, however, a reduction to strong axis bending MOE is also observed. Layup E showed a minimal reduction to strong bending stiffness along with a substantial increase in shear stiffness over layup A. The layups with 30 and 60 degree alignment show similar strong bending stiffness with variation in weak bending stiffness and shear modulus. Layup D shows similar stiffness in all three categories creating a well-rounded panel.

The selection of panel layup orientations is based on expected outcomes and ease of manufacturing. Due to current manufacturing ability, layup patterns with 30 and 60 degree orientations cannot be achieved. With a goal to increase shear modulus while limiting the reduction to strong bending stiffness, layup B was manufactured and tested. Layup A should be manufactured and tested to create a baseline data set.

Table B1. OSU Laminates alignment research summary

Input Information:

Material: Douglas Fir Rotary

Total Panel Thickness: 0.5" or 12.7 mm

Suggested panels to test: ●

Results:

		Flexure, Mpa		In-Plane, Mpa
Layup Orientation	Layup	MOE - Strong	MOE - Weak	G, Shear Stiffness
0/90/0	A ●	14,022	1,137	760
0/-45/+45/+45/-45/0	B ●	10,916	1,408	2,711
0/-45/+45/90/+45/-45/0	C	10,130	1,742	2,433
0/90/-45/+45/+45/-45/90/0	D	9,058	5,153	2,223
0/0/-45/+45/-45/+45/0/0	E	13,009	1,016	2,223
0/-30/+30/-60/+60/90/+60/-60/+30/-30/0	F	9,735	1,733	2,356
0/-30/+30/+45/-45/-45/+45/+30/-30/0	G	9,991	1,291	2,809
0/-60/60/90/+60/-60/0	H	9,668	3,068	2,014
0/-30/+30/-60/+60/+60/-60/+30/-30/0	I	10,102	1,494	2,516

For Comparison:

0/0/0/0		14,500.00	620.00	760.00
45/-45/-45/45		2,220.38	2,220.38	3,686.88
90/90/90/90		620.00	14,500.00	760.00
30/-30/-30/30		4,657.18	1,149.86	2,955.16
60/-60/-60/60		1,149.86	4,657.18	2,995.16

APPENDIX C

Preliminary Research

Before the main research study was carried out, a preliminary study was performed to guide the main research plan. This preliminary study involved manufacturing eight OSB panels and performing ASTM D3043 bending, ASTM D1761 nail connection, and ASTM D3044 plate twist shear tests. Four panels were made from hybrid poplar, or Pacific Albus, strands and 4 were made from southern pine strands. The goal of the preliminary study was to evaluate the effectiveness of the strand alignment on in-plane shear and bending properties, as well as, test the reliability and effectiveness of the resin pump control and proposed press schedule. During the pressing of the first panel, made from southern pine, the OSB mat was placed into the hot press and a lengthy amount of time passed before the mat was pressed due to interruptions. The result was the first panel did not bond well due to pre-curing of the resin. Therefore the preliminary testing only included 7 panels of which 4 were hybrid poplar and 3 were southern pine OSB panels. One commercial panel was included in all the testing procedures.

The southern pine strands were first dried from a moisture content from 12.1% to 5-7% using a rotating drum dryer. The resin application process and press schedule followed the same procedure as the main research study presented in the above manuscript. The hybrid poplar panels seemed to show large bumps on the panel surface due to moisture not able to escape during the pressing. The moisture would build up pressure within the panel, and when the press platens were released the internal pressure would cause uplift creating a bump.

The bending and nail connection test procedure was similar to the procedures used in the manuscript. However, the shear test procedure was different, in that ASTM D3044 (ASTM 2011b) method was followed. ASTM D3044 involves subjecting a square plate to a twisting force. One pair of diagonal corners are fixed and the other pair are deflected. The ASTM D3044 procedure requires measuring the deflection of the surface of the panel relative to the center using dial gauges. To save time, this measurement was performed using DIC. The surface strain was measured and the equation for G from ASTM D3044 was used to calculate the shear modulus. The ASTM D3044 standard called for turning the specimen 90° and testing a second time and averaging the results. This is shown on Table C1 with the “A” and “B” notation on the southern pine panels. This second measurement was not performed on the hybrid popular panels. Shear strength could not be measured using ASTM D3044. Table C1 shows the results from the bending test and the plate twist in-plane shear test. The results showed that [0/+45/-45]s alignment had evidence of improving the in-plane shear modulus when compared to 0/90/0. However, there was very high variation in the bending tests.

Table C1. Bending and in-plane shear results of preliminary study

			Bending				
			Parallel To Strong		Perpendicular to Strong		In-Plane Shear
Panel #	*Species/Alignment*		MOE, Gpa	MOR, Mpa	MOE, Gpa	MOR, Mpa	G, Gpa
1	Hybrid Poplar		8.5	67.1	1.7	18.6	2.7
		SD	0.69	8.25	0.35	5.43	
	[0/-45/+45]s	COV (%)	8.2	12.3	20.2	29.2	
2	Hybrid Poplar		7.2	49.6	2.1	24.5	2.3
		SD	0.76	8.29	0.28	3.63	
	[0/-45/+45]s	COV (%)	10.5	16.7	13.7	14.8	
3	Hybrid Poplar		7.9	57.2	1.8	19.1	2.1
		SD	1.72	15.46	0.52	3.86	
	[0/90/0]	COV (%)	21.6	27.0	28.6	20.3	
4	Hybrid Poplar		8.8	63.2	2.0	26.4	2.4
		SD	0.47	3.58	0.39	6.15	
	[0/90/0]	COV (%)	5.4	5.7	19.5	23.3	
5	Southern Pine		0.8	4.3	0.7	5.1	0.9
		SD	0.43	1.42	0.23	1.63	0.95 A
	[0/90/0]	COV (%)	55.2	33.0	33.0	31.8	0.95 B
6	Southern Pine		4.6	24.0	1.5	12.2	1.5
		SD	0.89	5.28	0.26	3.56	1.49 A
	[0/-45/+45]s	COV (%)	19.5	22.0	17.6	29.1	1.52 B
7	Southern Pine		4.7	26.8	1.2	8.9	1.7
		SD	1.15	8.33	0.28	3.39	1.72 A
	[0/-45/+45]s	COV (%)	24.4	31.1	24.3	38.3	1.66 B
Commercial			5.3	31.0	1.9	15.5	2.0
		COV (%)	7.4	6.2	13.4	21.3	

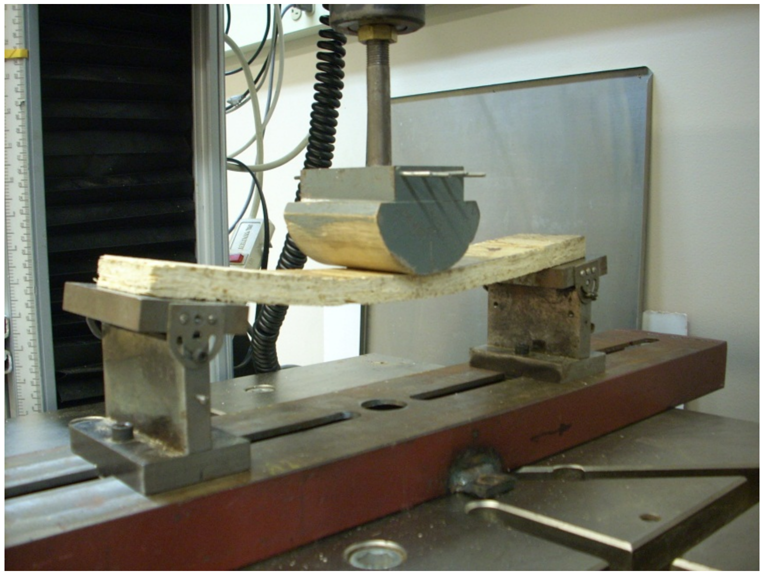

Figure C1. Bending test of preliminary study

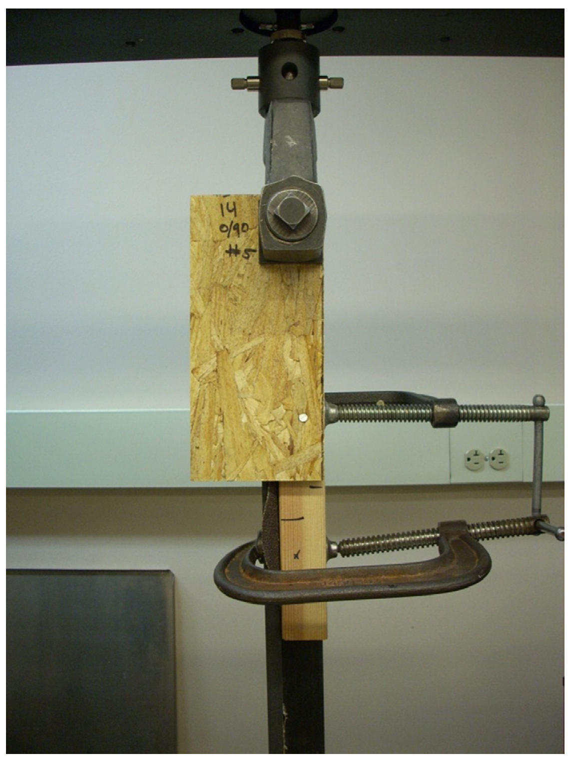

Figure C2. Nail connection test of preliminary study

APPENDIX D

Manufacturing Details

OSB wood strands were donated by Weyerhaeuser Natural Resources Company (Federal Way, Washington). The stands were mostly Aspen. The wood strands were dried by Weyerhaeuser Natural Resources Company (Federal Way, Washington) to a moisture content of 6% to 8%. The moisture content was measured using a Mettler-Toledo HB43-S Halogen Moisture Analyzer. The wood strands were approximately 100 mm in length.

The strands were placed into a rotating drum blender which was set to spin at 5 RPM. A spinning disk atomizer sprayed the adhesive onto the wood strands inside the blender. The atomizer received resin from a custom, electronically controlled resin pump. The piston and cylinder are removable for ease of cleaning and refilling. The electronic controller positions the piston from a specified start position and stops at a specified end position. By knowing the volume of the cylinder, precise volumetric control of resin can be achieved. Exactly the same amount of resin was used for every panel manufactured. The resin was liquid phenol formaldehyde (PF) with a solids content of 55.49%. The resin was donated by Momentive Specialty Chemicals Inc. (Springfield, Oregon).The PF resin was assumed to have a 0.0011 g/mm^3 density. 599 grams of resin were required for each panel. Thus, 599g / 0.0011 g/mm^3 equates to 545 ml of resin per panel.

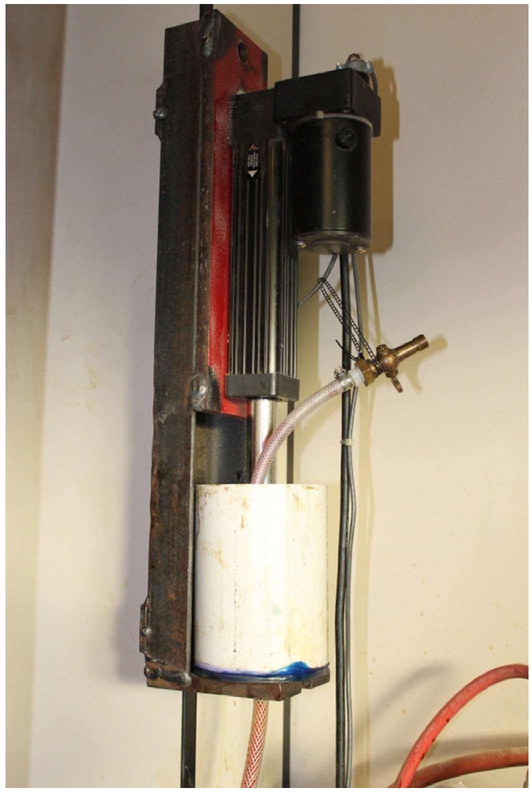

Figure D1. Gear driven piston resin pump

Figure D2. Electronic pump controller

PARTICULATE COMPOSITE MANUFACTURING SPECIFICATIONS	Created by: Sinha (based on Kamke's input) Cells highlighted must be input.
Project: OSB layup optimization	Name: Kenton Alldritt, Sinha, Miller
Panel No.	Date: 3/24/2012

PANEL

					English Units:	
OD Target Density (g/cm3):	0.64	Resin Solids, $100k_r$ (%):	4.0		OD Target Density (lb/ft3):	39.95
Thickness (cm):	1.3	Wax Solids, $100k_s$ (%):	0.0		Thickness (in):	0.51
Length (cm):	94	Furnish MC, M_f (%):	8.9		Length (in):	37.01
Width (cm):	94				Width (in):	37.01
Volume (cm3):	11487				Volume (in3):	700.97
Number of mats to blend:	1					
Compaction ratio (panel density / wood density):	1.60	<<< OK				

WOOD

Species:	Aspen	
Particle Size:	4" lab strands	
Solid wood OD density (g/cm3):	0.40	Wood Handbook 2010, Table4-7
Wood MC, M_w (%):	6.000	
OD Wood, S_o = (Density x Vol.) / $(1 + k_r + k_s)$ (g):	7069	
Blending & Forming Losses, L_B (%):	12.0	
OD Wood & Losses, $S_{o+} = S_o (1+ L_B/100)$ (g):	7917	
Wood + Losses, $S_{w+} = S_{o+} (1 + M_w / 100)$ (g):	8392	
Wood added to blender (g):	**8392**	18.5 lbs

NEAT RESIN		NEAT WAX		CATALYST	
Resin Type:	liq.PF	Wax Type:	Emulsion	Catalyst Type:	
Resin Solids Content, $100k_{nr}$ (%):	55.49	Wax Solids Content, $100k_{ns}$ (%):	50.0	Catalyst Solids (%):	
Resin Solids Wt, $S_r = k_r S_{o+}$ (g):	317	Wax Solids Wt, $S_s = k_s S_{o+}$ (g):	0	% of Resin Solids:	
Neat Resin Wt., $S_{nr} = S_r/k_{nr}$ (g):	571	Neat Wax Wt., $S_{ns} = S_s/k_{ns}$ (g):	0	Catalyst Solution (g):	#DIV/0!
Neat resin added to blender (g):	**571**	**Neat wax added to blender (g):**	**0**	**Catalyst added to blender (g):**	**#DIV/0!**

WATER

Desired water in Furnish, $W_f = (M_f)(S_{o+})(1 + k_r + k_s) / 100$ (g):	730
Water in Wood, $W_w = M_w S_{o+} / 100$ (g):	475
Water in Resin, $W_r = S_{nr} - S_r$ (g):	254
Water in Wax, $W_s = S_{ns} - S_s$ (g):	0
Added Water = $W_f - (W_w + W_r + W_s)$ (g):	0
Water added to blender (g):	**0**

FURNISH

OD Furnish Wt., $S_f = S_o (1+ k_r + k_s)$ (g):	7352		
OD Furnish & Water = $S_f (M_f + 100) /100$ (g):	8003		
Expected Squeeze-out, L_S (%):	2.0		
Total Furnish Wt. = $(Sf (M_f + 100) /100)(1+L_S/100)$ (g):	**8163**	**<<<< Furnish added to mat.**	18.0 lbs

Figure D3. Furnish inputs and calculations

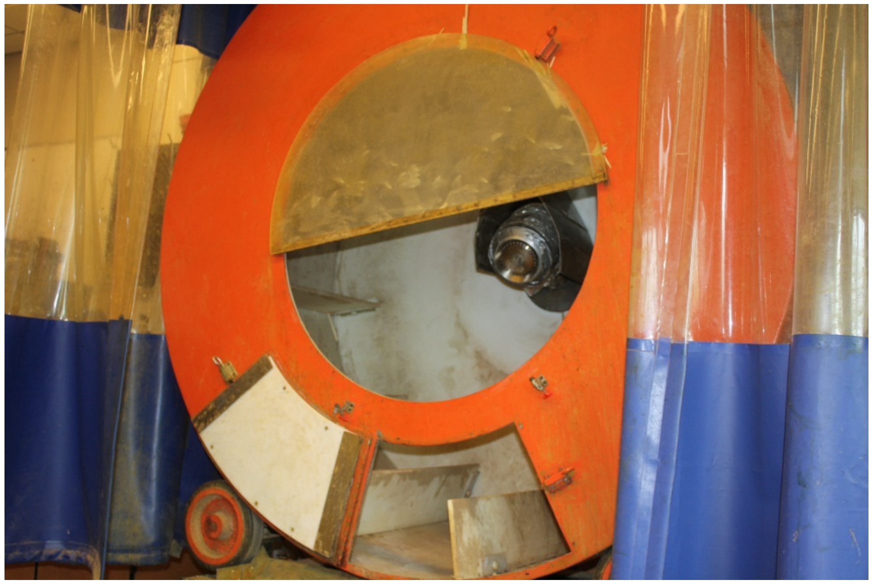

Figure D4. Drum strand blender

Figure D5. Drum blender and atomizer control box

Figure D6. Resin atomizer after blending panels.

The rate of the spinning disk atomizer was 10000 rpm. The target density of each panel was 0.64g/cm^3 with a target thickness of 12.7 mm. The calculated amount of resin added to the blender was 524 milliliters. Typical weight of resin coated wood strands per layer was 2674 grams for the 0/90/0 panels and 1337 grams for the $[0/+45/-45]_s$ panels. The resin was liquid phenol formaldehyde with a solids content of 55.49%.

MOMENTIVE Page 1 of 1

Momentive Specialty Chemicals Inc.

Certificate of Analysis

Customer #:	100026	**Ship Date:**	07/31/2012
Customer Address:		**DDN:**	83606381
OREGON STATE UNIVERSITY		**Customer - PO#:**	TODD MILLER

DEPT WOOD SCIENCE 234 RICHARDSON H
3180 SW JEFFERSON WAY
CORVALLIS OR 97331-5751

SAP Product #: 368892

Tank Number: 78
Product Description: Cascophen(TM) AM1661

Property	Value	Units
Alkalinity, Total	**2.57**	**%**
pH, 25C	**9.78**	
Refractive Index	**1.4929**	
Solids, Refractive Index	**55.49**	**%**
Temperature, Shipping	**17**	**°C**
Viscosity, Brookfield	**190**	**cPs**

Dave R IWANYSHYN
Quality Assurance

SHIPPED FROM: Momentive Specialty Chemicals ● 12621 156th Street NW
Edmonton, AB T5V 1E1 ● Phone: 780/447-1270

Figure D7. Certificate of Analysis of resin

Strand alignment was achieved by passing the strands by hand through a vibratory screen consisting of aluminum vanes spaced at 50 mm as shown in Fig. D8. The vanes were 127 mm deep. The forming box was 914 mm by 914 mm with the alignment screen having an adjustable height above the surface of the strand mat. The free-fall distance of the wood strands from the bottom of the alignment vanes to the surface of the mat was not greater than the typical length of a wood strand being approximately 100 mm. The vibration was achieved from a variable speed electric motor attached to the side of the forming box. The motor was connected to an off-center counter weight. The speed of the motor was adjusted to achieve the greatest amount of vibration of the forming screen. Two forming screens were used consisting of vanes set to 0° and 45°. The forming screens were removed, rotated 90°, and reinstalled to create the different alignment patterns. The 0°, 90°, and ±45° patterns of the OSB strands before pressing are shown in Figures 5, 6, 7, and 8. A thin thermocouple wire was placed in the center of the panel to monitor core temperature during pressing. The weight of strands used in each panels was held constant. The weight ratio for the 0/90/0 panels was 1/3:1/3:1/3 and of the [0/+45/-45]s panels was 1/6:1/6:1/6:1/6:1/6:1/6. Fig. D3 states that total weight of furnish was 8163 g, however the actual furnish weight used in all panels was 8023 g due to calculation error.

Figure D8. Dropping strands into vibratory alignment box

Figure D9. Switching alignment screen in alignment box. 0°/90° screen shown

Figure D10. Switching alignment screen in alignment box. +45°/-45° screen shown

Figure D11. Electric counter-weight motor to achieve vibration

After forming the mat of OSB strands, the mat was placed into a hydraulic hot-press. The platen temperature was maintained at 180°C. The panel was pressed using displacement control until the press reached the desired thickness of 12.7 mm. The panel was held in the press until the core temperature reached 180°C. The panels were pressed for an average of 9 minutes. The pressed panel was then removed and allowed to cool to room temperature.

Figure D12. Hot press

Figure D13. Control panel for hot press

APPENDIX E

Panel Cut Pattern Layout

914 mm by 914 mm panels were manufactured. To reduce edge effects from manufacturing, 67 mm was removed from the entire panels around the perimeter. Seven parallel bending specimens that were 51 mm wide were cut from the top left and top right corners. Six perpendicular bending specimens were cut from the lower section of the panel. One in-plane shear test specimen was cut per panel. Removing the 67 mm perimeter of the panel assisted in reducing the variation within the bending test specimens, however, specimens #1, 7, 10, and 13 seemed to show a lower density then the interior specimens.

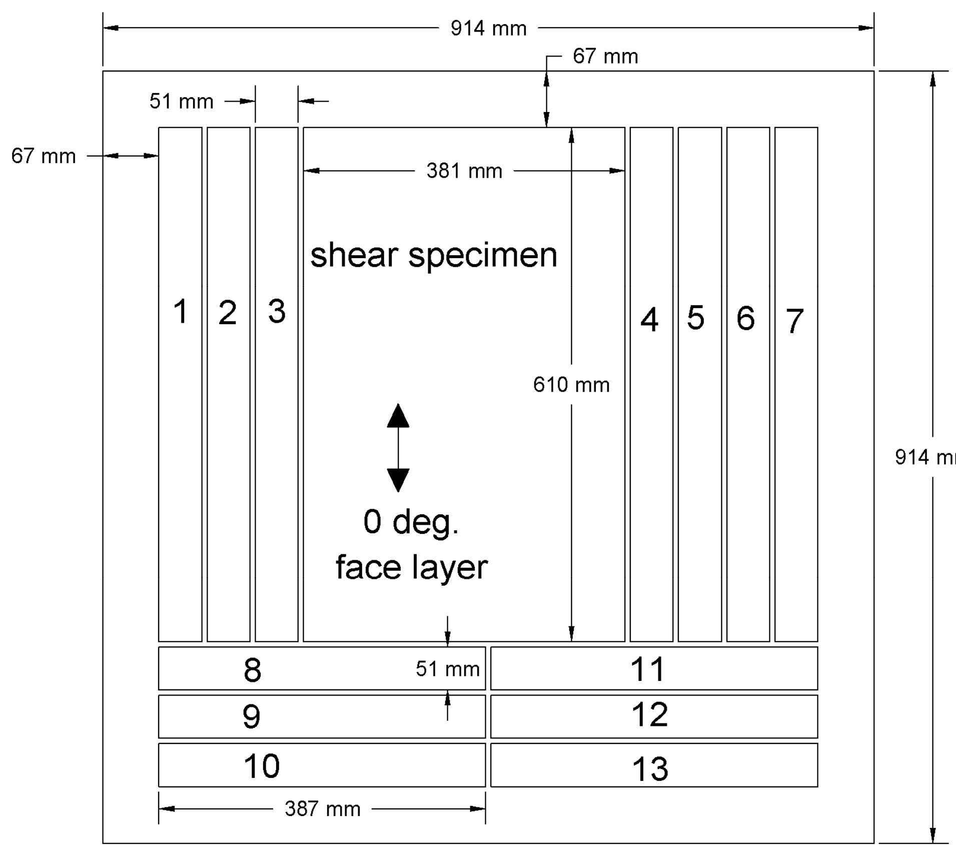

Figure E1. Specimen cut pattern layout

APPENDIX F

Derivation of Equations for In-Plane Shear Test

ASTM D2719 Method C refers to the in-plane shear modulus as:

$$G = 0.5\ (P_g / \Delta)(l/Lt)$$

Where:

G = modulus of rigidity in the plane of the plies
(P_g / Δ) = slope of force/deformation diagram
l = gage length
L = length of shear area
t = average thickness of shear area

DIC surface strain measurement was used to find the shear strain of the specimen. Therefore, there was no gauge length. A new derivation of shear strain was needed to calculate the shear modulus, G. Based on mechanics of materials, the constant of proportionality between the shearing stress, τ_{xy}, and the shearing strain, γ_{xy}, is the shear modulus, G. Vic-3D 2010 outputs the average shear strain of a selected area as ε_{xy} and is associated with the corresponding applied load. An ε_{xy} versus applied load graph can be produced. ε_{xy} is referred to as engineering shear strain which is equal to half of the total strain, γ_{xy}. Thus:

$$\gamma_{xy} = 2^* \varepsilon_{xy} = \tau_{xy}/G$$

Rewrite:

$$G = \tau_{xy}/(2^* \varepsilon_{xy})$$

$$\text{Average Shear Stress} = P/L = \tau_{xy}$$

Where:

P = force

t * L = shearing area

Rewrite:

$$G = (P/(L*t))(1/(2*\varepsilon_{xy})$$

Rewrite:

$$G = (P/ \varepsilon_{xy})*(1/(L*t*2))$$

The slope in the linear region of the force vs. shear strain, ε_{xy}, graph will be considered to be (P/ ε_{xy}).

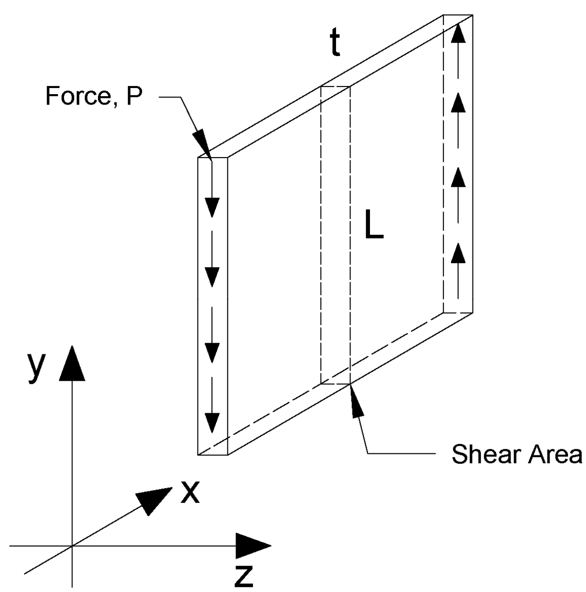

Figure F1. Reference coordinate system for shear modulus derivation

APPENDIX G

In-plane Shear Test Apparatus

The modified ASTM D2719 testing apparatus was machined from 19 mm A36 steel plate. A total of 4 plates were made. It included 14 (7 on each side) 13 mm holes for bolts to clamp the specimen to the brackets.

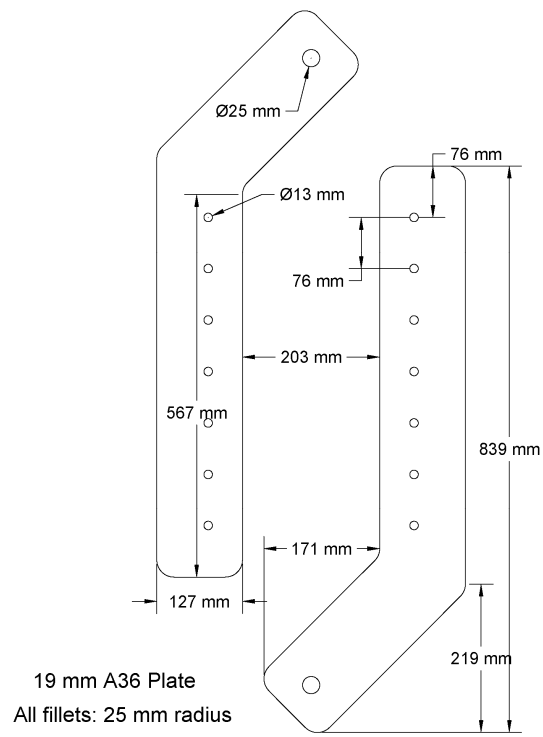

Figure G1. Dimension of in-plane shear testing plates

APPENDIX H

Density of Test Specimens

Density of each test specimen was recorded directly before the test occurred. Density is referred to weight of specimen in grams divided by the volume of the specimen in cm^3. Tables are listed for in-plane shear and bending. Cut #4 and #5 of the bending tests specimens were reused for the parallel and perpendicular nail test specimens respectfully. The density of the shear wall specimens was not recorded.

Table H1. Measured density of in-plane shear test specimens

Density, g/cm^3

	0/90/0		[0/+45/-45]s		Commercial
Panel #					
1	0.703	3	0.707	1	0.574
2	0.706	4	0.707	2	0.598
5	0.699	7	0.701	3	0.586
6	0.646	8	0.682	4	0.556
9	0.773	12	0.706	5	0.600
10	0.779	13	0.721	6	0.527
11	0.681	14	0.735	7	0.600
15	0.838	18	0.809	8	0.567
16	0.863	19	0.824	9	0.591
17	0.799	20	0.822	10	0.585
Average	0.749		0.741		0.578
SD	0.072		0.055		0.023
COV, %	9.6		7.4		4.0

Table H2. Measured density of bending test 0/90/0 specimens

Density, g/cm^3

0/90/0	Panel #												
Cut #	1	2	5	6	9	10	11	15	16	17	Average	SD	COV
1	0.632	0.700	0.749	0.603	0.677	0.693	0.645	0.637	0.677	0.701	0.671	0.043	6.4
2	0.662	0.697	0.748	0.678	0.747	0.781	0.658	0.771	0.776	0.783	0.730	0.051	7.0
3	0.685	0.691	0.728	0.692	0.790	0.747	0.698	0.813	0.836	0.811	0.749	0.059	7.8
4	0.674	0.753	0.721	0.655	0.734	0.753	0.698	0.905	0.833	0.799	0.753	0.076	10.1
5	0.700	0.779	0.704	0.657	0.799	0.752	0.672	0.864	0.909	0.816	0.765	0.084	10.9
6	0.676	0.769	0.688	0.644	0.829	0.781	0.673	0.805	0.840	0.796	0.750	0.072	9.7
7	0.650	0.713	0.635	0.569	0.760	0.770	0.616	0.776	0.760	0.745	0.699	0.075	10.8
8	0.742	0.746	0.755	0.728	0.853	0.752	0.716	0.819	0.802	0.758	0.767	0.043	5.6
9	0.749	0.781	0.715	0.757	0.814	0.753	0.675	0.785	0.790	0.737	0.756	0.040	5.3
10	0.665	0.704	0.703	0.658	0.707	0.712	0.556	0.640	0.635	0.591	0.657	0.053	8.1
11	0.744	0.737	0.690	0.707	0.813	0.742	0.673	0.801	0.746	0.802	0.745	0.048	6.4
12	0.739	0.724	0.729	0.734	0.800	0.709	0.656	0.726	0.714	0.769	0.730	0.038	5.2
13	0.680	0.657	0.693	0.614	0.706	0.675	0.586	0.616	0.644	0.670	0.654	0.038	5.9
Average	0.692	0.727	0.712	0.669	0.771	0.740	0.656	0.766	0.766	0.752			
SD	0.039	0.038	0.033	0.055	0.054	0.033	0.046	0.088	0.082	0.065			
COV	5.7	5.2	4.6	8.2	7.0	4.5	7.0	11.5	10.7	8.7			

Table H3. Measured density of bending test [0/+45/-45]s specimens

Density, g/cm^3

[0/+45/-45]s	Panel #												
Cut #	3	4	7	8	12	13	14	18	19	20	Average	SD	COV
1	0.801	0.750	0.691	0.738	0.660	0.696	0.651	0.729	0.745	0.643	0.710	0.051	7.2
2	0.805	0.704	0.707	0.736	0.732	0.764	0.720	0.829	0.815	0.818	0.763	0.049	6.5
3	0.724	0.641	0.732	0.690	0.734	0.736	0.731	0.841	0.837	0.872	0.754	0.073	9.7
4	0.765	0.702	0.709	0.679	0.746	0.763	0.721	0.781	0.815	0.785	0.747	0.043	5.8
5	0.782	0.679	0.718	0.727	0.756	0.775	0.690	0.820	0.864	0.858	0.767	0.066	8.6
6	0.770	0.630	0.701	0.771	0.716	0.810	0.637	0.833	0.843	0.821	0.753	0.079	10.4
7	0.730	0.598	0.674	0.707	0.657	0.777	0.640	0.745	0.717	0.702	0.695	0.053	7.7
8	0.795	0.693	0.737	0.717	0.729	0.757	0.807	0.808	0.810	0.750	0.760	0.042	5.6
9	0.784	0.735	0.716	0.765	0.724	0.729	0.741	0.720	0.719	0.687	0.732	0.027	3.7
10	0.642	0.617	0.633	0.756	0.646	0.657	0.683	0.641	0.675	0.600	0.655	0.043	6.6
11	0.679	0.761	0.660	0.734	0.728	0.759	0.665	0.795	0.772	0.754	0.731	0.047	6.5
12	0.746	0.693	0.668	0.685	0.751	0.730	0.671	0.706	0.728	0.744	0.712	0.032	4.4
13	0.695	0.644	0.634	0.724	0.698	0.653	0.624	0.650	0.674	0.620	0.662	0.035	5.3
Average	0.747	0.681	0.691	0.725	0.713	0.739	0.691	0.761	0.770	0.743			
SD	0.051	0.052	0.035	0.029	0.037	0.046	0.052	0.069	0.065	0.089			
COV	6.8	7.6	5.0	4.0	5.2	6.3	7.5	9.0	8.4	11.9			

Table H4. Measured density of bending test Commercial specimens

Density, g/cm^3

Commercial	Panel #												
Cut #	1	2	3	4	5	6	7	8	9	10	Average	SD	COV
1	0.602	0.672	0.006	0.594	0.589	0.623	0.572	0.602	0.621	0.576	0.546	0.192	35.1
2	0.612	0.672	0.631	0.597	0.560	0.623	0.557	0.599	0.628	0.568	0.605	0.036	6.0
3	0.631	0.652	0.598	0.588	0.584	0.608	0.612	0.578	0.670	0.597	0.612	0.030	5.0
4	0.598	0.571	0.600	0.546	0.605	0.556	0.600	0.584	0.588	0.577	0.582	0.020	3.4
5	0.544	0.557	0.589	0.537	0.636	0.555	0.615	0.569	0.589	0.598	0.579	0.032	5.6
6	0.564	0.545	0.601	0.569	0.609	0.569	0.612	0.570	0.574	0.563	0.578	0.022	3.8
7	0.597	0.563	0.595	0.564	0.633	0.582	0.616	0.563	0.590	0.564	0.587	0.024	4.2
8	0.588	0.631	0.573	0.606	0.670	0.636	0.610	0.593	0.576	0.649	0.613	0.032	5.3
9	0.555	0.631	0.622	0.621	0.607	0.606	0.616	0.618	0.589	0.611	0.608	0.022	3.6
10	0.586	0.623	0.641	0.593	0.595	0.602	0.616	0.587	0.595	0.600	0.604	0.018	2.9
11	0.618	0.566	0.615	0.584	0.604	0.589	0.645	0.569	0.567	0.614	0.597	0.026	4.4
12	0.622	0.546	0.605	0.622	0.603	0.598	0.674	0.589	0.583	0.600	0.604	0.033	5.4
13	0.589	0.554	0.627	0.592	0.555	0.597	0.689	0.588	0.569	0.591	0.595	0.039	6.6
Average	0.593	0.599	0.562	0.586	0.604	0.596	0.618	0.585	0.595	0.593			
SD	0.026	0.049	0.168	0.026	0.031	0.025	0.035	0.016	0.029	0.024			
COV	4.4	8.2	29.9	4.4	5.1	4.2	5.7	2.7	4.8	4.1			

APPENDIX I

Load, Deflection, and Strain Curves

The following graphs include load versus deflection from the in-plane shear tests and the bending tests and nail tests. A box and whisker plot of results from the bending test are also included as well as the load vs. shear strain plots from the in-plane shear tests. Deflection refers to the testing machine head deflection.

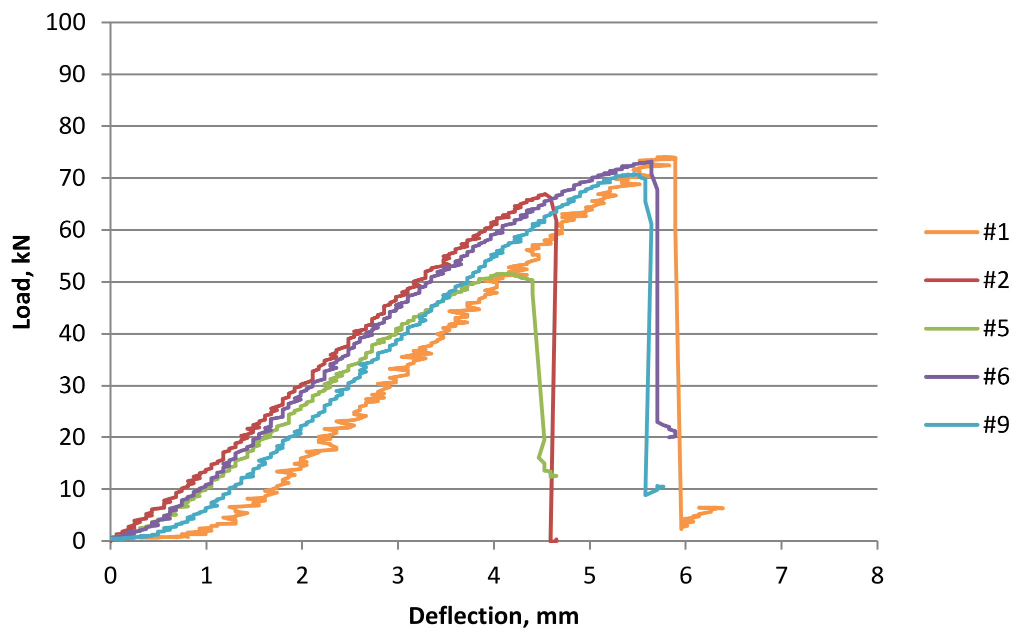

Figure I1. In-plane shear load-deflection graph for 0/90/0 panels

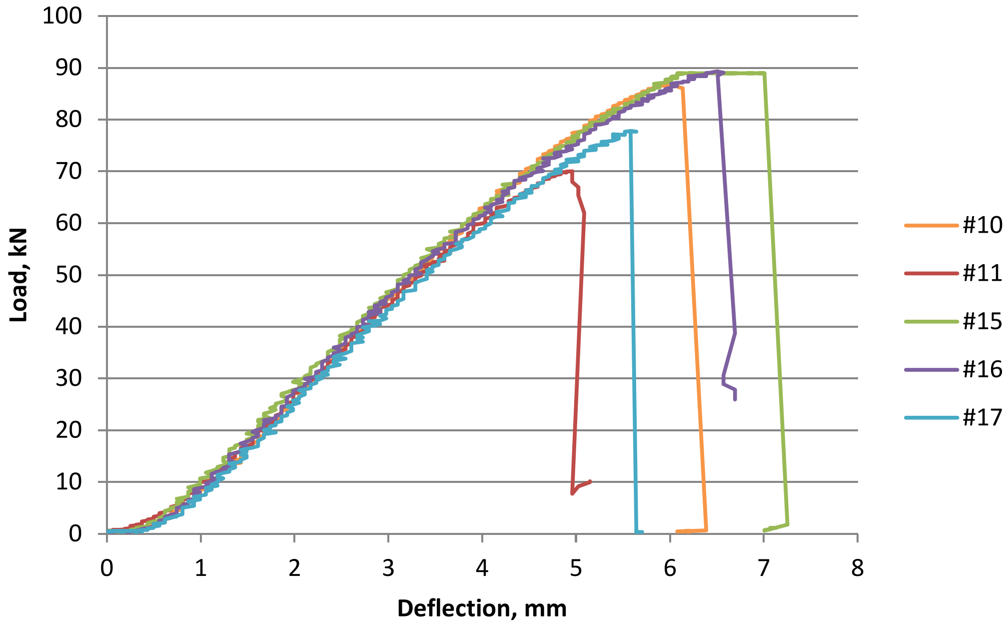

Figure I2. In-plane load-deflection graph for 0/90/0 panels

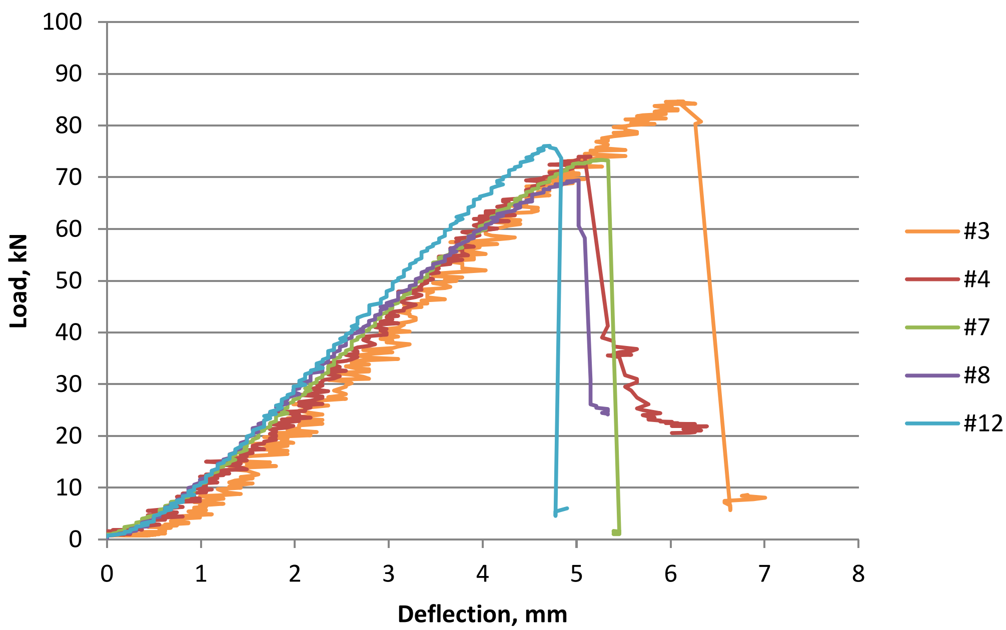

Figure I3. In-plane shear load-deflection graph for [0/+45/-45]s panels

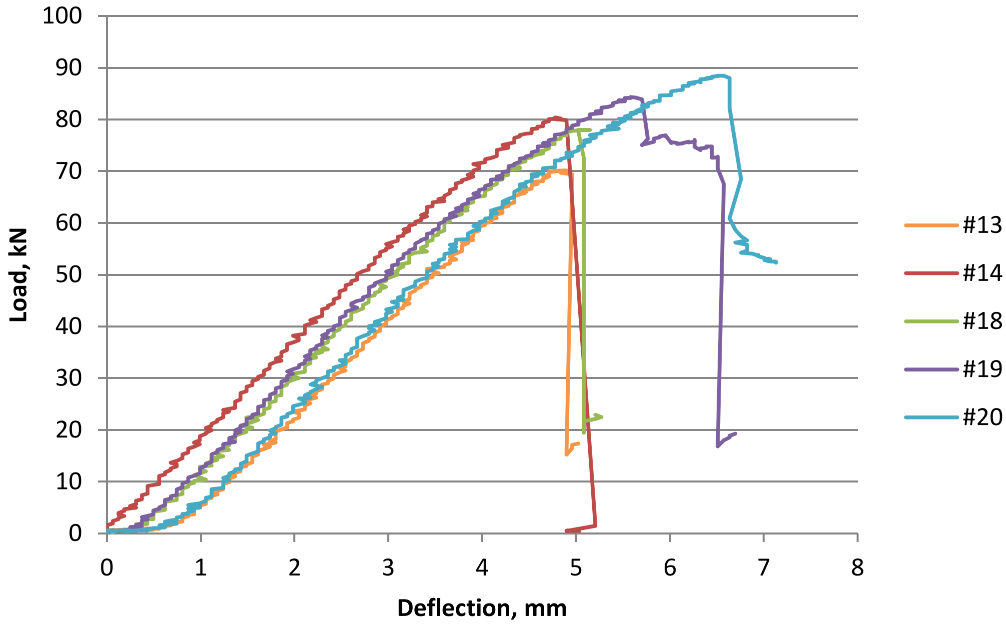

Figure I4. In-plane shear load-deflection graph for [0/+45/-45]s panels

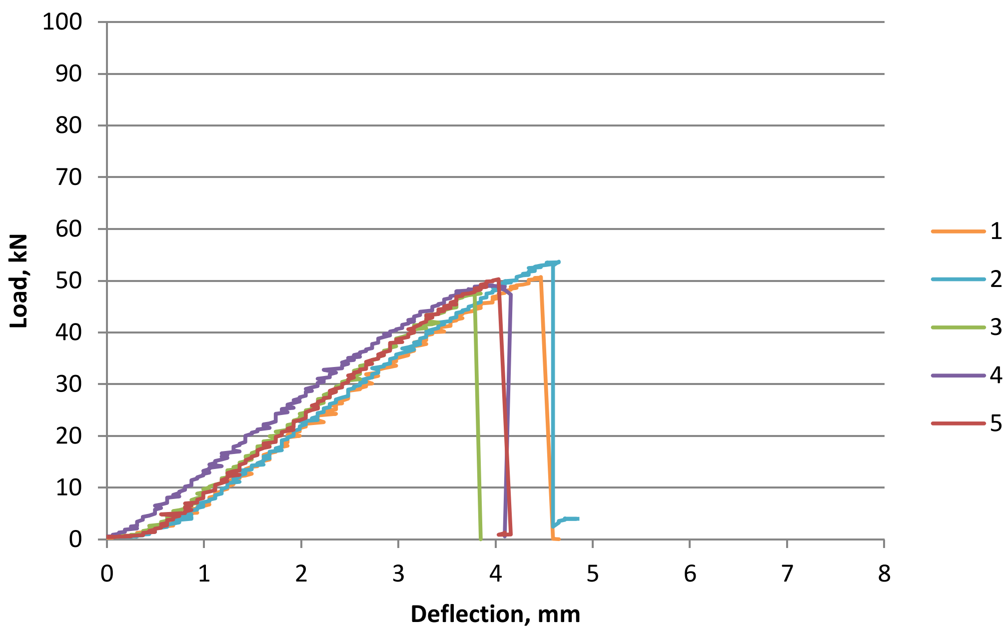

Figure I5. In-plane shear load-deflection graph for commercial panels

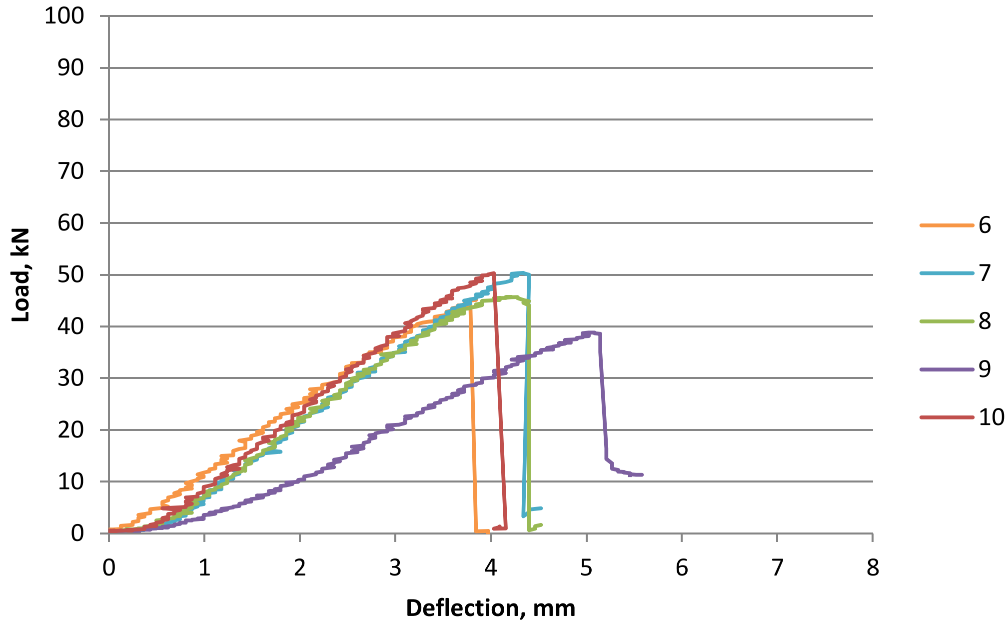

Figure I6. In-plane shear load-deflection graph of commercial panels

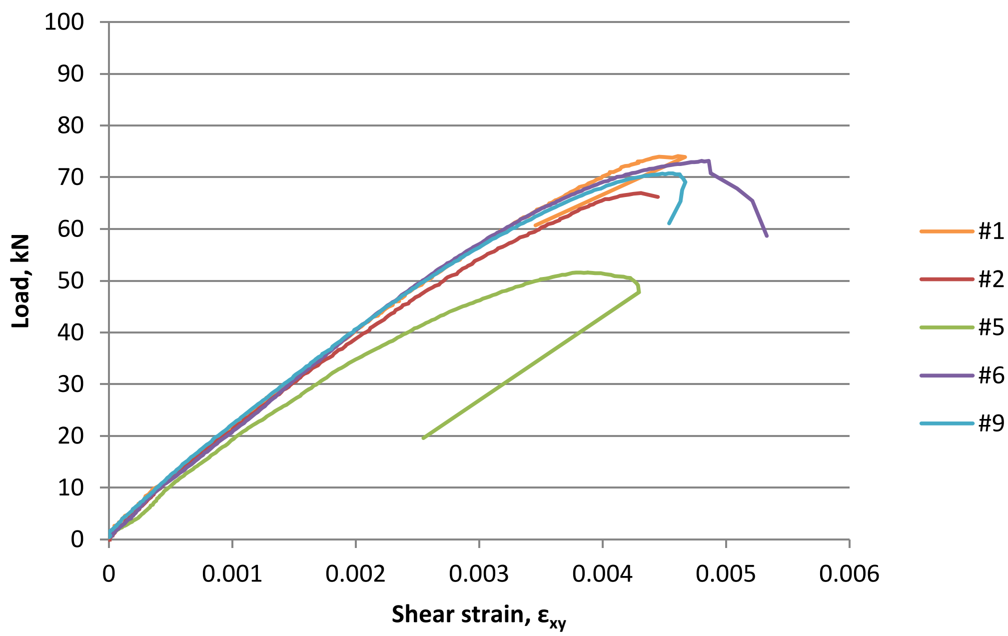

Figure I7. In-plane shear load-shear strain graph of 0/90/0 panels

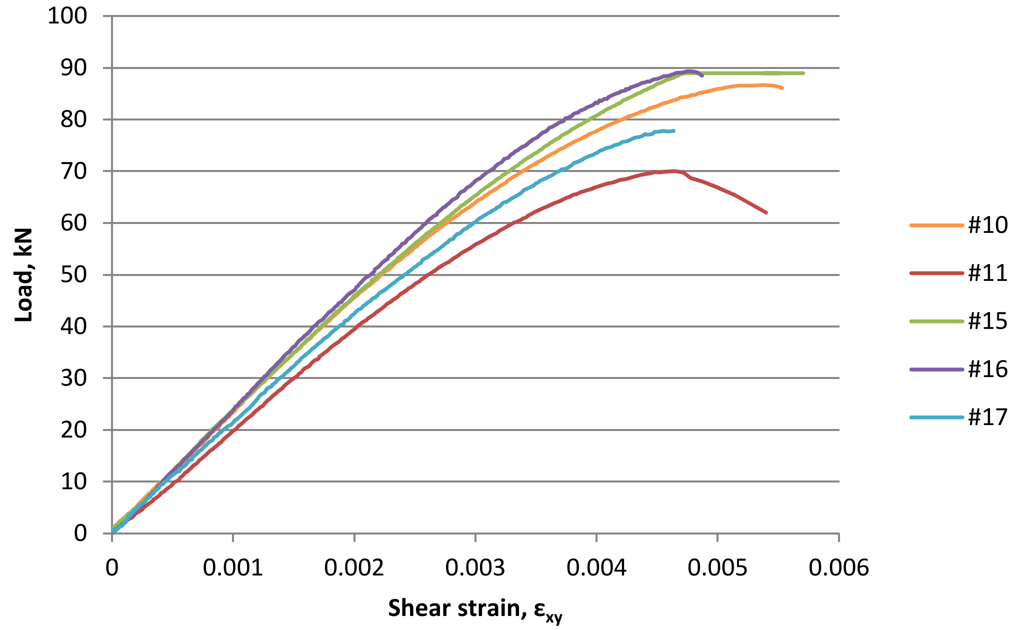

Figure I8. In-plane shear load-shear strain graph of 0/90/0 panels

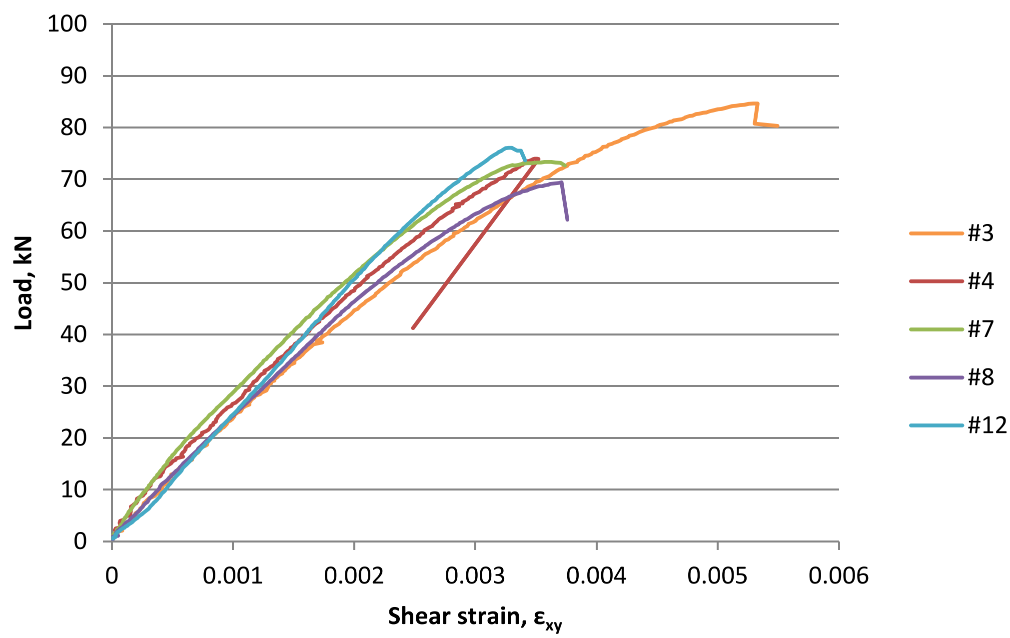

Figure I9. In-plane shear load-shear strain graph of [0/+45/-45]s panels

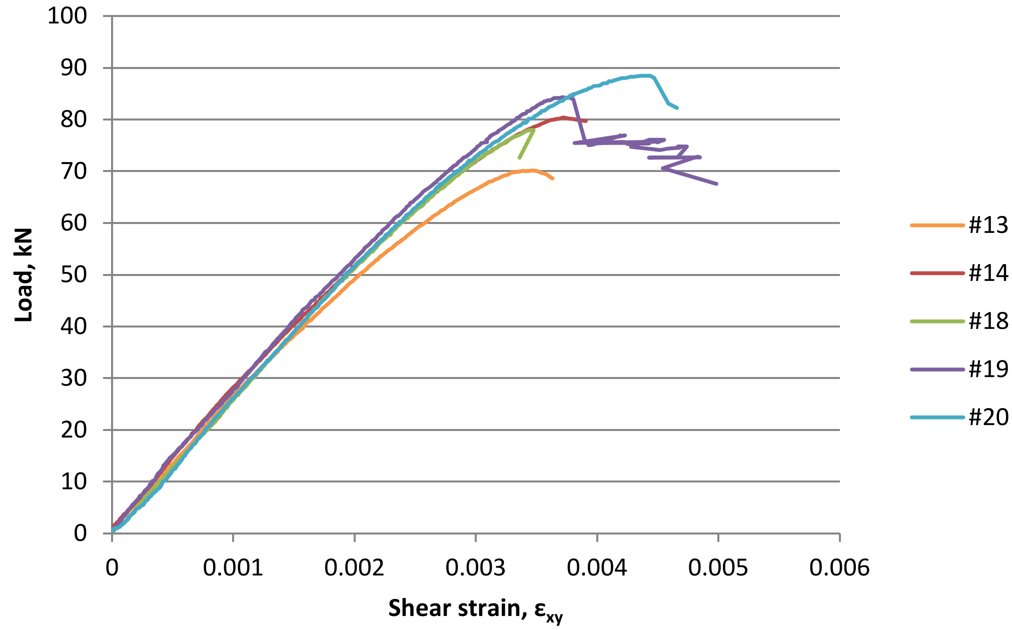

Figure I10. In-plane shear load-shear strain graph of [0/+45/-45]s panels

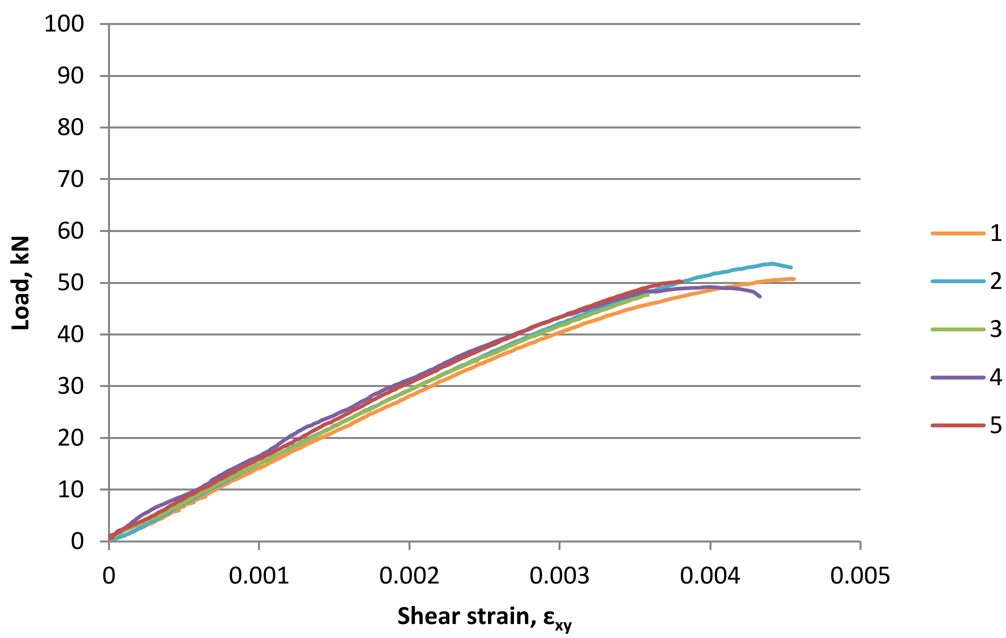

Figure I11. In-plane shear load-shear strain graph of commercial panels

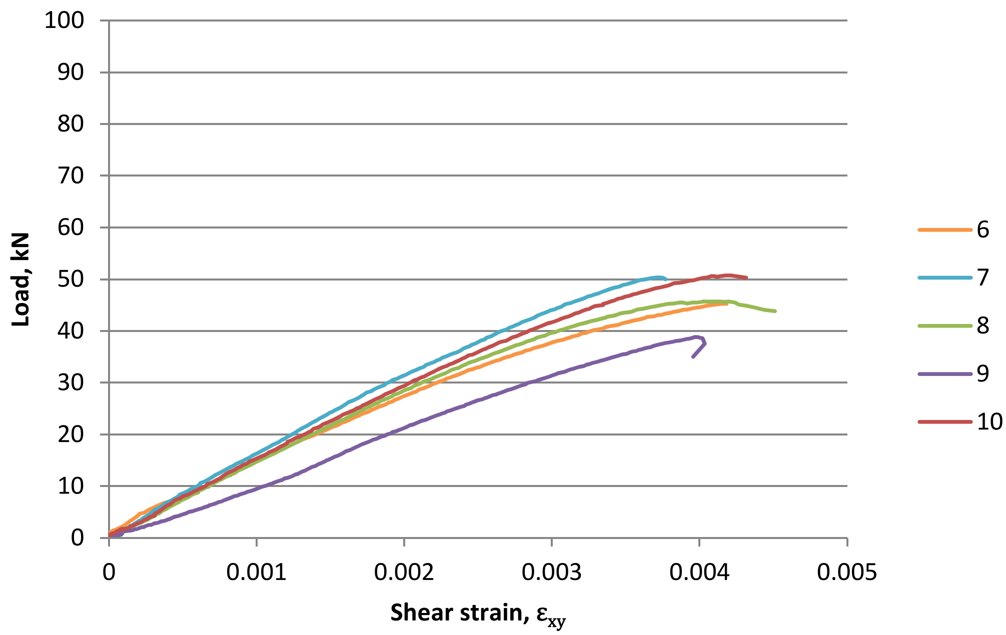

Figure 12. In-plane shear load-shear strain graph of commercial panels

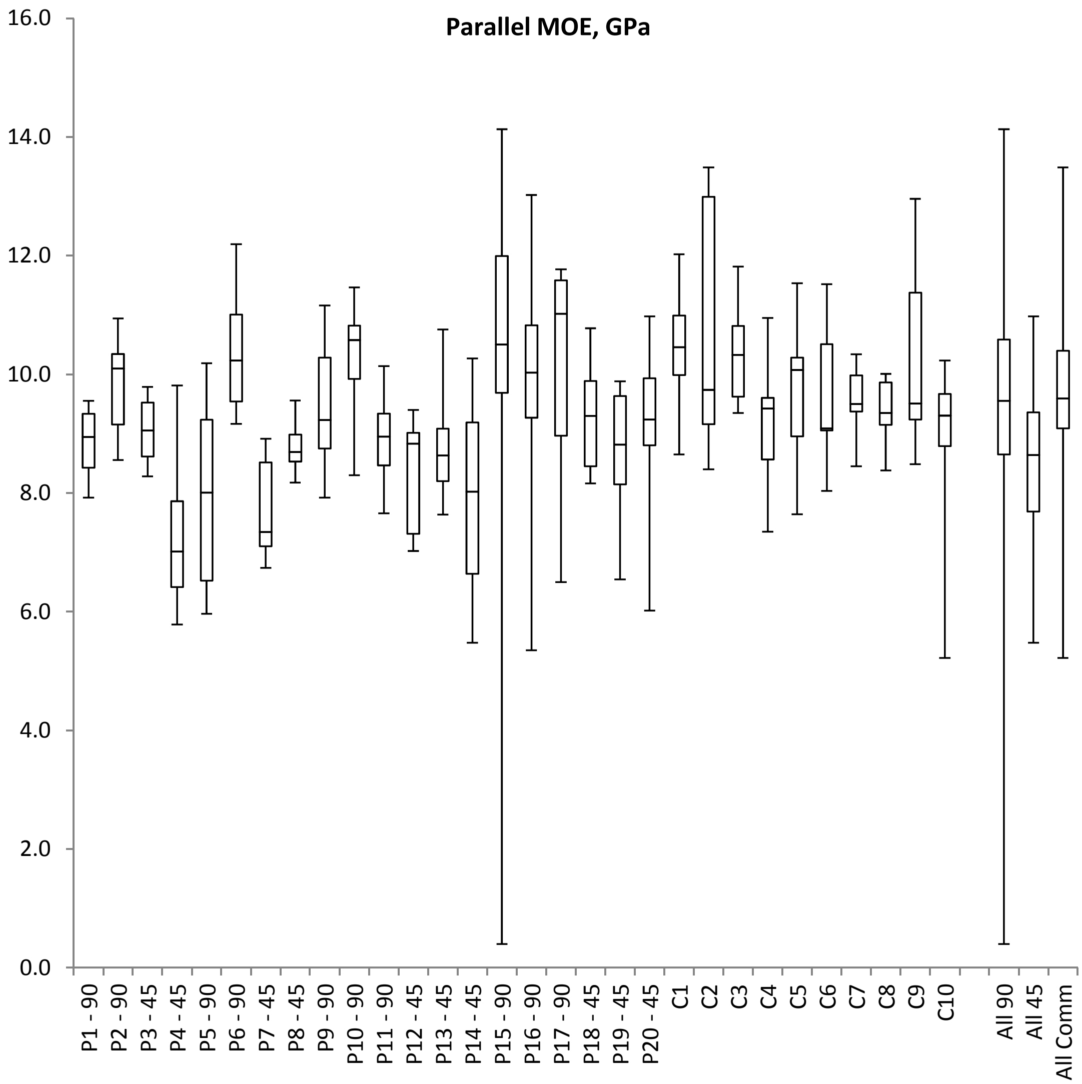

Figure I13. Parallel bending MOE box and whisker plot of all panels

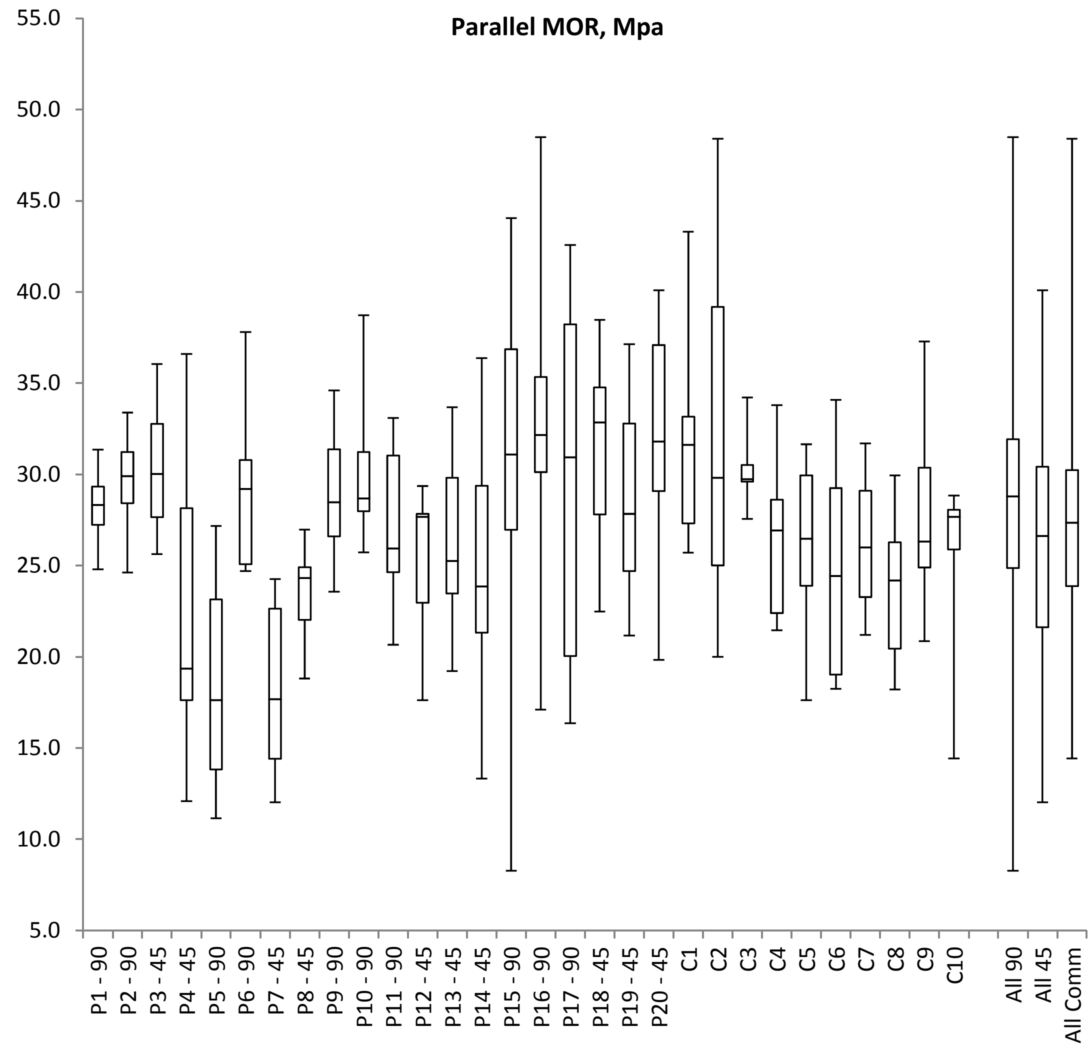

Figure I14. Parallel bending MOR box and whisker plot of all panels

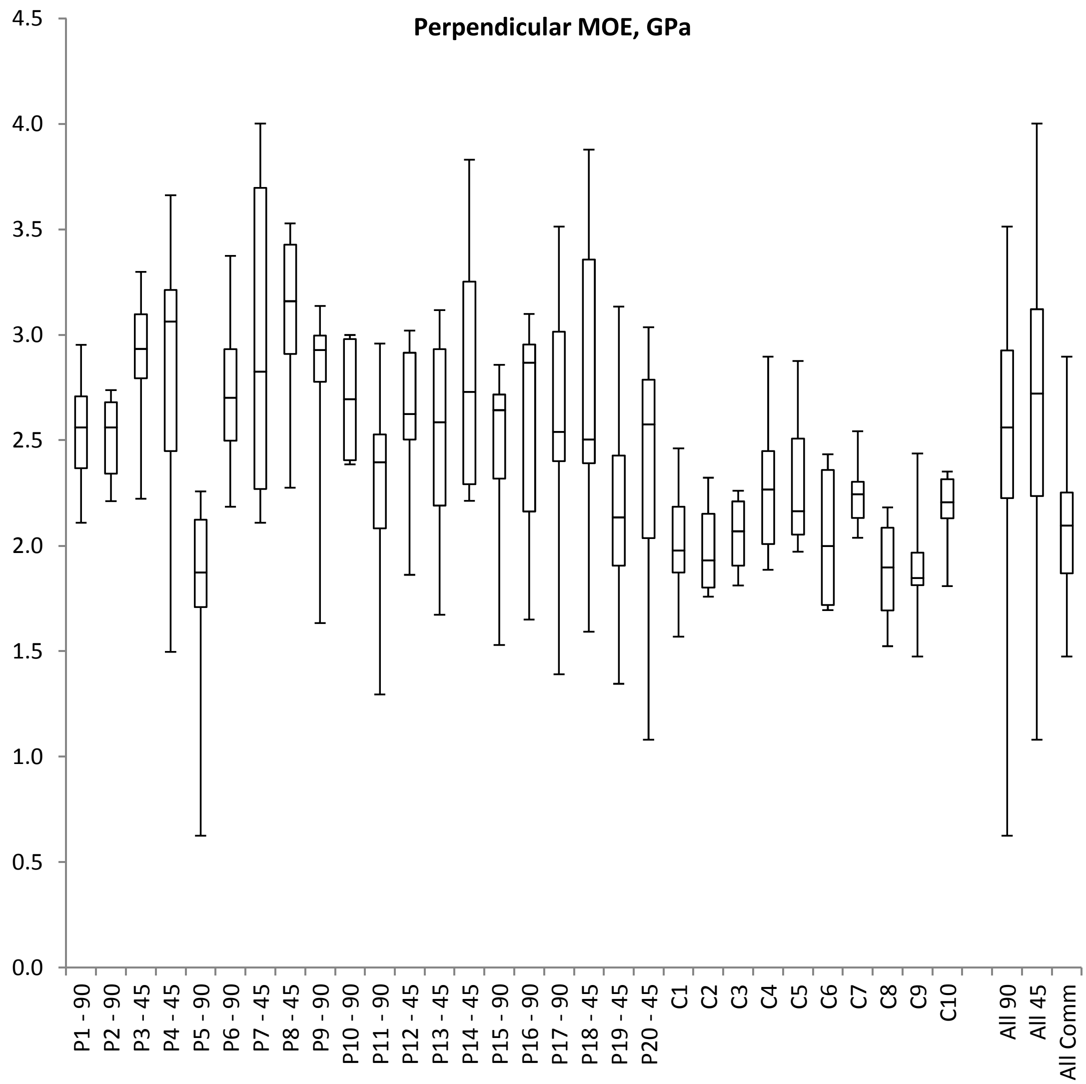

Figure I15. Perpendicular bending MOE box and whisker plot of all panels

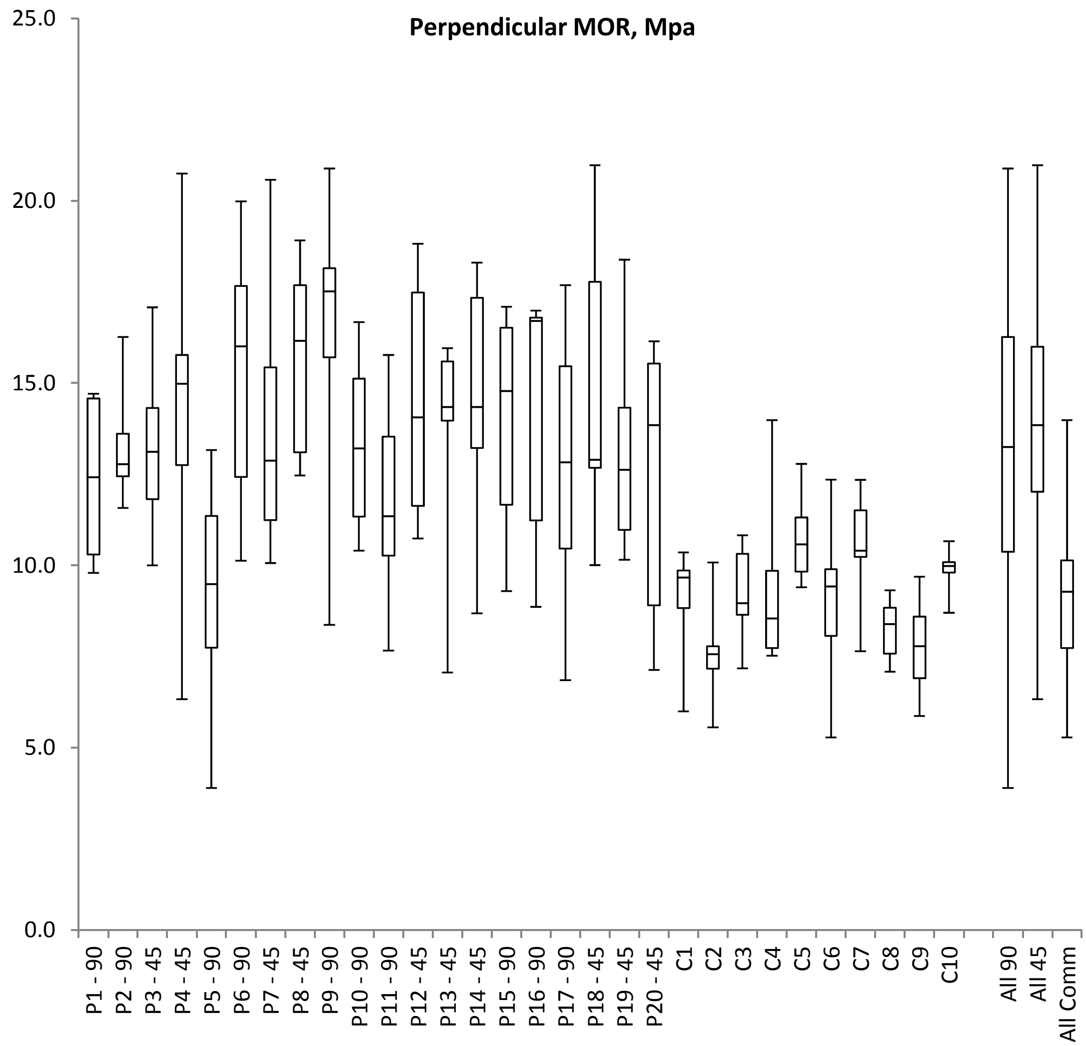

Figure I16. Perpendicular bending MOR box and whisker plot of all panels

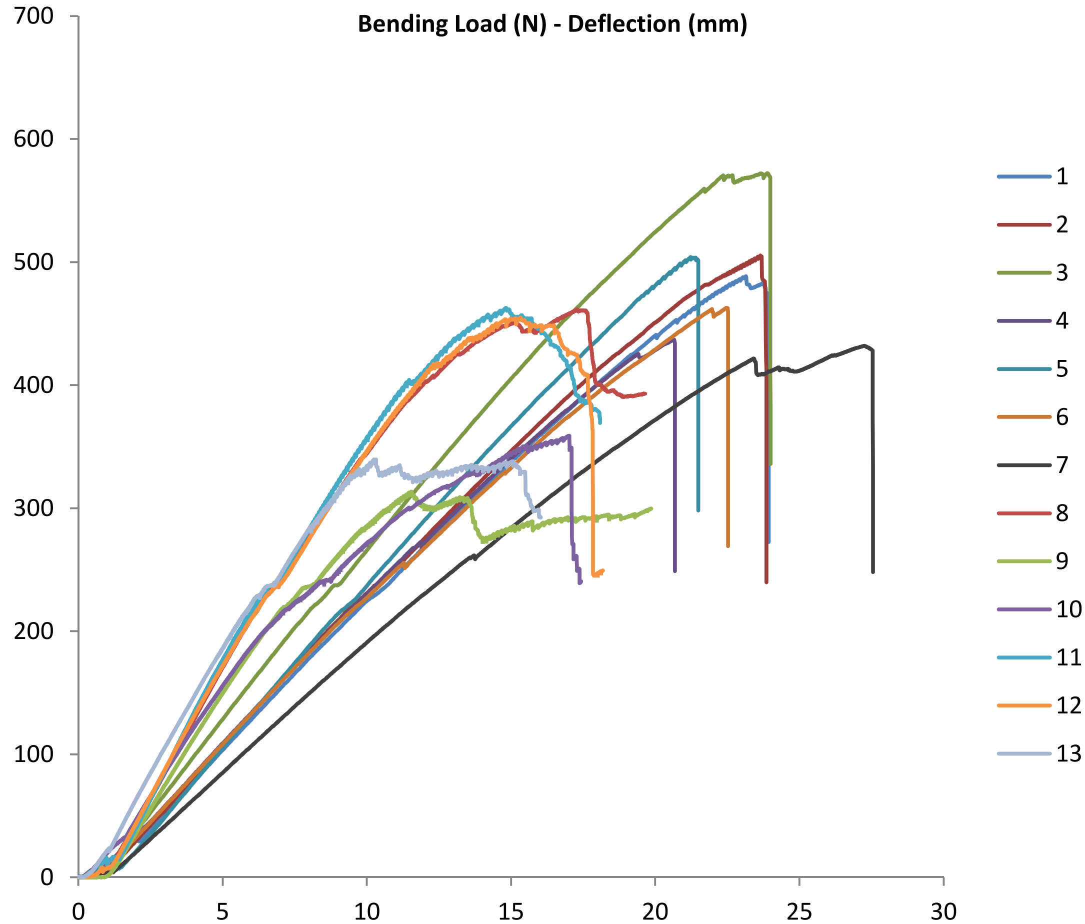

Figure I17. Load vs. deflection graph of panel #1 (0/90/0). Cuts #1-7 are parallel bending, Cuts #8-13 are perpendicular bending.

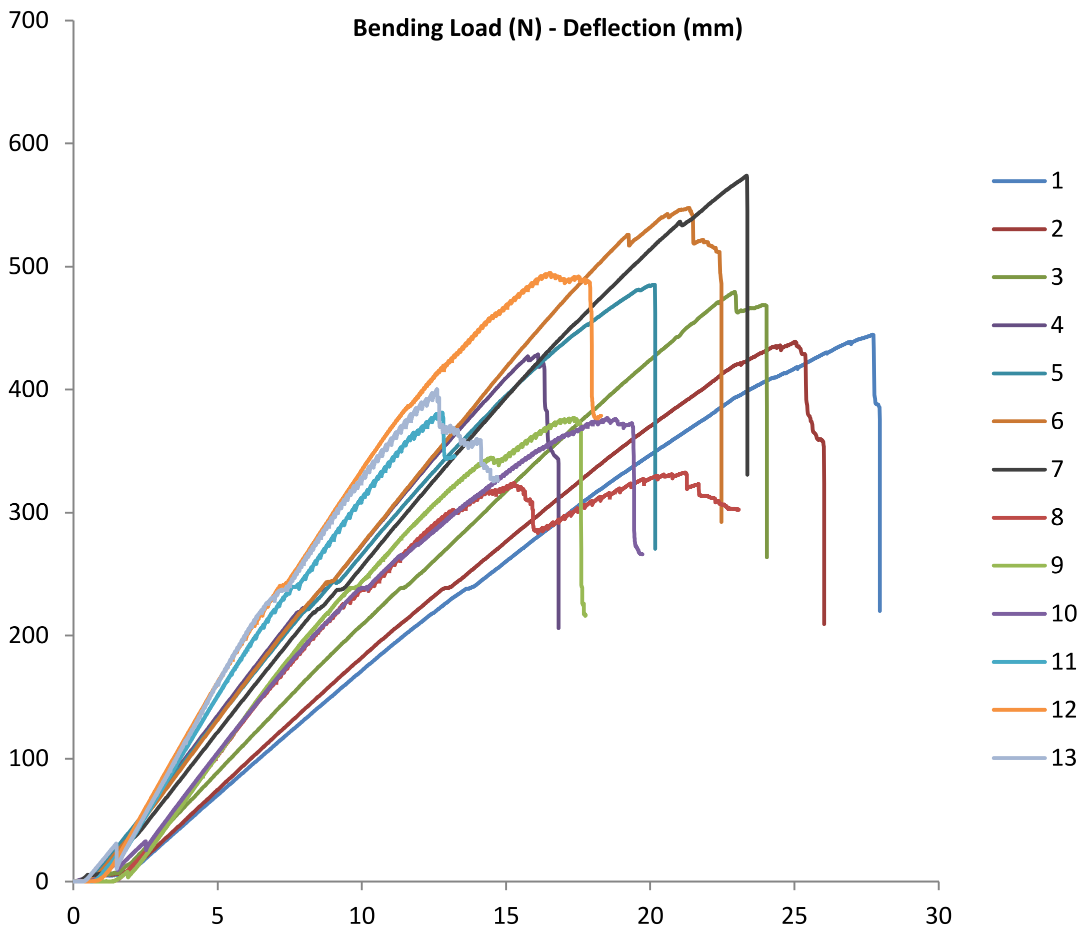

Figure I18. Load vs. deflection graph of panel #2 (0/90/0). Cut #1-7 are parallel bending, Cut #8-13 are perpendicular bending.

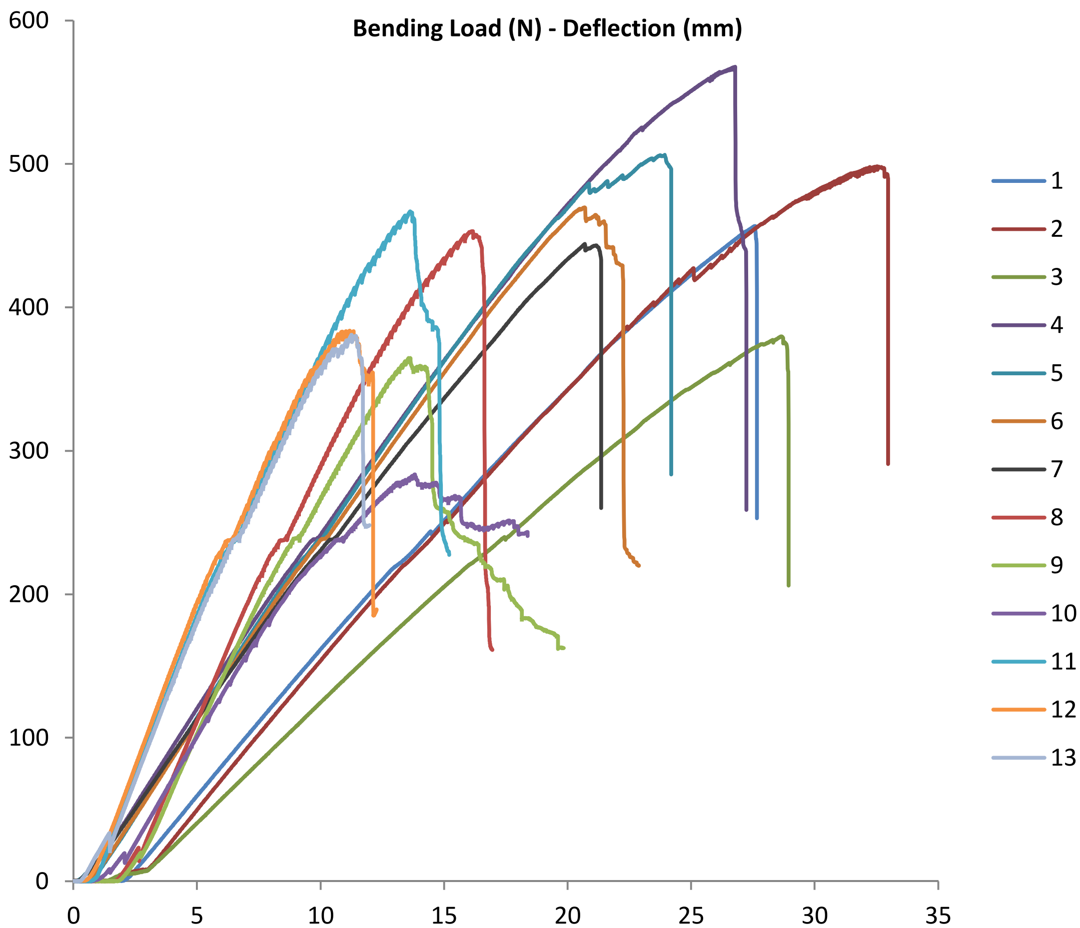

Figure I19. Load vs. deflection graph of panel #3 [0/+45/-45]s Cut #1-7 are parallel bending, Cut #8-13 are perpendicular bending.

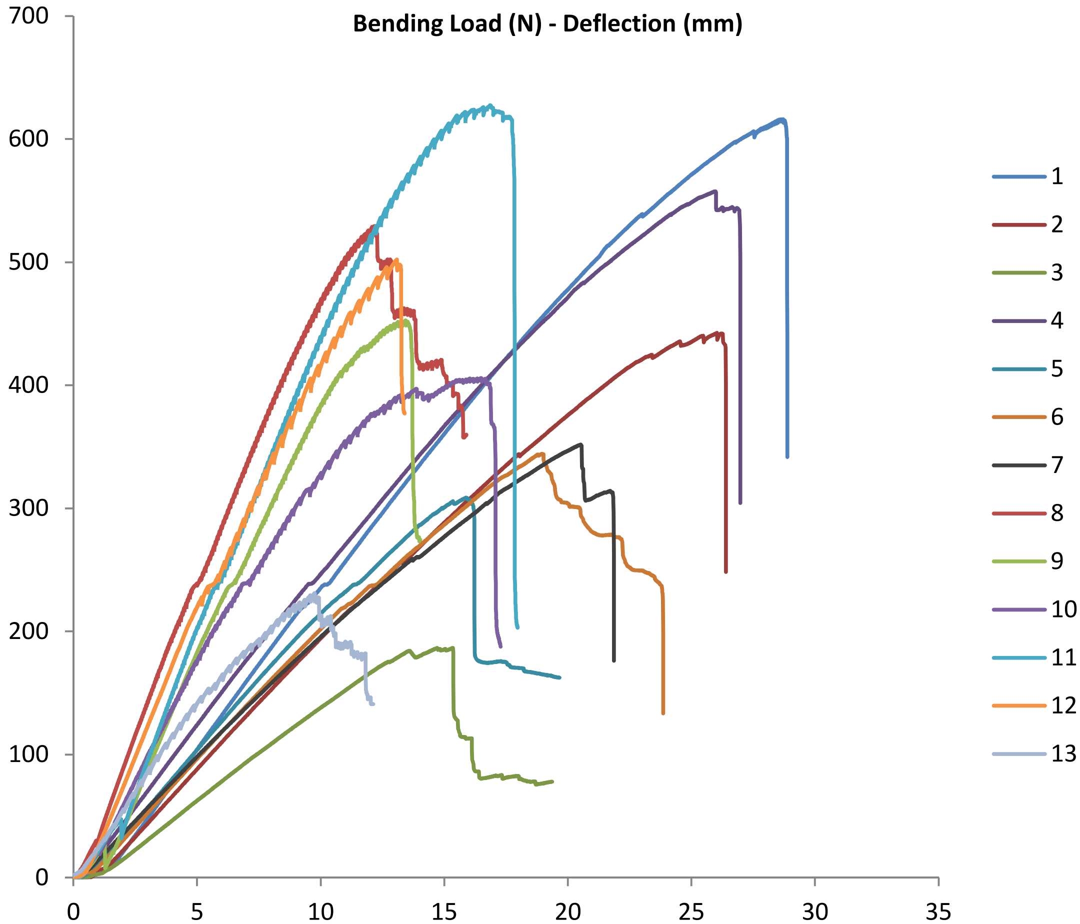

Figure I20 Load vs. deflection graph of panel #4 [0/+45/-45]s Cut #1-7 are parallel bending, Cut #8-13 are perpendicular bending.

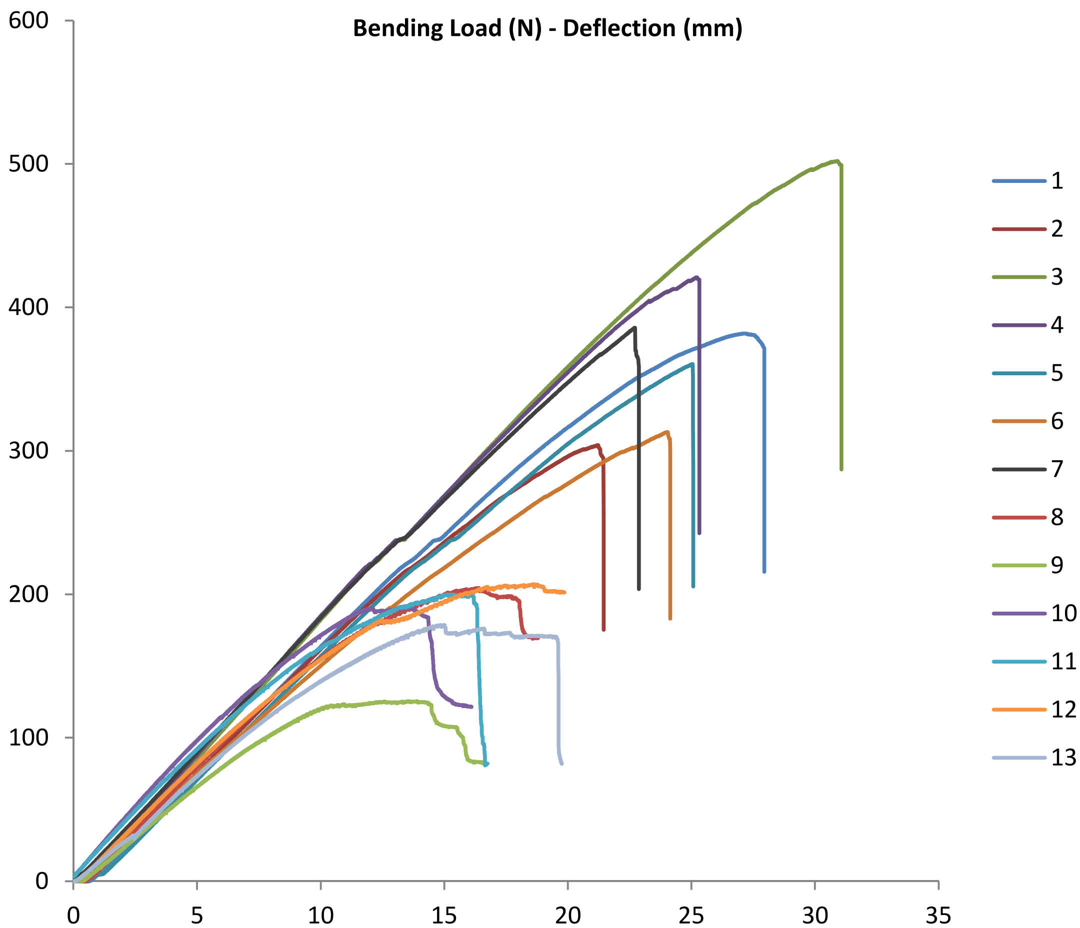

Figure I21. Load vs. deflection graph of commercial panel #1. Cut #1-7 are parallel bending, Cut #8-13 are perpendicular bending.

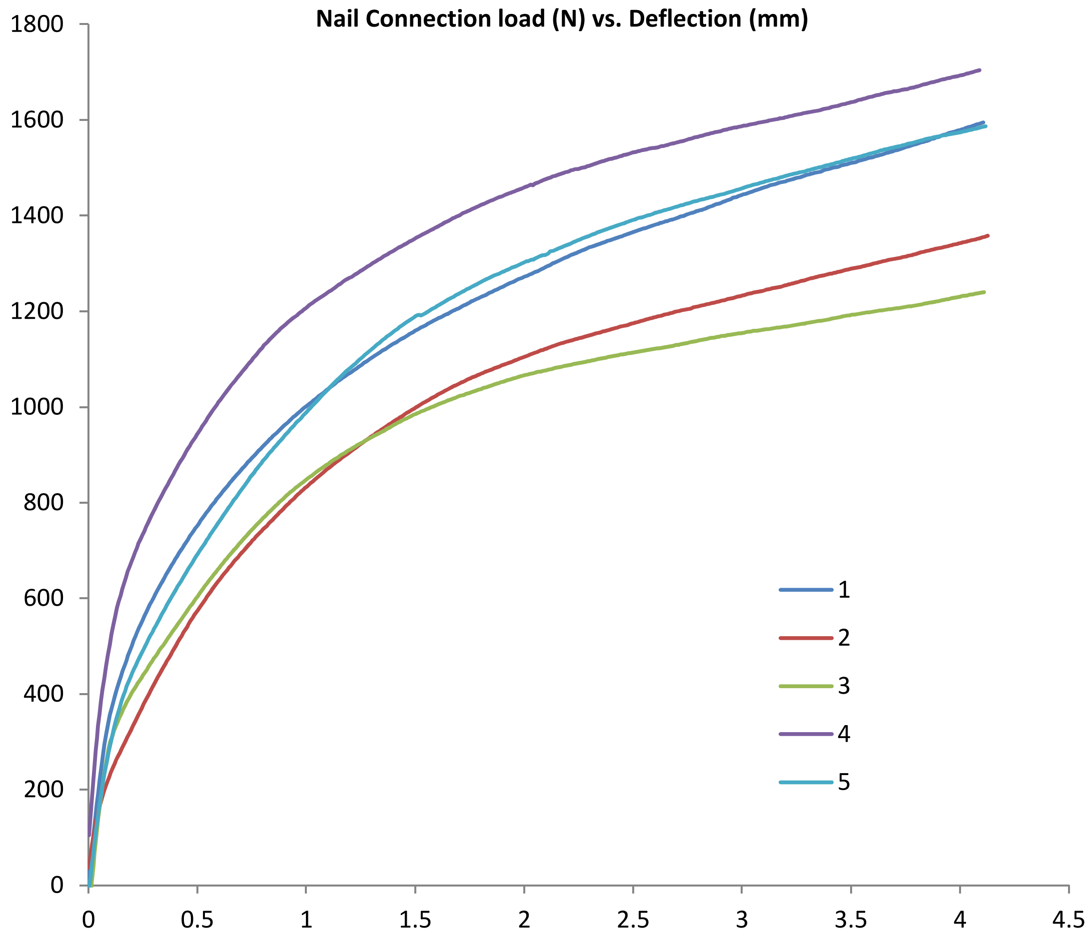

Figure I22. Load vs. deflection graph of parallel lateral nail connection test of laboratory manufactured panels #1-5.

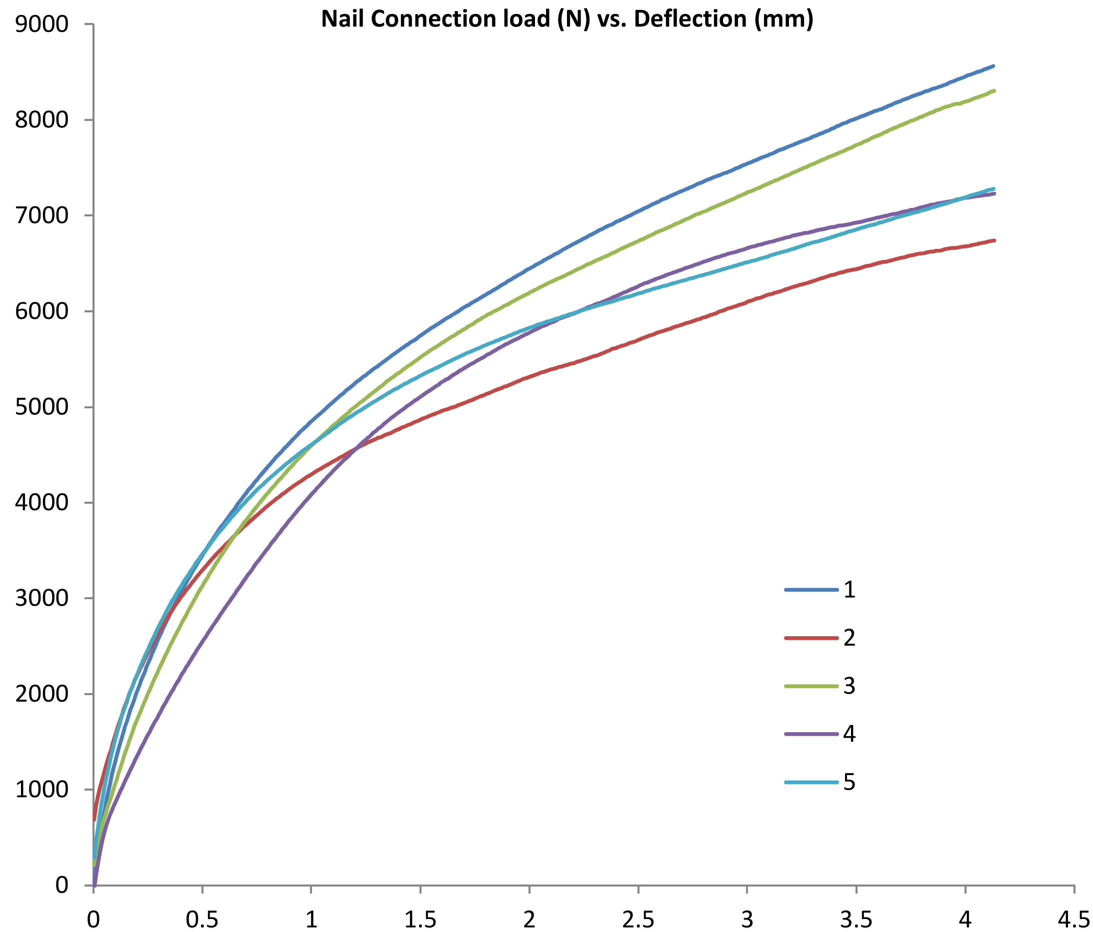

Figure I23. Load vs. deflection graph of parallel lateral nail connection test of commercially manufactured panels #1-5.

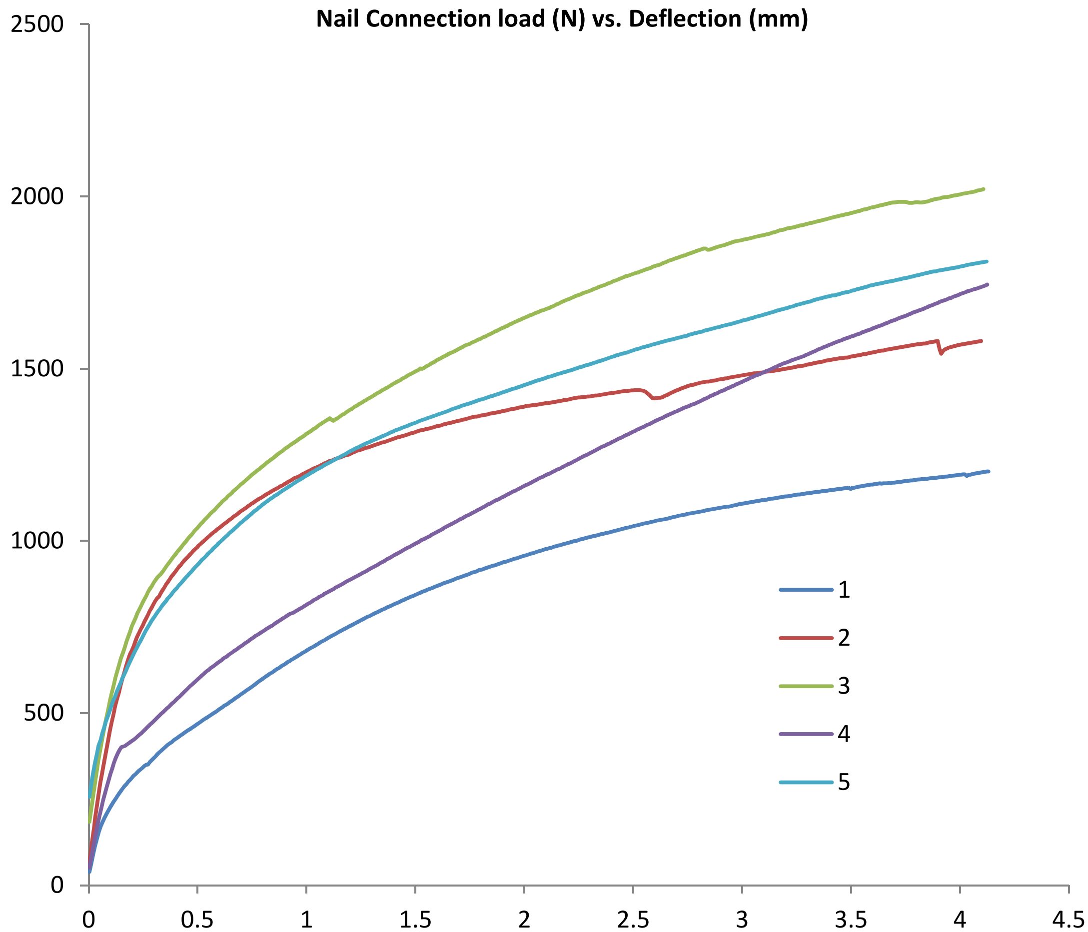

Figure I24. Load vs. deflection graph of perpendicular lateral nail connection test of laboratory manufactured panels #1-5.

APPENDIX J

In-Plane Shear Test Shear Strain Contour Plots

Below are the DIC shear strain output color contour plots. The scale for the color contours is shown in Fig. J1. The panels shown from left to right are commercial #3, panel #17 (0/90/0), and panel #19 [0/+45/-45]s.

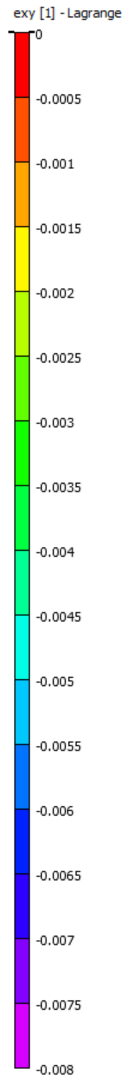

Figure J1. Shear strain color contour plot scale

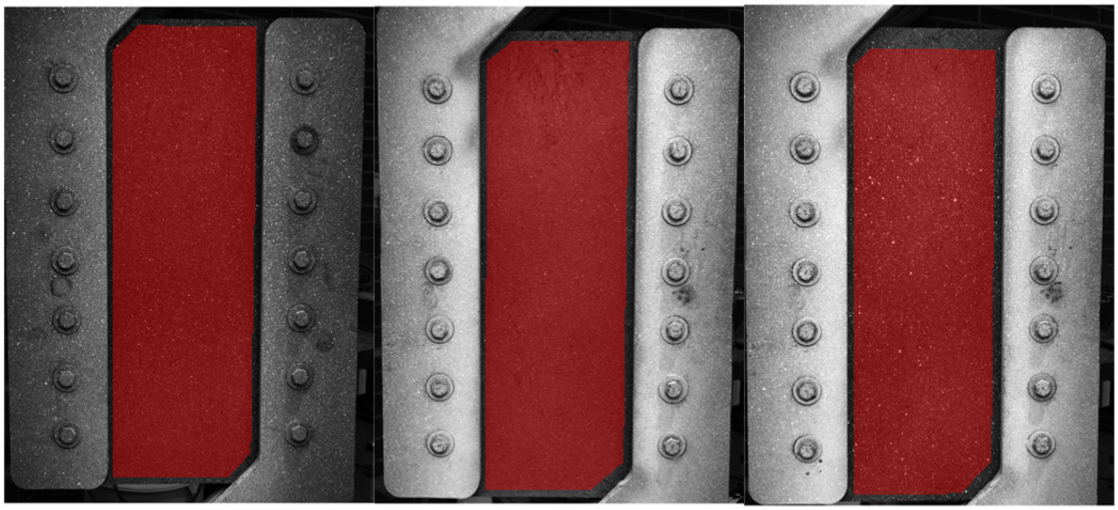

Figure J2. Shear strain at 0kN

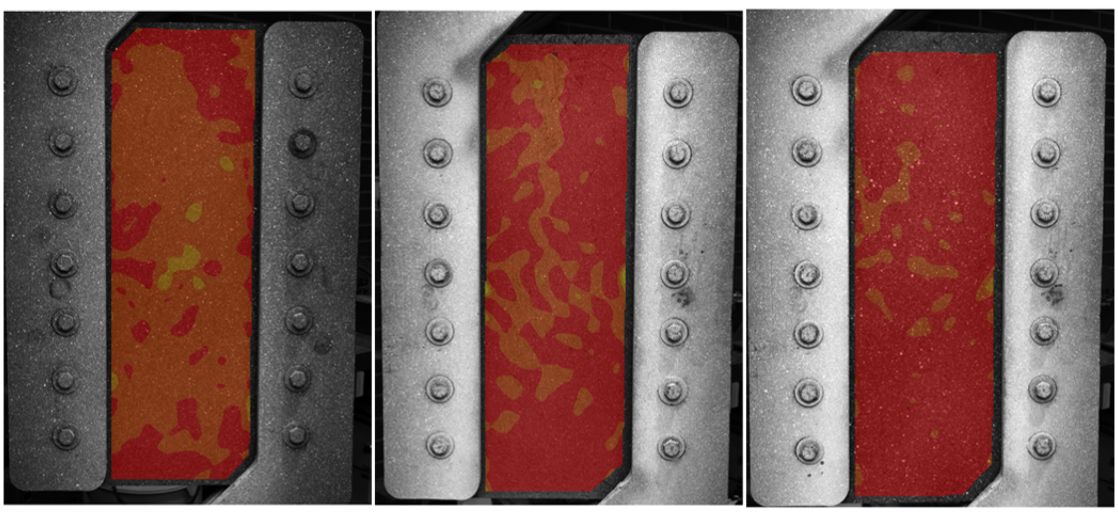

Figure J3. Shear strain at 10kN

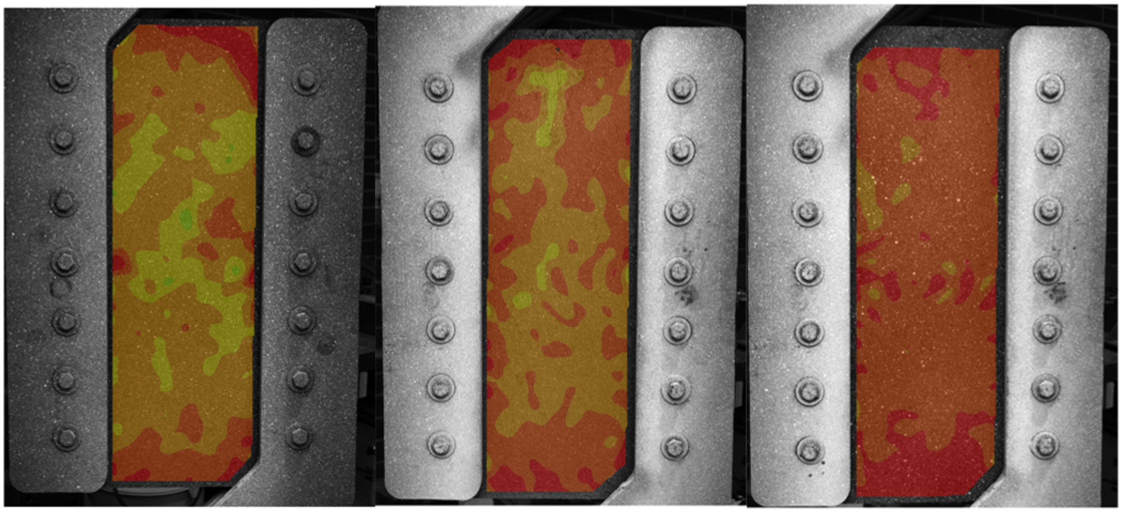

Figure J4. Shear strain at 20kN

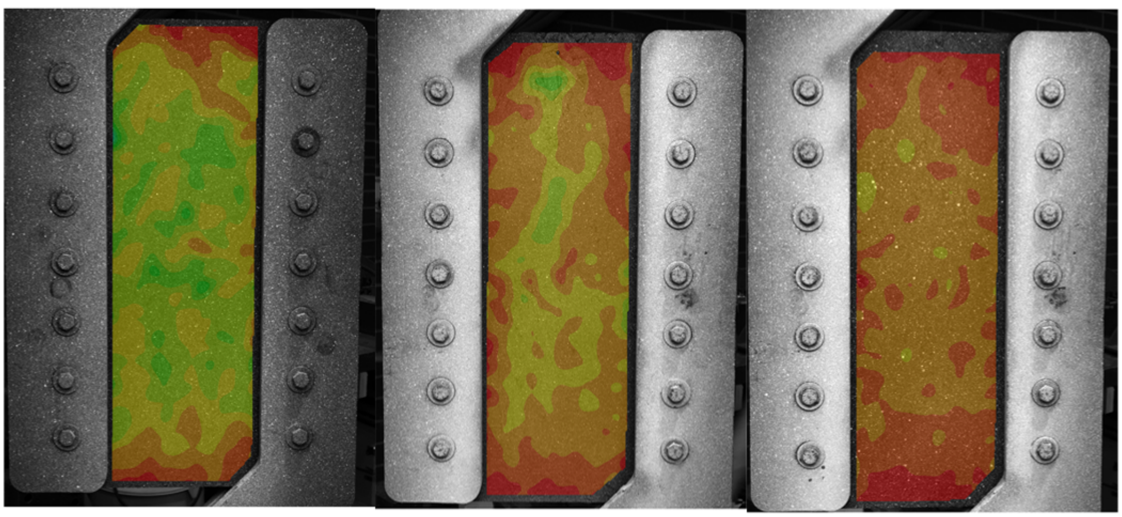

Figure J5. Shear strain at 30kN

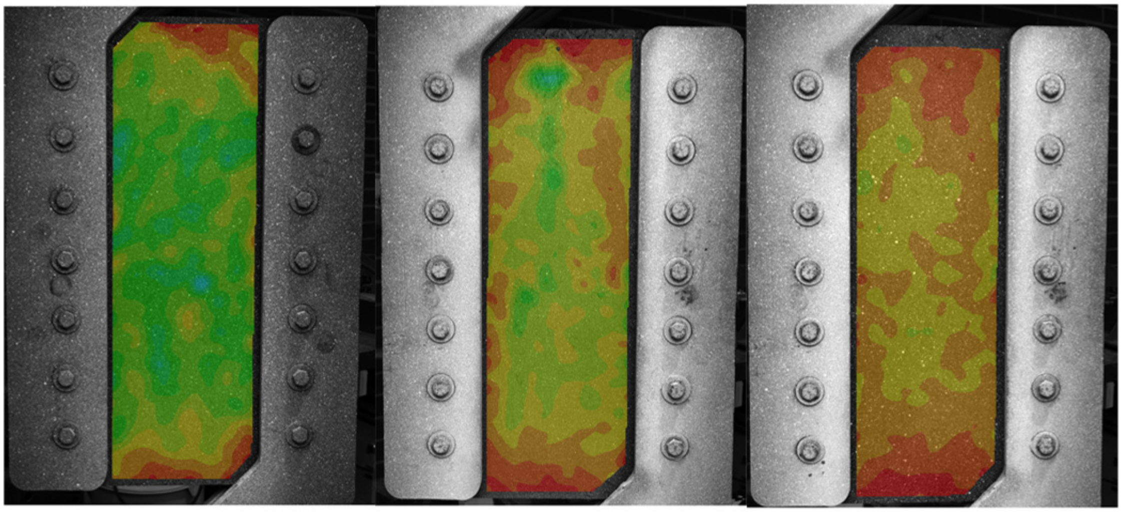

Figure J6. Shear strain at 40kN

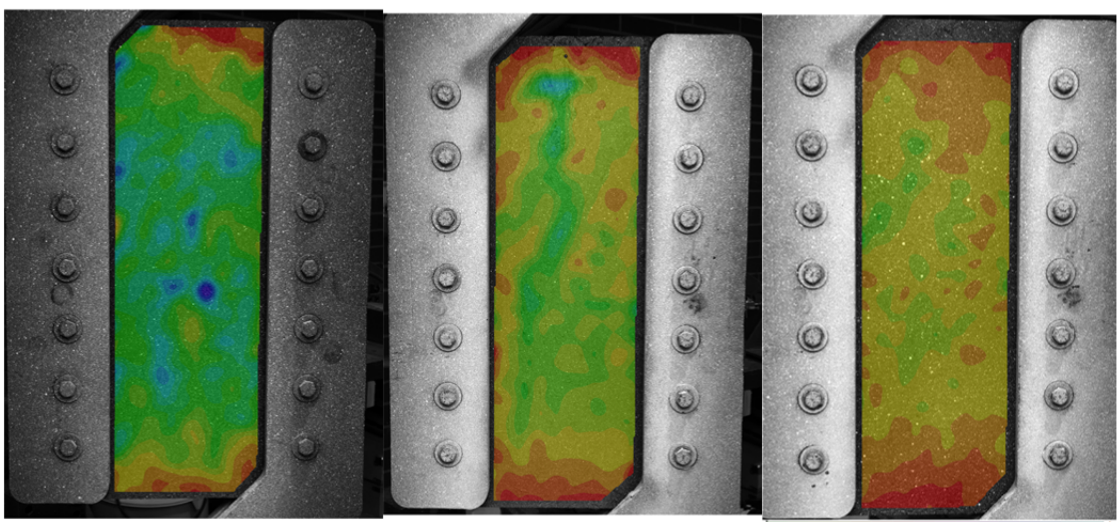

Figure J7. Shear strain at 47.7kN. The commercial panel failed at 47.7kN

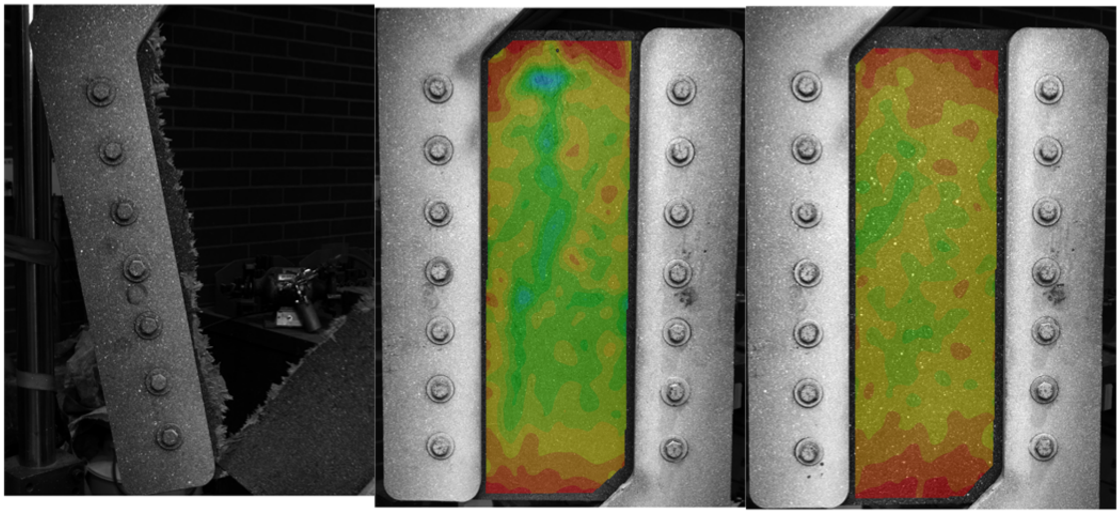

Figure J8. Shear strain at 50kN

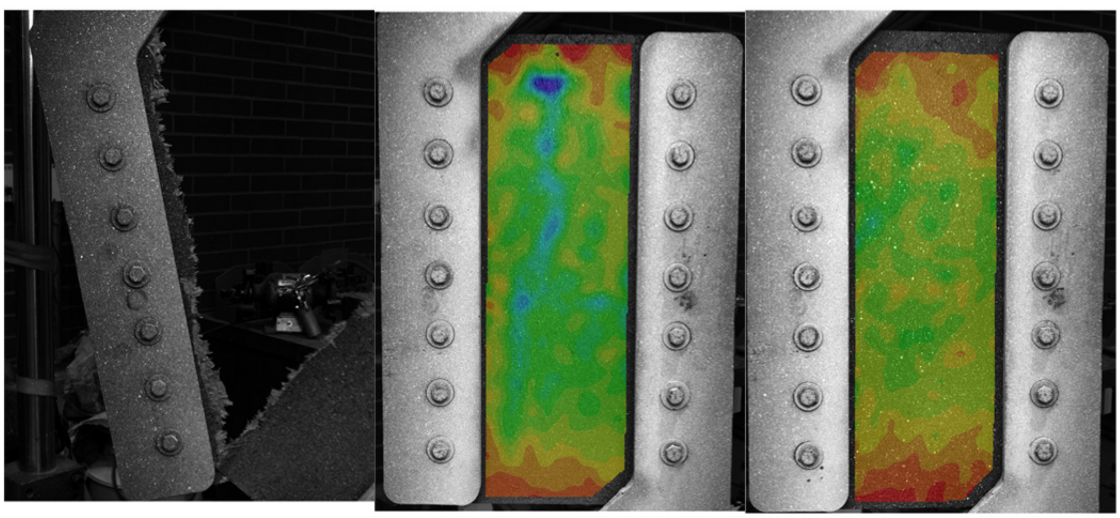

Figure J9. Shear strain at 60kN

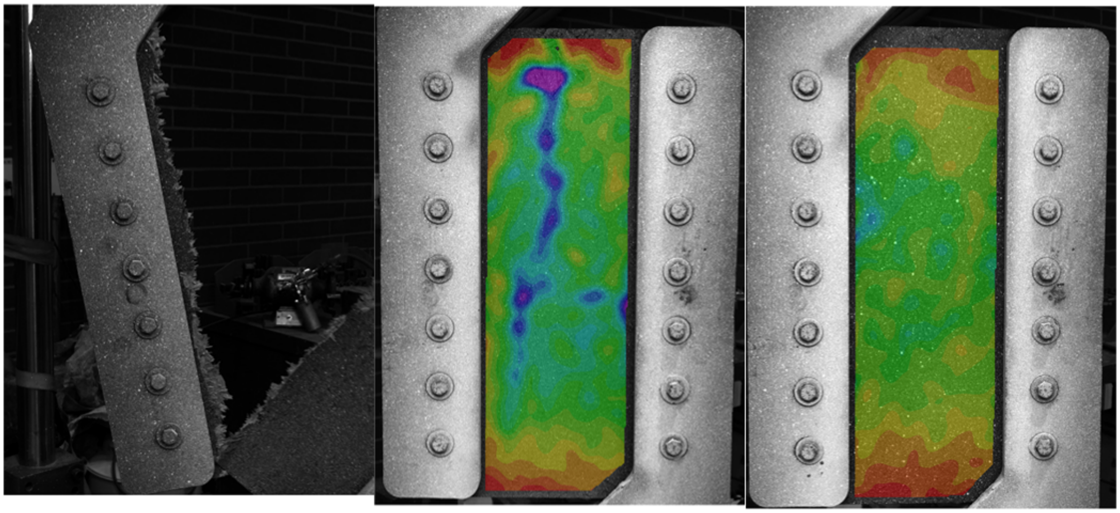

Figure J10. Shear strain at 70kN

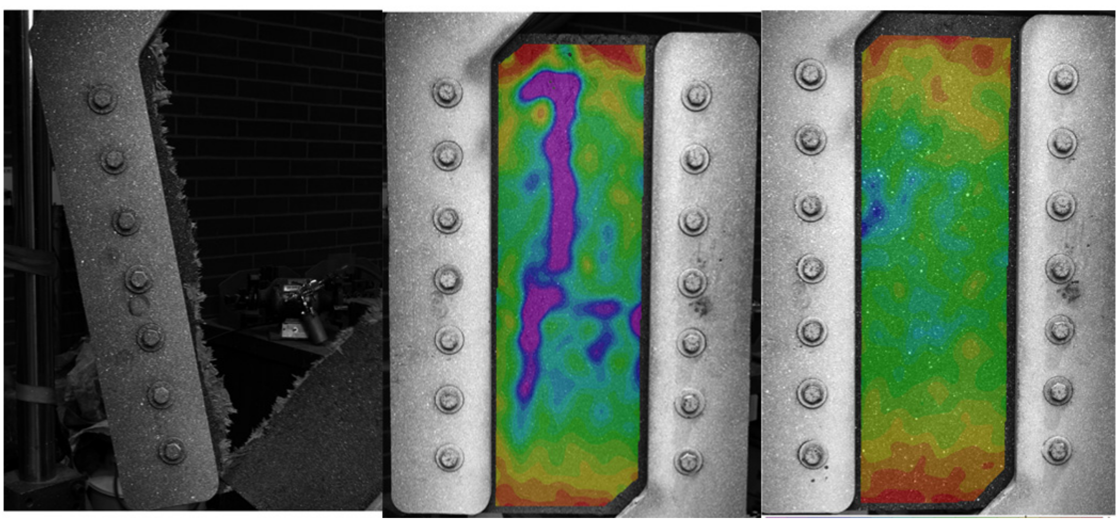

Figure J11. Shear strain at 77.8kN. The 0/90/0 panel failed at 77.8kN

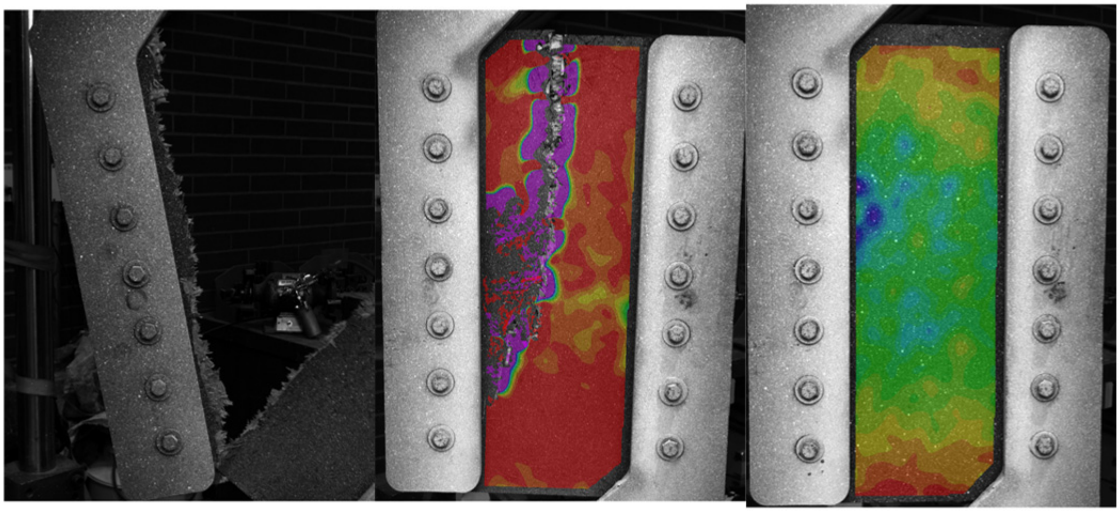

Figure J12. Shear strain at 80kN

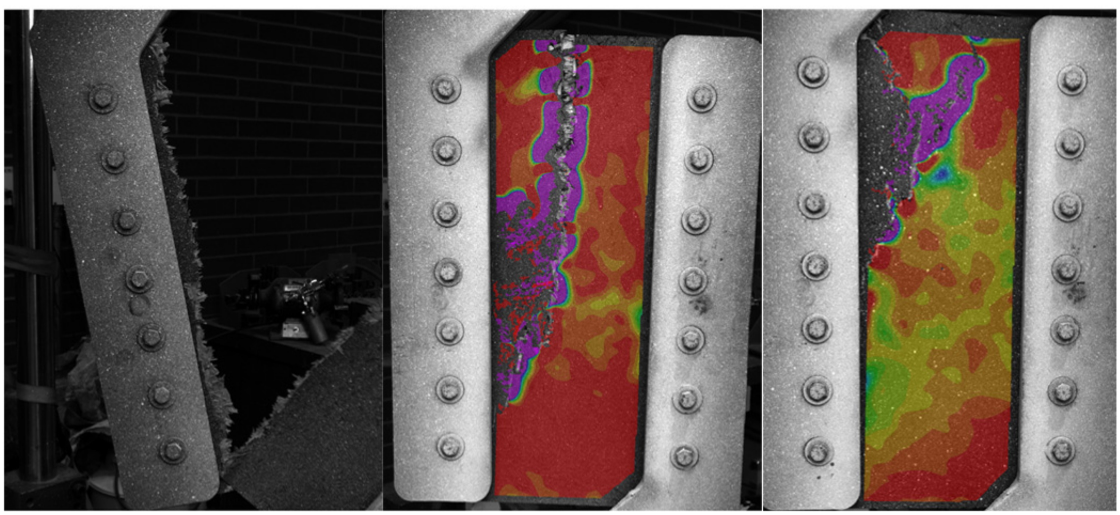

Figure J13. Shear strain at 84.4kN. The [0/+45/-45]s panel failed at 84.4kN

APPENDIX K

Small-Scale Shear Wall Shear Strain and Deflection Contour Plots

Below are the DIC shear strain output color contour plots. The scale for the color contours is shown in Fig. K1 The panels shown from left to right are commercial #5, panel #22 (0/90/0), and panel #27 [0/+45/-45]s.

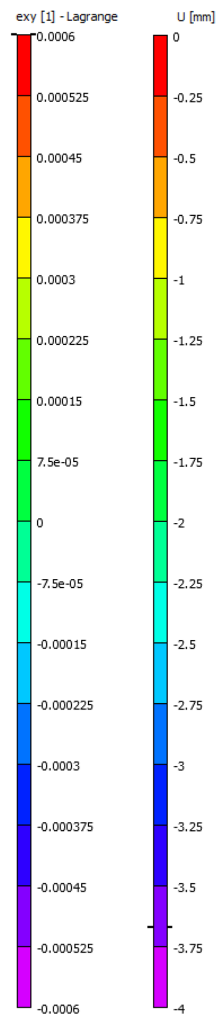

Figure K1. Shear strain (left) and wall deflection (right) color contour plot scale

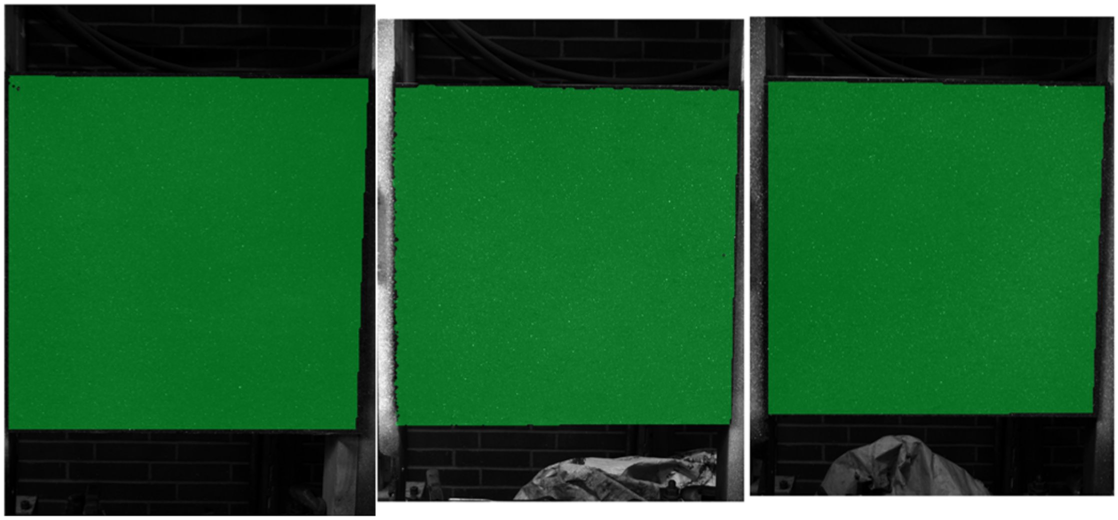

Figure K2. Shear strain color contour at 0kN

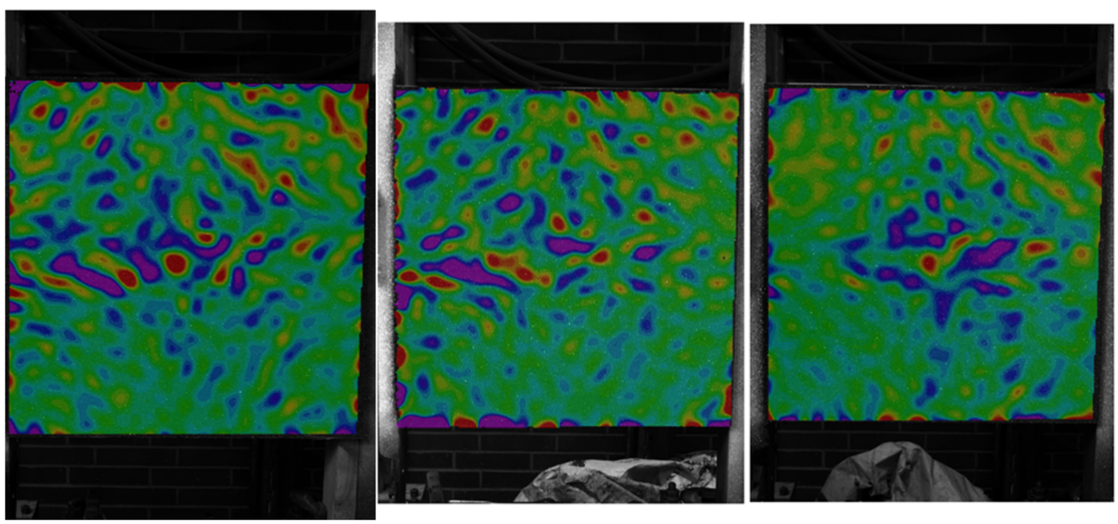

Figure K3. Shear strain color contour at 0.5kN

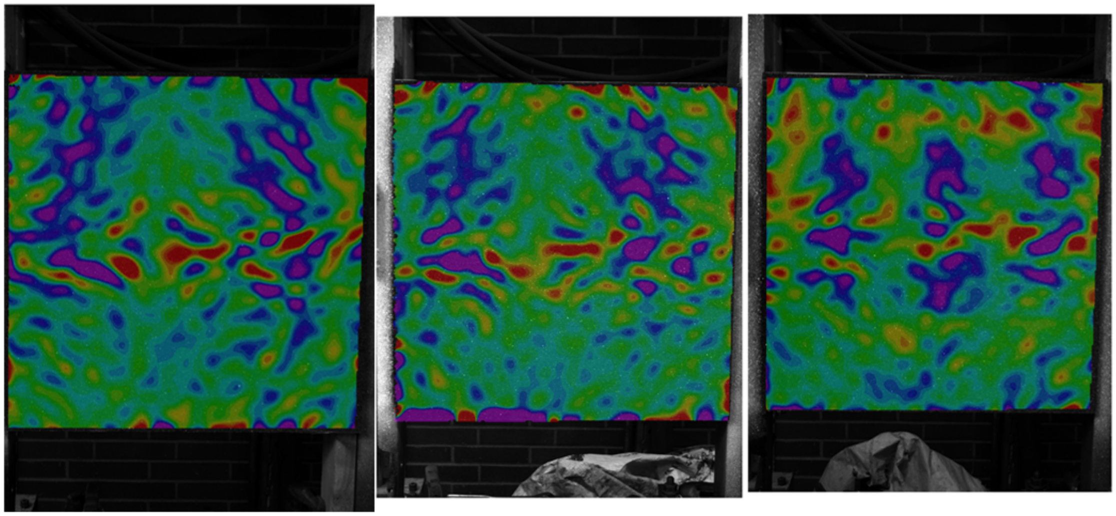

Figure K4. Shear strain color contour at 1.0kN

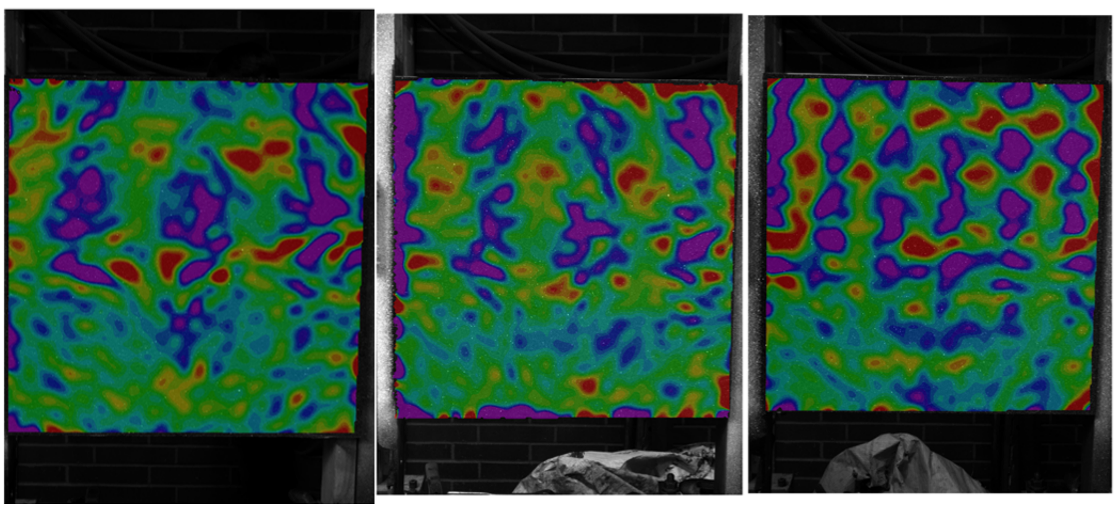

Figure K5. Shear strain color contour at 1.5kN

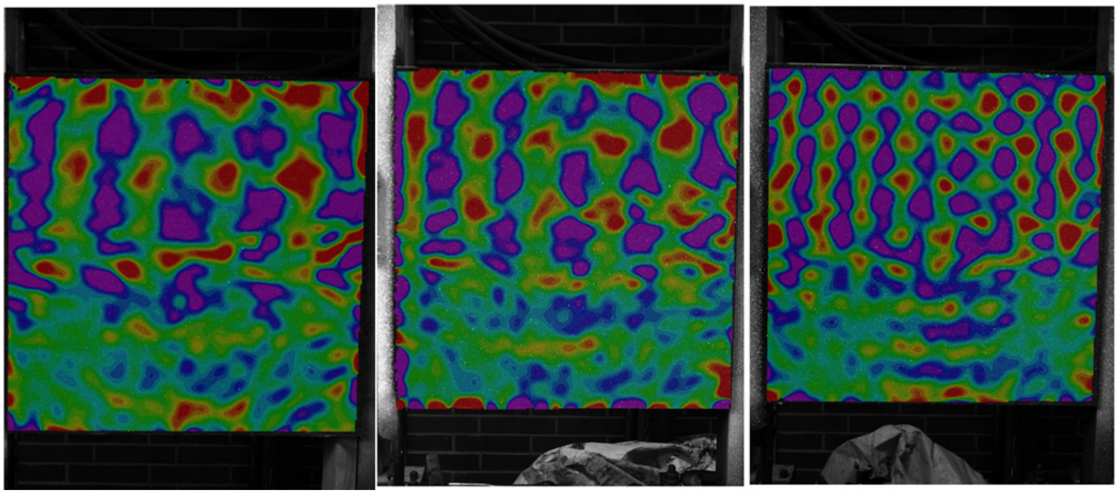

Figure K6. Shear strain color contour at 2.0kN

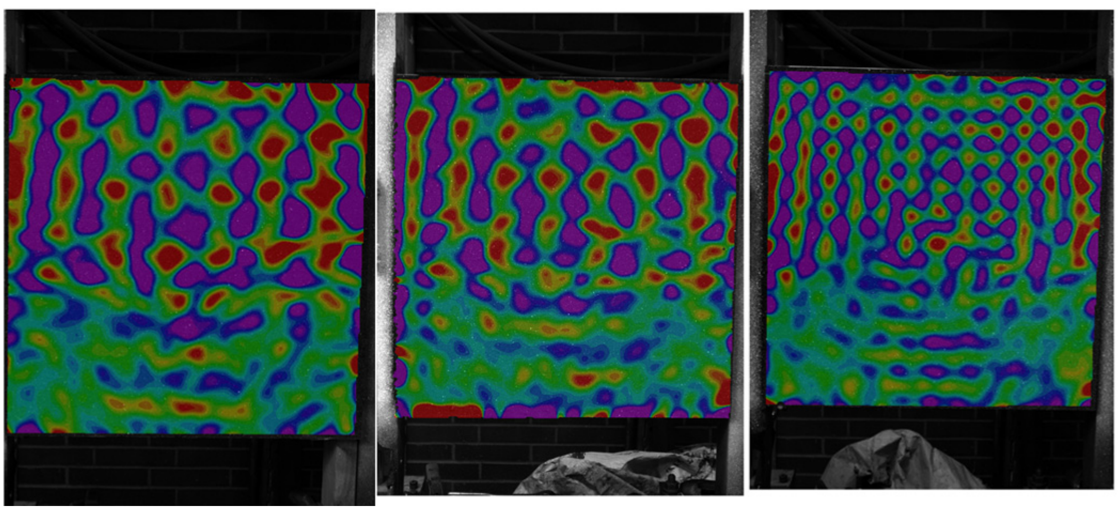

Figure K7. Shear strain color contour at 2.5kN

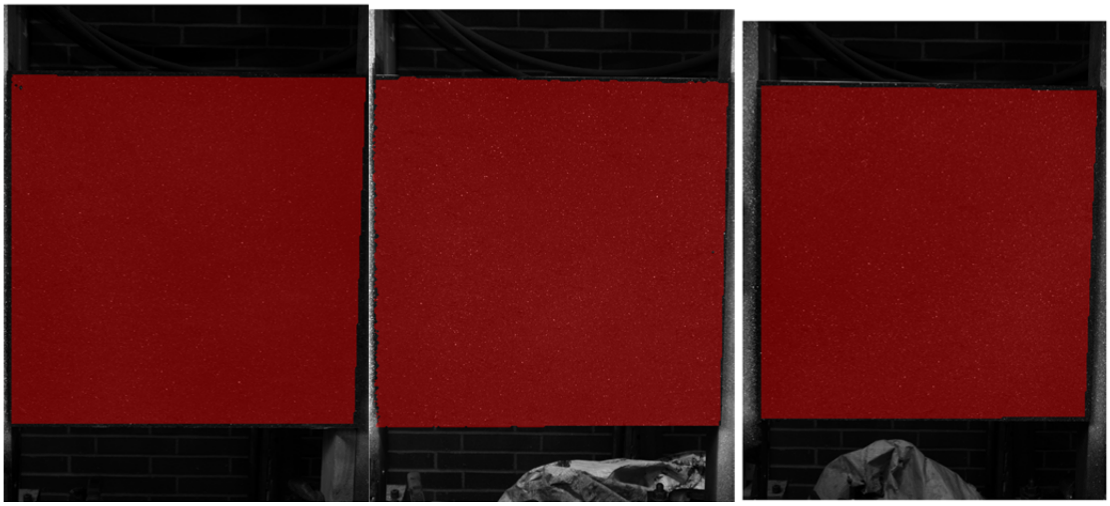

Figure K8. Wall deflection color contour at 0kN

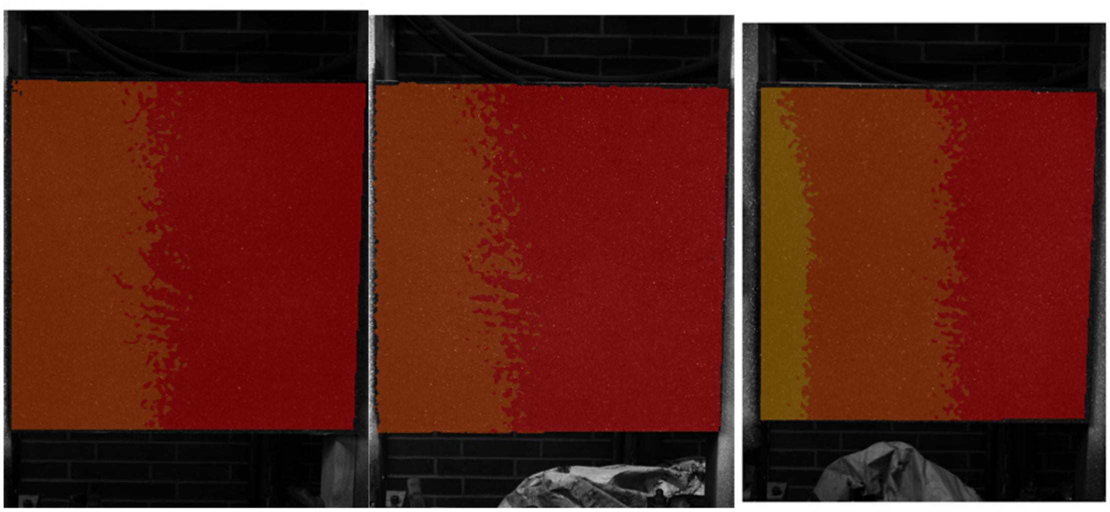

Figure K9. Wall deflection color contour at 0.5kN

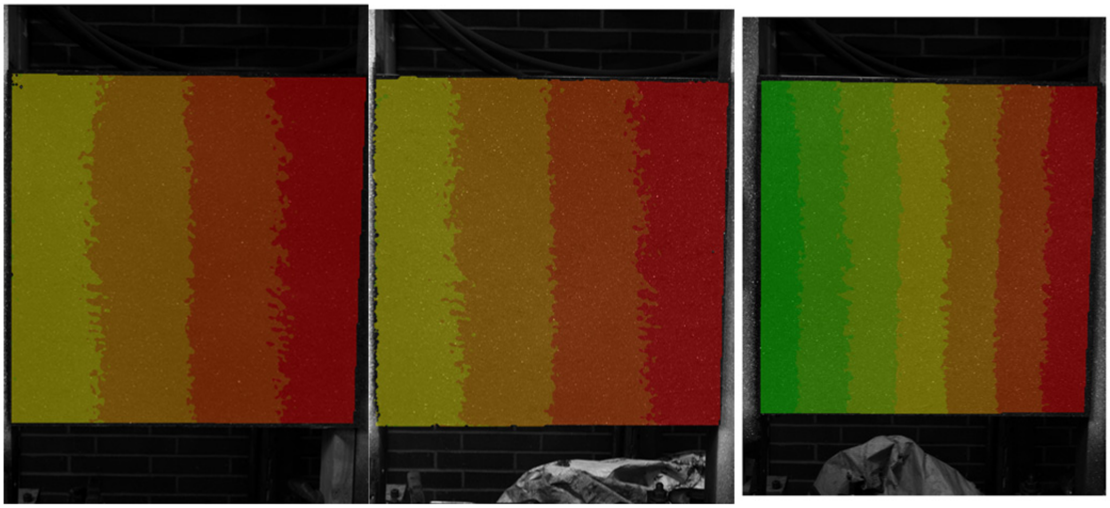

Figure K10. Wall deflection color contour at 1.0kN

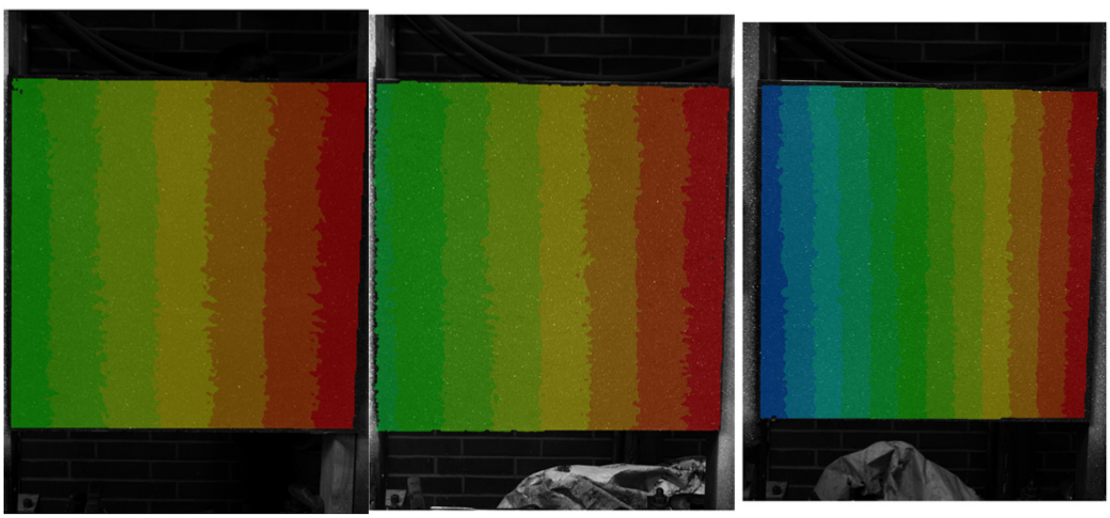

Figure K11. Wall deflection color contour at 1.5kN

APPENDIX L

Non-Destructive Testing of Studs

Before the wall studs were cut to length and nailed to the OSB specimens, non-destructive MOE evaluation of the stud at full length was performed. This was to assist in data interpretation due to wall deflection being affected by quality and strength of the studs.

Table L1. Measured MOE using non-destructive test

NDT MOE, MPa	
Board #	
1	17,323
2	9,963
3	11,083
4	11,773
5	11,135
6	11,514
7	21,977
8	7,757
9	20,960
10	17,720
11	12,928
12	14,445
13	8,136
14	9,825
15	9,136
16	9,584
17	12,997
18	11,204
19	7,826
20	12,755
21	13,927
22	10,963
23	13,031
24	9,446

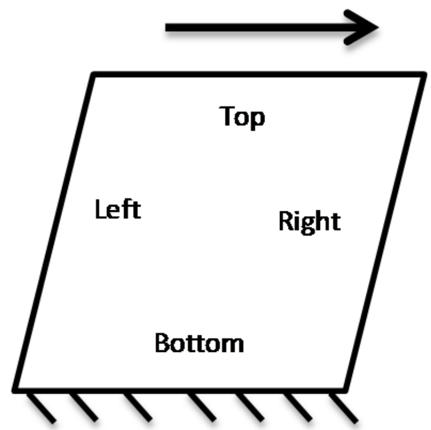

Figure L1. Coordinate system for stud location in small-scale shear wall test

Table L2. Board number of studs in small-scale shear wall test

		Board #		
Panel #	Top	Bottom	Left	Right
21	10	10	1	1
22	10	10	1	1
23	18	18	5	5
24	4	4	6	6
25	19	19	8	8
26	3	18	5	22
27	7	7	9	9
28	7	10	1	9
29	3	3	22	22
30	16	16	24	24
31	16	2	14	24
32	2	2	14	14
Commercial				
1	15	15	13	13
2	11	11	20	20
3	12	12	21	21
4	19	15	13	8
5	23	23	17	17
6	12	23	17	21

APPENDIX M

EEEP Curves Analysis

To assist in wall comparisons, equivalent energy elastic-plastic curves (EEEP) were created. The EEEP curves create a simplified perfectly elastic-plastic curve based on specific calculated parameters from the load-deflection curve and allow for comparisons of wall performance on an energy basis. The EEEP curve parameters are:

P_{peak} = Measured peak load

Δ_{peak} = Measured displacement at peak load

Δ_{yield} = Calculated yield displacement from EEEP curve (P_{yield}/K_e)

$\Delta_{failure}$ = Measured post peak displacement at 80% peak load

K_e = Calculated elastic shear stiffness (0.4 $P_{peak}/\ \Delta_{0.4peak}$)

E = Calculated energy under the curve to failure

μ = Calculated ductility factor $\Delta_{failure}/\Delta_{yield}$

D = Calculated ductility ratio $\Delta_{peak}/\Delta_{yield}$

The EEEP curves were produced but did not allow definite conclusions to be made about increased shear properties affecting shear wall deflection. The EEEP curves are shown in Fig. M2. The EEEP curve data are shown in Table M1. The "-" represents a test where no Δ_{fail} was determined due to the failures being highly ductile and the test being stopped before a maximum deflection was reached.

Table M1. EEEP curve data parameters

Panel #	Ppeak, N	Δpeak, mm	Δ fail, mm	Ke, N/mm	Energy, J	Δ yield, mm	μ	D
21	2997.3	10.7	-	574.8	23.3	4.2	-	2.6
22	4800.1	16.4	16.6	631.1	51.9	6.1	2.7	2.7
23	4626.3	17.9	18.7	439.1	53.7	8.4	2.2	2.1
24	3605.5	10.2	10.4	542.5	22.2	5.3	1.9	1.9
25	3942.1	14.4	14.6	497.2	36.2	6.3	2.3	2.3
26	5093.3	15.4	-	488.7	51.9	8.3	-	1.8
27	4311.4	15.8	-	629.0	50.3	5.5	-	2.9
28	5093.3	16.9	-	761.5	65.0	5.4	-	3.2
29	2801.9	15.8	-	292.9	30.3	7.7	-	2.1
30	4952.1	24.6	27.2	446.6	90.0	8.9	3.1	2.8
31	5060.7	20.3	-	875.9	81.2	4.6	-	4.4
32	3062.5	10.9	13.6	821.6	29.6	3.0	4.6	3.7
C1	3355.7	21.0	-	583.7	55.7	4.6	-	4.6
C2	2780.1	22.4	-	578.3	50.5	3.8	-	5.8
C3	3562.1	23.6	-	293.4	60.2	9.7	-	2.4
C4	2280.6	31.1	-	388.3	58.2	4.7	-	6.6
C5	2704.1	17.4	-	468.7	36.5	4.6	-	3.8
C6	4181.1	23.9	32.7	508.4	98.5	6.6	5.0	3.6

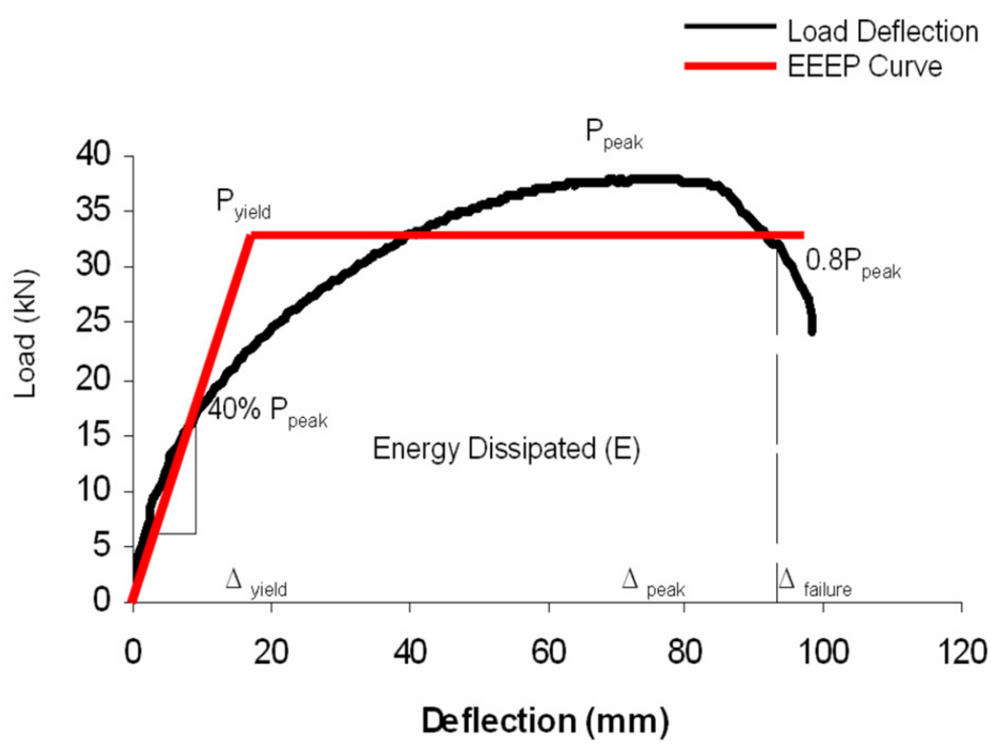

Figure M1. Typical EEEP curve with corresponding definition from Sinha and Gupta (2009).

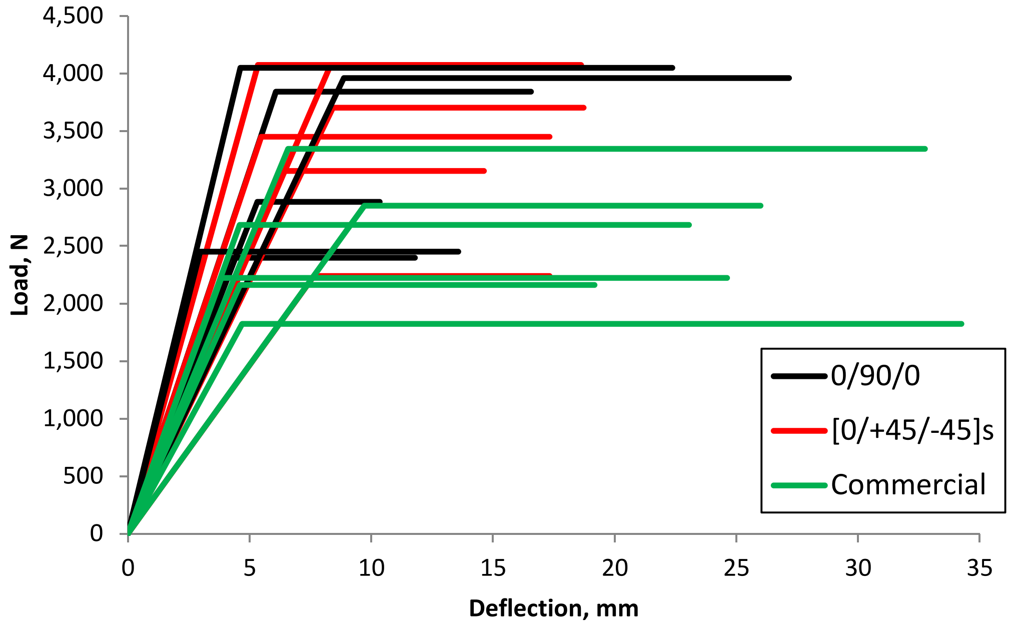

Figure M2. Small-scale shear wall EEEP graph

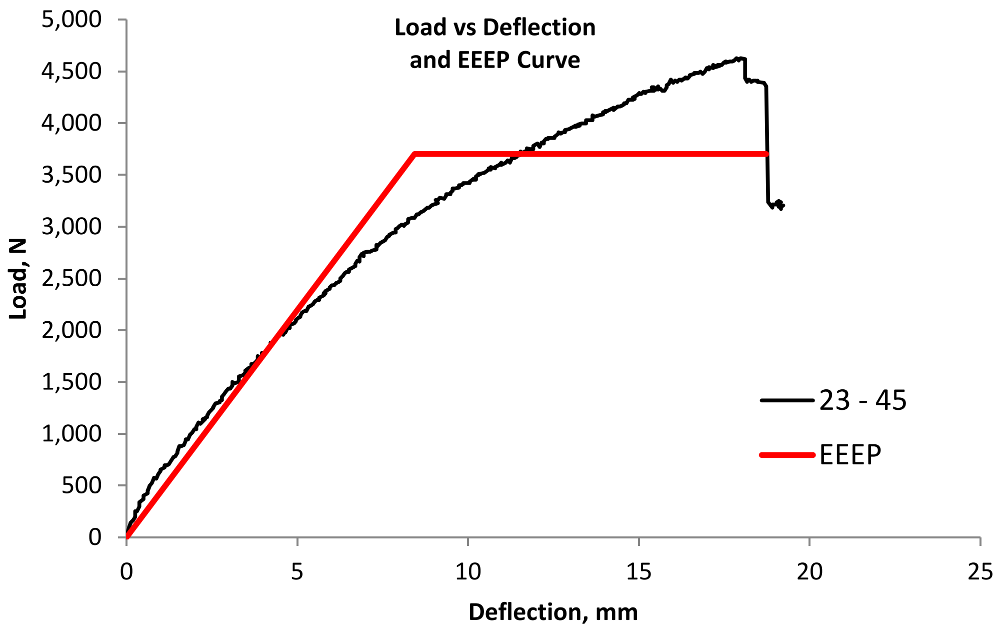

Figure M3. Wall deflection and EEEP comparison for panel #23 with [0/+45/-45]s

Table M2. Area under the EEEP Curve comparison

EEEP Area, N-mm	0/90/0	[0/+45/-45]s	Commercial
	23,298	53,712	55,722
	51,902	36,155	50,488
	22,201	51,947	60,222
	90,027	50,301	58,189
	81,228	64,976	36,472
	29,622	30,258	98,517
Average	49,713	47,892	59,935
SD	29,938	12,623	20,733
COV	60.2	26.4	34.6

Table M3. Statistical summary of EEEP area-under-curve comparison between 0/90/0 and [0/+45/-45]s

t-Test: Two-Sample Assuming Unequal Variances
Units: N-mm

	Variable 1	*Variable 2*
Mean	49713	47892
Variance	896309537	159340841
Observations	6	6
Hypothesized Mean Difference	0	
df	7	
t Stat	0.137	
P(T<=t) one-tail	0.447	
t Critical one-tail	1.895	
P(T<=t) two-tail	0.895	
t Critical two-tail	2.365	

APPENDIX N

Statistical Summaries

Two-sample t-tests were performed on results and are presented below. The tests were performed in Microsoft Excel 2010.

Table N1. Statistical output comparing measured shear modulus between 0/90/0 and [0/+45/-45]s panels.

Shear Modulus, GPa
t-Test: Two-Sample Assuming Equal Variances

	Variable 1	*Variable 2*
Mean	1.224	1.522
Variance	0.042	0.024
Observations	10	10
Pooled Variance	0.033	
Hypothesized Mean Difference	0	
df	18	
t Stat	-3.660	
P(T<=t) one-tail	0.0009	
t Critical one-tail	1.734	
P(T<=t) two-tail	0.0018	
t Critical two-tail	2.101	

Table N2. Statistical output comparing measured shear strength between 0/90/0 and [0/+45/-45]s panels.

Shear Strength, MPa
t-Test: Two-Sample Assuming Equal Variances

	Variable 1	*Variable 2*
Mean	9.161	9.497
Variance	3.391	1.239
Observations	10	10
Pooled Variance	2.315	
Hypothesized Mean Difference	0	
df	18	
t Stat	-0.493	
P(T<=t) one-tail	0.314	
t Critical one-tail	1.734	
P(T<=t) two-tail	0.628	
t Critical two-tail	2.101	

Table N3. Statistical output comparing measured bending MOE in parallel direction between 0/90/0 and [0/+45/-45]s panels.

Parallel MOE, GPa

t-Test: Two-Sample Assuming Equal Variances

	Variable 1	*Variable 2*
Mean	9.527	8.496
Variance	3.818	1.545
Observations	70	70
Pooled Variance	2.681	
Hypothesized Mean Difference	0	
df	138	
t Stat	3.7270	
P(T<=t) one-tail	0.0001	
t Critical one-tail	1.6560	
P(T<=t) two-tail	0.0003	
t Critical two-tail	1.9773	

Table N4. Statistical output comparing measured bending MOR in parallel direction between 0/90/0 and [0/+45/-45]s panels.

Parallel MOR, MPa

t-Test: Two-Sample Assuming Equal Variances

	Variable 1	*Variable 2*
Mean	28.426	26.353
Variance	53.003	46.377
Observations	70	70
Pooled Variance	49.690	
Hypothesized Mean Difference	0	
df	138	
t Stat	1.740	
P(T<=t) one-tail	0.042	
t Critical one-tail	1.656	
P(T<=t) two-tail	0.084	
t Critical two-tail	1.977	

Table N5. Statistical output comparing measured bending MOE in perpendicular direction between 0/90/0 and [0/+45/-45]s panels.

Perpendicular MOE, GPa

t-Test: Two-Sample Assuming Equal Variances

	Variable 1	*Variable 2*
Mean	2.481	2.694
Variance	0.294	0.431
Observations	60	60
Pooled Variance	0.362	
Hypothesized Mean Difference	0	
df	118	
t Stat	-1.945	
P(T<=t) one-tail	0.027	
t Critical one-tail	1.658	
P(T<=t) two-tail	0.054	
t Critical two-tail	1.980	

Table N6. Statistical output comparing measured bending MOR in perpendicular direction between 0/90/0 and [0/+45/-45]s panels.

Perpendicular MOR, MPa

t-Test: Two-Sample Assuming Equal Variances

	Variable 1	*Variable 2*
Mean	13.233	13.994
Variance	12.779	12.058
Observations	60	60
Pooled Variance	12.418	
Hypothesized Mean Difference	0	
df	118	
t Stat	-1.182	
P(T<=t) one-tail	0.120	
t Critical one-tail	1.658	
P(T<=t) two-tail	0.240	
t Critical two-tail	1.980	

Table N7. Statistical output comparing measured lateral nail connection yield load in parallel direction between 0/90/0 and [0/+45/-45]s panels.

Parallel Yield Load, N

t-Test: Two-Sample Assuming Equal Variance

	Variable 1	*Variable 2*
Mean	631.0	626.6
Variance	18613.7	9740.5
Observations	10	10
Pooled Variance	14177.1	
Hypothesized Mean Difference	0	
df	18	
t Stat	0.082	
P(T<=t) one-tail	0.468	
t Critical one-tail	1.734	
P(T<=t) two-tail	0.936	
t Critical two-tail	2.101	

Table N8. Statistical output comparing measured lateral nail connection yield load in perpendicular direction between 0/90/0 and [0/+45/-45]s panels.

Perpendicular Yield Load, N

t-Test: Two-Sample Assuming Equal Variances

	Variable 1	*Variable 2*
Mean	637.7	671.3
Variance	45390.8	23679.5
Observations	10	10
Pooled Variance	34535.2	
Hypothesized Mean Difference	0	
df	18	
t Stat	-0.403	
P(T<=t) one-tail	0.346	
t Critical one-tail	1.734	
P(T<=t) two-tail	0.691	
t Critical two-tail	2.101	